ACIBADEM MEHMET ALİ AYDINLAR UNIVERSITY
INSTITUTE OF HEALTH SCIENCES

MOLECULAR MODELLING OF ANTIMICROBIAL PEPTIDES AND POLYMERS

SENA ATASEVER

M.Sc. THESIS

DEPARTMENT OF MEDICAL BIOTECHNOLOGY

SUPERVISOR
Asst. Prof. Tuğba Arzu Özal İldeniz

SECONDARY SUPERVISOR
Asst. Prof. Nihan Ünübol

ISTANBUL-2023

ACIBADEM MEHMET ALİ AYDINLAR UNIVERSITY
INSTITUTE OF HEALTH SCIENCES

MOLECULAR MODELLING OF ANTIMICROBIAL PEPTIDES AND POLYMERS

SENA ATASEVER

M.Sc. THESIS

DEPARTMENT OF MEDICAL BIOTECHNOLOGY

SUPERVISOR
Asst. Prof. Tuğba Arzu Özal İldeniz

SECONDARY SUPERVISOR
Asst. Prof. Nihan Ünübol

ISTANBUL-2023

Department	:	Medical Biotechnology
Program	:	Master
Thesis Title	:	Molecular Modelling of Antimicrobial Peptides and Polymers
Student's name and Surname	:	Sena Atasever
Date of Defence	:	18/01/2023

This is to certify that I have examined this copy of master thesis. I have found that she/he prepared after fulfilling the specified requirements in the associated legislations before the final examining committee whose signatures are below.

Jury Member (Head of the Defense)	Asst. Prof. Tuğba Arzu Özal İldeniz Acıbadem Mehmet Ali Aydınlar University , Institute of Health Sciences, Faculty of Engineering And Natural Sciences	Signature
Jury Member (Thesis Supervisor)	Asst. Prof. Tuğba Arzu Özal İldeniz Acıbadem Mehmet Ali Aydınlar University, Institute of Health Sciences, Faculty of Engineering And Natural Sciences	Signature
Jury Member (Thesis co-advisor)	Asst. Prof. Nihan ÜNÜBOL Acıbadem Mehmet Ali Aydınlar University Vocational School of Health Sciences, Medical Microbiology, Natural Sciences	Signature
Jury Member	Prof Dr. Özge CAN Acıbadem Mehmet Ali Aydınlar University, Faculty of Engineering And Natural Sciences	Signature
Jury Member (Non.-Uni. Member)	Prof. Dr. Tarık EREN Yıldız Technical University, Faculty of Art and Science	Signature
Jury Member (Non.-Uni. Member)	Asst. Prof. Öznur YAŞAR DİNER Kadir Has University Faculty of Engineering and Natural Sciences	Signature

DECLARATION

I declare that this thesis work is my own work, I had no unethical behavior at any stages from the planning to the writing of the thesis, I obtained all the information in this thesis in accordance with academic and ethical rules, I cited all the information and comments that were not obtained with this thesis work, and I provided resources in the list of references. I also declare that there was no violation of any patents and copyrights during the study and writing of this thesis.

04/01/2023

Sena Atasever

PREFACE AND ACKNOWLEDGEMENT

First and foremost, I would like to express my deep and sincere gratitude to my dear advisor, Asst. Prof. Tuğba Arzu ÖZAL İLDENİZ, who gave me the opportunity take part in the project in which she was performing the modelling part, for guiding me with her invaluable knowledge and experiences, for her contributions, and supports not only for this research but also for all the process. Again, I would like to thank to my co-adviser Asst. Prof. Nihan ÜNÜBOL for being always kind to me and giving me the opportunity to take part in her project. I would also like to thank to Prof.Dr. Özge CAN and Prof. Dr. Tarık EREN for allowing me to benefit from their projects.

I extremely grateful to my mother, my greatest chance, Seher TUNCER, and to my other chance in life, my sister, Aslı ATASEVER, for supporting me with their endless love and caring. Besides all, I would like to thank my dearest friend Aleyna ERMİŞ who has always been there for me with all her support and encouragements. I am also very thankful for my beloved friend Ziver AYBİRDİR who always listens to me and understands me, and to my friend Cemre Su TURHAN for her friendship. Last but not least, I would like to express my longing and to dedicate my thesis to my precious grandmother, Nuriye TUNCER who passed away last year.

Lastly, I would like to give very special thanks to Prof. Dr. Tanıl KOCAGÖZ and Asst. Prof. Erkan MOZİOĞLU for giving me the opportunity to begin my master journey at Acıbadem University and made this thesis study possible.

This thesis study was supported by TÜBITAK with the 118Z859, 217Z155 and 217S060 coded projects, and was conducted by İTAO Molecular Modelling Laboratory at ACIBADEM MEHMET ALİ AYDINLAR UNIVERSITY.

TABLE OF CONTENTS

LIST OF ABBREVATION AND SYMBOLS

Å	Angstrom
AI	Artificial Intelligence
AMBER	Assisted Model Building With Energy
AMP	Antimicrobial Peptide
AP	Antimicrobial Polymer
CC.	Coupled Cluster Theory
CHARMM.	Chemistry at Harvard Molecular Mechanics
CI	Configuration Interaction
CPU	Central Processing Unit
DFT	Density Functional Theory
DMPC	*1,2-Dimyristoyl-sn-glycero-3-phosphocholine*
DPPC	*1,2-Dipalmitoyl-rac-glycero-3-phosphocholine*
EPS	Extracellular polymer Subtance
FDA	Food and Drug Administration
ffTK	Force field Toolkit
fs.	femtosecond
FTIR	Fourier Transform infrared spectroscopy
GPC	Gel Permeation Chromatography
HF	Hartree-Fock Canculation
HGT	Horizontal Gene Transfer
HPD	Host Defence Peptide
kDa	Kilodaltons
MAP	Membrane Active Peptides
MCSCF	Multiconfgurational Self-Consistent Field
MD	Molecular Dynamics
μ.	Micro
MIC	Minimum of Inhibitory concentration
ML	Machine Learning
MM	Molecular Mechanics
NAMD	Nanoscale Molecular Dynamicss

NCBI	National Center for Biotechnology Information
NMR	Nuclear Magnetic Resonance
ns	nanosecond
PBC	Periodic Boundary Conditions
PDB	Protein Data Bank
POPE	phosphatidylethanolamine bilayers
ps	picosecond
QM	Quantum Mechanics
QMC	Quantum Monte Carlo
QSAR	Quantitative Structure-Activity Relationship
QSPR	Quantitative Structure-Property Relationship
RCSB	Research Collaboratory for Structural Bioinformatics
RMSD	Root-mean-square deviation
UFF	Universal Force Field
VMD	Visual Molecular Dynamicss
XRD	X-Ray Diffraction

LIST OF FIGURES

LIST OF TABLES

ÖZET

Antimikrobiyal Peptit ve Polimerlerin Moleküler Modellemesi

Son yıllarda, ilaca dirençli bakteriler artış göstermiştir. Dirençli bakteriler nozokomiyal enfeksiyon riskini arttırır ve bu da hastanelerde morbidite ve mortalite oranlarını yükseltir. Bu nedenle antibiyotiklere karşı yeni ve etkili alternatiflere duyulan ihtiyaç gündeme gelmeye başlamıştır. Antimikrobiyal peptitler (AMP'ler), araştırma alanında, terapötik ajanlar olarak çok çekici bir alternatif haline gelmiştir. Diğer bir alternatif ise daha ekonomik ve daha yüksek miktarlarda üretilmeleri, daha uyumlu olmaları ve kimyasal uyum için esnek bir yapıya sahip olmaları gibi avantajlara sahip olan antimikrobiyal polimerlerdir (AP'ler). Bu tez çalışması, antimikrobiyal ajanları tasarlamayı ve etkinliklerini incelemeyi amaçlamaktadır. Doğal antimikrobiyal peptitlere benzer AMP'ler ve AP'ler tasarlamak için moleküler modelleme ve hesaplama yöntemleri kullanılmıştır. İlk olarak, tüm olası moleküllerin 2 boyutlu yapıları, sentetik orijinal moleküller ve kimyasal moleküllerin hesaplamalı olarak çizilmesiyle bir yazılım araclığıyla elde edildi. Ardından, kompütasyonel hesaplama yöntemleri ile moleküllerin yük, atomlar arası açılar, bağ uzunlukları ve 3 boyutlu yapılar gibi parametreleri belirlenmiştir. Parametreler daha sonra moleküler dinamik simülasyon yöntemi için girdi olarak kullanılmış ve tasarlanan moleküllerin hem membran hem de sulu ortamlarda nasıl davrandığı gösterilmiştir. Ayrıca, tasarlanan moleküllerin diğer moleküllerle etkileşimlerinin incelenmesi moleküler yerleştirme adı verilen bir yöntemle yapılmıştır. Böylece moleküllerin etkileştiği bölgeler belirlenerek, antimikrobiyallerin etki mekanizmaları incelenerek yeni tasarlanan moleküllerin rasyonel temellere dayandırılması amaçlanmıştır. Bu bulgular, moleküllerin proteazlara dirençli hale getirilmesinde, etkinliklerinin arttırılmasında ve toksisitelerinin azaltılmasında yol gösterici bir rol oynar.

Anahtar Sözcükler: Antimikrobiyal peptit, antimikrobiyal polimer, ilaç tasarımı, moleküler modelleme, moleküler dinamik simülasyonu.

ABSTRACT

Molecular Modelling of Antimicrobial Peptides and Polymers

Multidrug-resistant bacteria have been on the rise over the past years. Resistant bacteria raise the risk of nosocomial infections, which in turn raises the rates of morbidity and mortality in hospitals. Need for new and efficient alternatives to antibiotics have become an issue. Antimicrobial peptides (AMPs) have grown to be a very attractive alternative to research as therapeutic agents in this area. Another alternative is antimicrobial polymers (APs) similar to natural antimicrobial peptides, which have the advantages of being produced more economically in higher quantities, being more compatible, and having a flexible structure for chemical adaptability. This thesis study aims to design antimicrobial agents, AMPs and APs, and to examine their effectiveness via molecular modelling and computational methods. First, 2D-structures of all possible molecules were obtained from a software by drawing synthetic original molecules computationally. Then, computational methods, the parameters of the molecules such as charge, interatomic angles, bond lengths and 3D-structures were determined. The parameters were then used as inputs for the molecular dynamics simulation method, showing how the designed molecules behave in both membrane and aqueous environments. Also, examining the interaction of molecules designed with other molecules have been done using a method called molecular docking. Thereby, it is ensured that the newly designed molecules are based on rational basis by examining the mechanisms actions of antimicrobials by determining the regions where the molecules interact. This plays a guiding role in making the molecules to be resistant to proteases, increasing their efficiency, and reducing their toxicity.

Keywords: Antimicrobial peptide, antimicrobial polymer, drug design, molecular modelling, molecular dynamics simulation.

1 INTRODUCTION AND AIM

In past several decades, multidrug-resistant bacteria have been emerging especially where clinical applications are applied, such as hospitals. There are several reasons causing this rapid emerging, for instance overuse or improper use of antimicrobial drugs causes bacteria to gain resistance. Resistant bacteria increase nosocomial infections and consequently increase in-hospital morbidity and mortality rates. To overcome this issue, novel, and effective alternatives other than antibiotics are needed to be developed. In this regard, antimicrobial peptides (AMPs) have become very popular option to investigate as therapeutic agents. Even though the AMPs are promising agents against bacteria and, they still needed to be improved. Only a few of them are evaluated for systemic therapy due to their poor drug properties in terms of rapid blood clearance, protease cleavage susceptibility and host cell toxicity (1). To improve these adverse effects, antimicrobial polymers can be another promising option as therapeutic agent since they display major advantages in that they can be made more affordably in larger quantities, are more compatible with drug distribution techniques, and offer a versatile structure for chemical alteration and adaptability. Antimicrobial polymers (APs) were developed to share some of the same mechanisms of action as AMPs while minimizing their drawbacks. According to studies in related topics, APs have predictable dose-dependent toxic effects towards mammalian cells, and they show better resistance to biodegradation by enzymatic proteolytic enzymes compared to AMPs (2–4).

Even though AMPs and APs have their own advantages and disadvantages, it is still quite costly and time consuming to produce and study both AMPs and APs. Taking into account of the drawbacks, it is logical to tend towards *in-silico* techniques before implementing *in-vitro* experimentations. Computational chemistry is a field of chemistry that uses computer simulation to investigate molecules' structure, mechanism of action and properties with the guide of theoretical chemistry knowledge (5). Molecular dynamics methods, which is one the methods of computational chemistry, is used to design AMPs and APs, then by performing molecular modelling methods, designed AMPs and APs are modeled and simulated by mimicking behaviors

of model peptides and polymers. With molecular modelling methods, molecules to be studied can be investigated prior to the *in-vitro* studies to determine whether the specific molecule is worth to study and to spend time and money.

The focus of this thesis is to provide more detailed about mechanism actions of antimicrobial agents in the context of this study, which are synthetically designed natural peptide inspired antimicrobial peptides and antimicrobial polymers, how they interact with each other or other microorganisms by using molecular modelling techniques, such as molecular dynamics simulation, docking and 3-dimensional structure prediction methods. To do so, we aim to compare previously designed peptides and polymer in the basis of which one is more efficient, has more antimicrobial effect, has resistant to proteases. In this way, we offer information for future *in-vitro* studies to produce synthetic derivatives of antimicrobial agents aimed to be novel and effective against drug-resistant bacteria infections. Another value of this thesis study is to improve computational methods and even build a new strategy for designing a drug molecule by *in-silico* methods.

2 BACKROUND

2.1 Computational Chemistry and Molecular Modelling

2.1.1 Computational chemistry

As a science field, chemistry studies elementary particles including electrons, atoms, and molecules. Besides that, it investigates material characteristics including composition, reactivity, and interactions with other chemicals. Molecules are made up of atoms with nuclei and electrons in combination. Since there are a huge variety of distinct molecules with various nuclei located in various nuclear positions in nature, it is a good possibility to find novel compounds. Fundamental branch of chemistry is theoretical chemistry which uses mathematical techniques to apply the physical laws to describe chemical reactions. Finding the most stable spatial configurations of the atoms in a molecule is the primary goal of theoretical chemistry. Theoretical chemistry can also be used to calculate a molecule's relative energy, dipole moment and other chemical and physical characteristics (6).

While a two-body system having interaction can be solved analytically, many-body systems containing higher than two electrons cannot be solved. Only numerical solutions can be obtained as a result of numerous mathematical problems for many-body systems. Those numerous mathematical problems can be solved with the help of powerful and fast computers. Computational chemistry has started to become relevant rapidly for the last decade and is still rapidly spreading in recent years. Computational chemistry is a sub-branch of theoretical chemistry which can be described as mathematical expression of chemistry while computational chemistry uses computer power for execution of mathematical expression to model and simulate the molecular systems as in biomolecules, inorganic/organic molecules, polymers, peptides, drugs etc. It was emerged as a result of computer advancement. Instead of creating a new method, the primary goal of computational chemistry is to find solutions to chemical issues using existing methods. The experimental component of theoretical chemistry is thus considered as computational chemistry. Though theoretical and computational

chemistry are often perceived as being distinct, there is a close relationship between the two (7). While certain theoretical approaches can be generated thanks to the outcomes of computer computations, new theoretical approaches can benefit in the study of computational issues.

The biggest challenge in computational chemistry is selecting an appropriate theoretical approach for the systems to be analyzed and evaluating the results (8). Fundamental concepts and methods that are most common in computational chemistry will be mentioned in the following sections.

2.1.1.1 Fundamental concepts of computational chemistry

Only way to implement computational chemistry thoroughly is to understand the terms of theory, model, and approximation concepts, and what they mean in the basis of computational chemistry (6). Every scientific study requires to bring out a ***hypothesis*** to be started. Hypothesis can be described as a rational assumption or outcome based on previously proven facts. If all experimentations' data is found to be viable with the hypothesis, the assumption is now called ***theory*** (9)**.** Theories can be expressed in mathematical representations. Following concept needed to be learnt is ***model*** that defines and allows researchers to estimate the scientific outcomes in a basic way. Models can be expressed as mathematical representation, and non-mathematical representation. Models are used by researchers with the purpose of comprehending a scientific topic and making assumption on that topic without implementing complex mathematical resolutions (10). In other words, models enable researchers to mimic of an original system. Even though it is a very useful concept, there can be always a possibility of a contradiction to rules of a model because model cannot provide an exact description of a system. One and very common example of a model is the Lewis Dot Representation that does not comprehend kinetic energies of the particles (11). Theory of quantum mechanics is needed to be involved to fully describe all the properties of a system. Even though quantum mechanics is one of the bases of describing chemical systems mathematically, it has never been certainly solved. Therefore, computational chemistry required to be used any other concept of

approximate solutions. ***Approximation*** is used in the situations where the mathematical calculations are significantly complex that solving them is not effectible for analyzation of chemical systems (6,11). One application of the approximation is to eliminate the complex part of the calculation altogether if quantitative measurements is required. Another implication is to use average mathematical description rather than complete description. Rest of the approximations techniques that have been using among computational chemists are variations, perturbations, simplified functions, and fitting parameters to regenerate experimental results (11).

2.1.1.2 Principles of the computational chemistry

2.1.1.2.1 Energy

Energy is one of the most fundamental terms in science. In the field of chemistry, energetic analyzation can provide answers on molecular processes. According to computational chemistry, molecular systems with the lowest energy are accepted as the most stable systems.

Kinetic energy and potential energy are the one which generate amount of total energy in a system. Both energy types are also divided into different categories based on some specifications within themselves (12). Kinetic energy is divided based on motions such as vibrational, rotational, translational, nuclear and electron motion. When it comes to potential energy differentiates into bond stretching energy, bond bending energy, conformational energy, and hydrogen bonding energy etc. Potential energy is expressed mainly by Coulomb's Law (13).

To represent molecules mathematically, different methods have been conducting based on how to treat energy. First, a reference system which has zero energy is required. In *Ab initio* and density functional methods (DFT), zero energy means that all nuclei and electrons have infinite distance between each other. The valence energy used by semiempirical methods is equivalent to removing the valence electrons and ionizing the resultant ions at an indefinite distance (14). Different molecular mechanics

techniques employ zero energy variations in different ways. Some molecular mechanics methods accept the zero value of chemical standards, whereas others accept the zero energy of strainless molecules. Additionally, some approaches to molecular mechanics view zero energy as arbitrary (13,14).

Total energy numbers in relation to the method's energy zero are frequently quite wrong, even within a certain approximation. This inaccuracy nearly always results from systematic error, which is something frequent to find. The relative energies produced by subtracting the total energy from various calculations give frequently the most precise calculations. This explains how the energy differences between conformers and bond dissociation energies can be calculated very accurately (15).

2.1.1.2.2 Electrostatics

Interaction between charged objects is investigated by electrostatics even though it is insufficient to examine whole molecular systems. Coulomb's Law is the mathematical definition of the electrostatics.

$$E = \frac{q_1 q_2}{r_{12}} \tag{2.1}$$

$$F = \frac{q_1 q_2}{r_{12}^2} \tag{2.2}$$

The Coulomb's Law equations for energy and the force between two particles with charges q_1 and q_2 at a distance r_{12}. The Coulomb's Law of equations below don't include constant 'k' because in computational chemistry, fundamental constants are assumed to be 1 according to "atomic unit system" (13).

The electrostatic potential (ϕ) is another important term that is specifically used in every aspect of three-dimensional real space. When a charged particle needs to be included at random point in space, electrostatic potential is involved into calculations. It is frequently said that the electrostatic potential is the energy of adding an

infinitesimal point charge to the system, which satisfies the constraint that there be no mobility of the current charges (polarization of electron density) (15).

The relation between electrostatic potential and density of charge (ρ) are described by the Poisson Equation that is utilized to determine a molecule's electrostatic characteristics (15).

$$\nabla^2 \phi = - \rho \qquad (2.3)$$

2.1.1.2.3 Atomic units

By setting numerous fundamental constants to 1, atomic unit system is applied to make mathematical problems easier to understand. This allows theorists to reduce their use of pencil lead and potential errors. Additionally, it cuts down on the lengthy computer time that is sometimes required for chemical computations. Besides, outcomes of theoretical calculations are unaffected by changes in the calculated values of physical constants (16).

2.1.1.2.4 Thermodynamicss

One of the most comprehensive mathematical representations of chemistry is thermodynamicss. Many of the ideas of energy, free energy, and entropy are defined by the field of thermodynamicss (17). Because of the thoroughness of prior and existing work had been done about thermodynamicss, it has not been investigated very often recently. Another reason for less research on thermodynamicss is the general incapacity to offer in-depth understanding of chemical processes. Over the years, many side of the chemistry have been successfully defined by basic mathematical expressions (18).

One significance of thermodynamicss in computational chemistry is that it can be correlated with computational results. Depending on the calculation, the output could be internal energies, free energies, or another type of energy. Similarly, different

entropy contributions can be calculated. Due to the terminologies used in computational chemistry and thermodynamicss, it might be frustrating that the program does not always make it clear which energy is being listed (19).

2.1.1.2.5 Quantum mechanics

To be able to accurately define electrons, so do the chemistry, Quantum Mechanics (QM) is the most reliable description that can be. Theoretically, QM can provide precise prediction of characteristics of an individual atom or molecule (20). When it comes to practice, the QM equations can be executed for systems with a single electron precisely. The answer for multiple electron systems has been approximated using a wide variety of techniques. To recognize when each estimate is legitimate and how accurate the outcomes are likely to be needs some knowledge on the side of the researcher, but these approximations can be very helpful (21).

Schröedinger and Heisenberg created two generic formulations of quantum mechanics. Schrodinger form serves as the foundation for almost all computational chemistry techniques.

$$\hat{\mathrm{H}}\,\Psi = E\ \Psi \tag{2.4}$$

Hamiltonian operator is described as *H*, wave function as Ψ and energy as *E*. the equation above is called eigen equation, so the Ψ is called eigenfunction while *E* is called eigenvalue in mathematical mean (22). The wave function describes nuclear position of electrons, thus also explaining the probabilistic behavior of the electrons. The Schroedinger equation can only be solved physically if the wave function is continuous, single-valued, normalizable, and antisymmetric with respect to the exchange of electrons (23).

The original Hamiltonian formulation is the time-independent, nonrelativistic form of Schrödinger equations. However, original Hamiltonian is not feasible for recently used software. Thus, researchers prefer to separate nuclear and electron

motions to simplify the problem by approaching Born-Oppenheimer approximation. Where a nuclei in a system is accepted as stationary, Hamiltonian formulation conducted by calculating individually the kinetic energy of electrons, attraction of electrons to nuclei and the repulsion between electrons. This entire formulation can be thought of as a potential energy surface on which nuclei move, which is how one can explain how nuclei move. Then the wave function can be obtained, and to do so, characteristics of a molecule can be described by taking the expectation value of the operator for a specific property. It is possible to get alternative measurable properties, such the dipole moment or electron density, by replacing other operators. Mostly, the Hamiltonian is preferred to be implied in frequently used computational chemistry methods to obtain wave function due to the other properties don't vary except energy (22,23).

The Hellmann-Feynman theorem can also be used to determine molecular characteristics. The Hellmann-Feynman theorem can also be used to determine molecular characteristics. The Hellmann-Feynman theorem is not adhered to by all approximation techniques (24). The Hellmann-Feynman theorem is only adhered to by variational approaches such as Hartree-Fock calculation (HF), multi-configurational self-consistent field (MCSCF), configuration interaction (CI) and coupled cluster theory (CC) (25).

2.1.1.2.6 Statistical mechanics

The mathematical method of calculating the thermodynamics characteristics of bulk materials out of a molecular representation of the materials called statistical mechanics. The theory of a large portion of statistical mechanics is not yet well developed (26). Statistical mechanicians lack even a baseline for a thorough estimation of the Schrödinger equation because quantum mechanicians are still unable to precisely solve it. Despite this restriction, it is still possible to get some excellent results for bulk materials (27).

Ab initio vibrational frequency calculations are needed to be done before statistical mechanics computations for gas-phase properties at low pressure. On the other hand, for condensed phase, application of molecular dynamicss or of Monte Carlo methods are necessary to reach statistical data (27).

According to principle behind, to identify a systems' geometry, in the case of presuming molecules as rigid, each molecule is depicted by its position and its rotational orientation. 6N dimensional space called phase space is created by designating 3 molecules each for position of a molecule and rotational orientation of the same molecule. In this generated phase space, there may be some configurations to occur that would never happen in a real system. Therefore, it is important to detect the occurrence of the configurations and its probability. The sum of the potential energy obtained from attraction of molecules, repulsion forces and resultant kinetic energy of molecular mobility gives the configuration occurring probabilistic (26,27).

The energy of the system, which is comprised of all molecules, differs from the energy of the single molecules. The total system contains a certain quantity of energy, which is quantifiable as the system temperature. But not every molecule will possess the same amount of energy. Depending on how they move and interact with other molecules, individual molecules will contain higher or lower energy. Whatever the energy, there is a chance that molecules will be present. The system's temperature T affects this likelihood. If the system has equal number of ways to be placed in both state of energy, Boltzmann distribution is applied (28).

At higher temperatures, there is frequently a greater likelihood of detecting high-energy molecules. Statistical average, also named as weighted average, is detected by calculating the value for each potential energy state belons to a specific system, then multiplying the result by the possibility of locating the system in that energy state. Nonetheless, it is not a feasible method for computer simulation of a real gas systems or condensed phase systems because even the insignificant calculations of all the potential energy states must be considered (28). There are other methods to estimate statistical average. First method called time average is time dependent and aims to

simulate molecular mobility by calculating the value for one molecule at each step and evenly distributing the value to all the time steps, thus the molecule will exist in more possible energy states at a higher percentage of the time. Final evaluation of the findings bases on number of time step and how correctly the simulation can mimic the actual system. Second method is the ensemble average which is used in simulations consisting vast number of molecules. Ensemble average method take value of every molecule in the simulation into account. Another technique is targets geometric configuration of molecules A point in phase space can be represented by a set of Cartesian coordinates, but the statistical propensity of molecules to orient themselves in a particular way is not presented. A radial distribution function, also known as a pair distribution function, provides this statistical analysis of geometry. This function calculates the likelihood of detecting atoms at different distances (29).

2.1.1.3 Computational chemistry methods

2.1.1.3.1 *Ab initio* calculations

Ab initio comes from the Latin word *"initium"* whose meaning is beginning, so the term *"ab initio"* is translated as "from the beginning". As a scientific term, *Ab initio* implies that the estimations are based on first principles and no empirical outcomes can be used (30). Schrödinger equations is resolved by ab initio computations, commonly known as the first principles approach. This technique enables atomistic level research into the atomic structure and material characteristics of many materials. This approach can be thought of as approximate quantum mechanical approach. The approximate solutions obtained for differential equations or functions are typically obtained through the use of simpler functional forms (31).

Ab initio calculations to determine the energy levels are frequently performed using the Hartree-Fock (HF) and density functional theory (DFT) approaches. Ab initio computations can be used to examine the structure of different polymers, big macromolecules, and minerals with the right wavefunction (32).

Hartree-Fock calculation is the most frequently used calculation in ab initio method. HF includes two approaches; one is the central field approximation and the second is the wavefunction. The calculation used in central field approximation does not account for Coulombic electron-electron repulsion. However, the evaluation takes into account its overall impact (32). The approximate energies estimated in this variational computation are all equal to or higher than the exact energy. The energies obtained by HF calculations exceed the precise energy due to the central field approximation and converge to a limiting value known as the Hartree-Fock limit. On the other hand, the wavefunction approximation have to be expressed by a linear function, that is mainly precisely understood for a several one-electron systems (5). Atomic orbitals or, more frequently, basis functions are combined in linear fashion to create the wavefunction. Due to this approximation, the calculated energy in the majority of HF simulations is higher than the Hartree-Fock limit. To minimize the errors of HF calculations, Quantum Monte Carlo (QMC) method have been using. Even though QMC calculations might require high amount of time, they are arguably the most precise ones available right now (5,32). In Density Functional Theory (DFT), the total electron density is used to express the entire energy instead of using the wavefunction (32). When total electron density is to be calculated, approximate Hamiltonian and approximate expression are used.

The advantage of ab initio approaches is that, once all approximations are sufficiently minimal in magnitude, they inevitably converge to the result. This convergence isn't really continuous, however. The simplest calculation might occasionally provide the greatest solution for a certain property. On the other hand, Ab initio techniques have also some disadvantages of being pricey. These techniques frequently need astronomical quantities of computer memory, CPU time, and storage space. Overall, the ab initio methods generally deliver ideal qualitative results and, as the size of the molecules in question decreases, increasingly precise quantitative conclusions (30,32).

2.1.1.3.2 Semi-empirical calculations

Semi-empirical methods use the same general principle of Hartree Fock calculation. According to this system, certain details, for instance the two electron integrals, are approximated or conveniently ignored (30). The system is parameterized by curve fitting within a few parameters or values to account for the inaccuracies created by ignoring a portion of the estimation to achieve the closest probable agreement with experimental data. The orbital approximation framework is used to derive the simplest description of a molecule's electronic structure, and the molecular orbitals are stated as a linear combination of atomic orbitals (33,34). The self-consistent field or Hartree-Fock equations are used to solve for the coefficients of the combination. This process is time-consuming and expensive since it requires an iterative (self-consistent) approach because there are a huge number of integrals to compile and manage. This is the case even more so when atomic orbitals or a large basis are used (34). The goal of the semi-empirical approaches is to substantially minimize calculation time and the amount of the tables that must be stored so that computations are possible and rapid on a limited lab computer (35).

When semi-empirical approach is to be applied, one should consider the strategies that ignoring a significant number of integrals in the energy of the interaction between two electrons, putting the majority of the remainder integrals into parametric form and modifying the parameters based on experimental evidence from atoms or molecules, and using the fewest selection of atomic orbitals available (35).

Semiempirical calculations have the advantage of being substantially quicker than ab initio calculations. The findings of semiempirical calculations may occasionally be imperfect. The results might be ideal if the molecule being computed is comparable to compounds in the database being used to parameterize the algorithm. The results could be quite poor if the molecule being calculated differs greatly from anything within the parameterization set (36).

2.1.1.3.3 Modelling the solid state

The investigation of the synthesis, composition, and characteristics of solid phase materials is known as solid-state chemistry, also known as materials chemistry (37). The same general strategy is used by computational chemical approaches in solid-state chemistry and molecules, with two exceptions. Two alternatives to the molecular atom-centered based functions exist: first, the solid's translational symmetry must be used; and second, entirely delocalized basis functions, such as plane waves, may be used (38).

In general, a band structure, which specifies the energy of electron orbitals for every spot in the Brillouin zone, describes the electrical structure of a crystal. Band structure calculations can use orbital energies obtained from ab initio and semi-empirical calculations. Calculating the energy for every single point in the Brillouin zone takes longer time than it does to compute the energy for a single molecule (39).

2.1.1.3.4 Molecular mechanics

Molecular mechanics (MM) has been using by researchers to identify conformational and molecular structure of a molecule, and energy differences between more than one molecule or to detect binding interactions of molecules (40).

It is still possible to simulate a molecule's behavior even if it is too large to successfully employ a semi-empirical approach by completely disregarding quantum mechanics methods. The techniques, known as molecular mechanics, establish a straightforward algebraic formula which doesn't require no wave function calculation or total electron density calculation for a compound's total energy (41). MM approximates the quantum mechanical energy surface, doing so it reduces the computational timescale and costs while simulating the large molecular systems. MM methods are required to be parameterized to obtain suitable results by using data of the composites (42).

When MM describing the energy of the molecules, classical equations, whose constants are needed to be provided by ab initio estimations and experimental outcomes, are involved. Bond stretching, bond angles, rotation (torsion) angles, non-bonded interactions such as van der Waals interactions, and hydrogen bonding interactions are taken into account in the case of MM method applications (40,43).

2.1.1.3.5 Molecular simulations

The term "molecular simulation" refers to both the molecular dynamicss and Monte Carlo computational techniques (44). The main goal of molecular simulation is to offer precise solutions to statistical mechanical questions rather than approximative answers. The characteristic of molecular simulation that sets it apart from other computer techniques, and also approximations is that the system's molecular coordinates are generated in compliance with an exact computation of the forces or energy interacting between molecules (45). It is appropriate to refer to molecular simulation as computational statistical mechanics. Molecular simulation enables us to identify observable features by implementing a computer program to precisely evaluate a theoretical model of a molecule's or a molecular system's behavior (46).

2.1.1.3.6 Thermodynamicss and statistical mechanics

Thermodynamicss investigates large sized molecular systems' characteristics at equilibrium level such as energy, pressure, volume, entropy, heat limitations and expansion coefficient. Thermodynamicss enables chemists to calculate such characteristics if some of them, which can be properties of the components of those large molecular systems and intermolecular interactions, are known by experimental equations (47). This is where the statistical mechanics comes in to use as it is applied to estimate composition of macroscopic molecular systems by using constituents of molecules in a system. Then, one can make prediction on behavior of related molecular system (47,48).

Advantage of the statistical mechanics is that it allows the researchers to make calculations with no unnecessary detailed forms of equations in which classical mechanics method is required. Calculations of classical mechanics methods are very time consuming, costly and are needed extremely high computational power because of the complexity of every little detail's estimation (48). In that sense, it can be said that the statistical mechanics method is the improved version of thermodynamicss (49). More detailed explanation of statistical mechanics is included previously.

2.1.1.3.7 Structure-property relationships

Structure and property relations are described by experimentally based on qualitative and quantitative measurements (50). Properties of a molecule can either physical properties or chemical properties; physical properties can be observed when a molecule do not undergo any chemical change, such as molecular weight, volume, mass, melting and boiling points, solubility, electrical conductivity, where the chemical properties can be observed once a molecule goes through chemical changes caused by compressibility, toxicity, reactivity of chemicals with each other. Physical properties enable to identify a substance where chemical properties provide information on how molecules and atoms react (50,51).

Structure of a molecule, on the other hand, depends on valence shell of electrons that controls how atoms join in the right proportions. It also depends on the type, orientation, and length of the bond. The position of the nucleus and the electron in a molecule can be used to predict its shape. It also depends on whether there are two or more bonded partners and how spatially oriented the covalent bonds are to the atoms (51). Theoretically, structure of a molecule can be determined with measuring the electron motion by using quantum mechanical equation. The Schrödinger equation can be used to determine it numerically which is a process requiring high-performance computers (52).

In the case of computational chemistry studies, quantitative mathematical relation between property and structure is the one that is considered the most (53). Quantitative

structure-property relationship is used when the property is specified as physical property (QSPR). Quantitative structure-activity relationship is used when the property is as a biological activity (QSAR) (54).

2.1.1.3.8 Artificial intelligence

Over the past several decades, interest in and scope for the use of artificial intelligence (AI) in computational chemistry have risen. AI has been regarded as a groundbreaking tool for the drug discovery process, and it will have a big influence. Main advantage of the AI in drug design is handling of large data sets from high-throughput experimental studies with profiles of gene expression for drug repurposing (55).

The combination of machine learning (ML) techniques, which is the most promising use of AI in material science research, and AI algorithms reduce the cost of computing electronic structure evaluations and can efficiently sample chemical spaces enables both rapid throughputs to look for new molecules with specific properties (56).

2.1.2 Molecular modelling

Molecular modelling is a method that uses both theoretical and computational techniques to mimic and to predict behavior of a molecule, chemical and biological system, and material formations (57). There are different approaches used to describe molecular systems. These approaches vary depending on the length and time scale (in Figure 1).

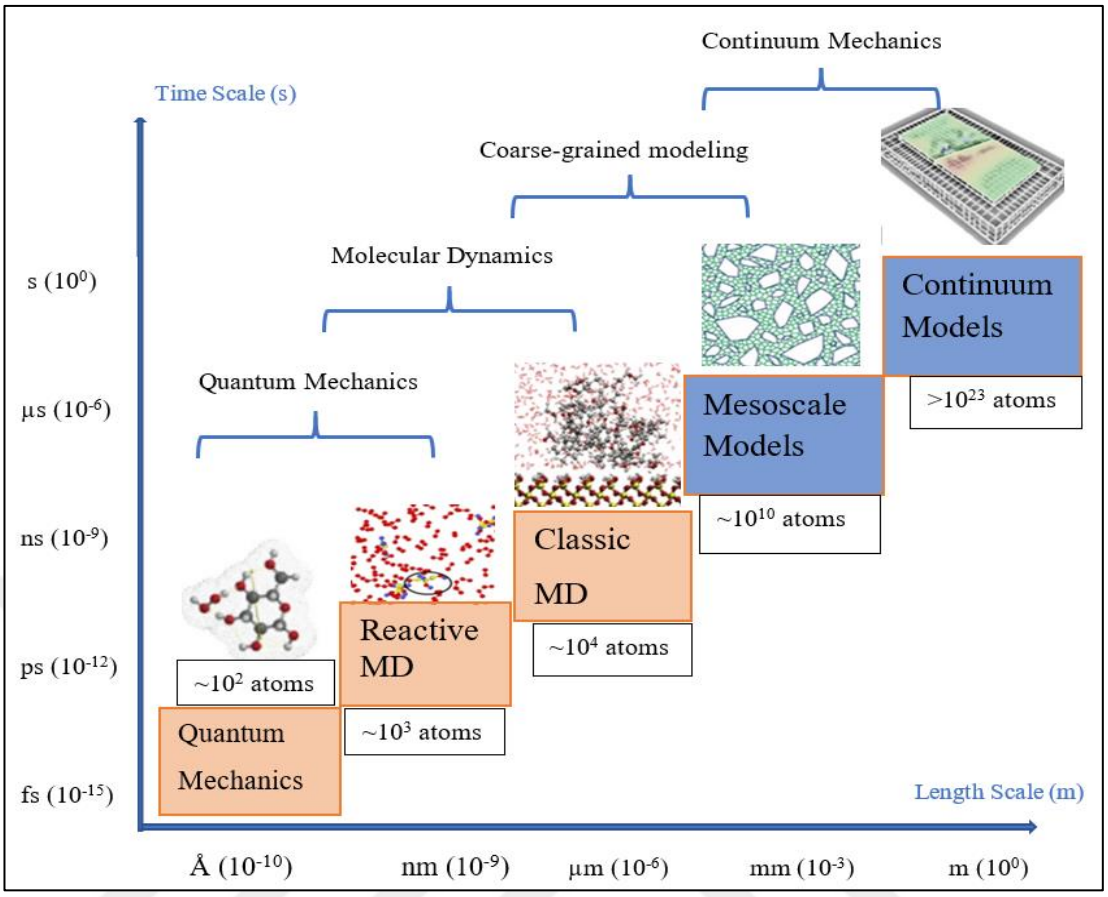

Figure 1. Illustration of Multi-scale Modelling based on time-length scale [modified according to Fenghua Nie et al. 2022 (58) via Microsoft Office Word]

Every modelling scale can be corresponding computational models classified by specific number of atoms. Quantum mechanics (QM) can be referred as theoretical chemistry while computational chemistry incorporates QM, MM (molecular mechanics), and simulation approach. Combination of theoretical and computational chemistry constitutes of molecular modelling's basis (59). QM describes energy of a molecule by using wave function used to predict the probability of finding an electron in a certain region of space while molecular mechanics does not consider explicitly electrons and is used to calculate potential energy of a molecule (60,61). Even though accuracy rate of QM is higher than MM, MM is faster and easy to threat large number of atoms.

One important concept of MM is force field that is used to explain potential energy of molecule or molecular system with optimized parameters and analytical expressions. Total potential energy of a system is called steric energy (V_{steric}). Derivative of the V_{steric} with respect the coordinates of the atoms give the force acting on atoms, which means force field. Every force field has a set of analytical expression of parameters. Total energy is divided up separate potential parameters. Equation of total energy is given below (62).

$$V_{steric} = \sum V_{terms} = V_{str} + V_{bend} + V_{oopb} + V_{tors} + V_{cross} + V_{vdW} + V_{es.} \quad (2.5)$$

(str: bond stretching, bend= bending, oopb= out-of-plane bending, tors: torsion, cross: cross terms, vdW: Van der Waals, es: electrostatic) (62)

Some force field examples are Chemistry at Harvard Molecular Mechanics (CHARMM), Universal Force Field (UFF), Assisted Model Building with Energy Refinement (AMBER), GROMOS, etc. (63)

Having total energy of the system to be studied means that now the atomic coordinates and force field parameters are known. After total energy of a system is known, further processes can be continued with several methods such as geometry optimization, conformational search, molecular dynamicss methods and Monte Carlo methods to model the related system (64). Geometry optimization serves to find the atomic coordinates required for total potential energy minimization while conformational analysis enables to make multiple geometry optimization by rotating the bonding molecules in different angles so that many different conformations can be obtained. The most stable conformers are identified and used for energy minimization (59,64).

Other modelling method is MD uses Newton's equation of motion to simulate a system based on its thermodynamics and kinetic characteristics.

Other than multiscale modelling methods, assorted experimental methods can be used to analyze behavior and interaction of molecules on different scales, such as X-ray diffraction (XRD), nuclear magnetic resonance (NMR), gel permeation chromatography (GPC), Fourier transform infrared spectroscopy (FTIR) (58).

2.1.2.1 Molecular dynamics simulation

Molecular Dynamicss (MD) depending on consecutively updating the positions and velocities of atoms in a system and calculating resultant potential energy of the related system (65). Basic steps of MD start with to draw the molecules and defining x-y-z coordinates (stored in .pdb/.xyz file formats) of the molecules then optimizing the system by using certain force field to lower the initial potential energy because it's high before starting MD simulation. After that, initial velocities of the system must be assigned by following the Maxwell-Boltzmann distribution. To assign the velocities, temperature in which system to be simulated is requires, must be known. Having all required information, potential energy (V_{steric}) can be calculated using the adopted force field. One can search literature to find force fields that is the most suitable with the molecular system to be studied or generate a force field of its own. By taking partial derivative of *Vsteric* with respect to the x-y-z coordinates, resultant force acting on each atom is found ($\boldsymbol{F = -\nabla Vsteric}$). This process is automatically done by the simulation software to be used. In the next step, new velocities and positions for each atom must be updated by using equation of Newton's Second Law ($\boldsymbol{F = ma}$). The steps of calculating potential energy, finding force acting on each atom and updating velocities and positions need to be repeated many times to generate trajectories and properties which then be used for simulation process (57,59,66).

A system is required to be described by statistical ensemble to be simulated. Statistical ensemble is used to make a system ideal by considering all the versions of that system that of each expresses a potential state in which the actual system might be. Ensemble term in MD means that collection of systems in thermodynamics equilibrium, each with total energy (67). There are different types of ensembles. One is NVT (canonical) ensemble in which number of particles, volume and temperature

are constant. Systems simulated by the NVT has Minimum Helmholtz free energy. Density is also constant while pressure can be low or high based on temperature, and other properties fluctuates. In NVT ensemble, macroscopic properties of a system can be predicted. Second one is NPT (isobaric-isothermal) ensemble in which number of particles, pressure and temperature are constant, volume and density fluctuates. In the case of NPT, systems to be simulated have Minimum Gibbs energy and the macroscopic properties of a real system can be predicted. Third ensemble is the μVT (grand canonical) ensemble where chemical potential, volume and temperature are constant. Particles may be generated or decimated. Heat exchanging occurs among systems. Systems simulated using μVT have maximum pressure and volume. Last one is NVE (microcanonical) ensemble where the number of particles, total energy and volume are kept at constant. Systems in NVE based simulation have maximum entropy (67–69).

In MD simulation, water box containing systems' atoms is generated. Because of the computational limitation, only the limited number of molecules can be simulated while millions of molecules wanted to be simulated present in a real system. Limited numbers of molecules most likely behave differently than the millions of molecules. That's why periodic boundary conditions (PBCs) are used to adjust a large system by using smaller portion of the system (unit cell). During simulation, one or more atoms may pass through one edge of unit cell and appears on the opposite section of the simulation box, however the atom number of the system in the simulation box must remain constant. Large systems have infinite number of small units, one of which is the original simulation box. During simulation, only the original one must be considered to propagate and to record. Molecules in original simulation box can move out while the same atom in the copied simulation box move into the original simulation box so that the molecule number in the original water box remain constant. PBCs is required for MD simulation to keep the number of atoms constant in the simulation box, to study the bulk system behavior and to avoid any surface effect (70,71).

Another terms to be considered for MD simulation is Ewald Sum to calculate total electrostatic interaction between charges involving in original simulation box obtaining by PBCs (59).

Molecular Dynamicss programs that can be used to model and to simulate a system or a molecule are GROMACS, CHARMM, AMBER, LAMMPS, NAMD, TINKER, OpenMM, Hyperchem, Schrödinger. Visualization programs for visually represent a simulation are VMD, PYMOL.

2.1.2.2 Molecular docking

A type of bioinformatic modelling called molecular docking includes the interaction of more than one molecule to produce a stable compound. It makes predictions about the three-dimensional structure of every compound based on the binding characteristics of ligand and target (72,73). Different potential adduct structures are generated by molecular docking and are scored and categorized using the software's scoring algorithm. Depending on the system's total energy, docking simulations forecast an optimum docked conformer. Despite all viable strategies, the difficulties still lay in ligand chemical reactions (tautomerism and ionization), receptor flexibility (single form of rigid protein), and scoring function (differentiate actual binding mode) (72,74).

Molecular docking is an appealing tool to comprehend drug biomolecular interactions for rational drug discovery and development in addition to the mechanism of action study. Working principle of docking is basically to incorporate a molecule functioning as a ligand molecule through the ideal binding region of the target segment of the DNA/protein functioning as a receptor molecule primarily in a non-covalent manner. The data gathered from the docking technique can be used to provide insights on the binding energy, free energy, and stabilization state of complexes (73). Currently, the docking technique is being utilized to make prediction on probable binding capabilities of the ligand-receptor compound.

Obtaining a ligand-receptor compound with an optimal configuration and the idea of having lower binding free energy is the primary focus of molecular docking (74).

In order to perform docking, two related processes must be taken: first, the ligand's structures in the protein's active site must be sampled; next, these structures must be ranked using a scoring function. The empirical binding form should ideally be reproducible by sampling methods, and it should also be given the best score among all created conformations (73,74).

There are mainly two types of strategies employed when conducting molecular docking; one is the simulations approach and the second is the shape complementarity approach. In simulation method, Physical separation between the ligand and target allows the ligand to attach into the pocket of the target after "specified durations of motion" in its conformational region. The movements contain internal (torsional angle rotations) or external (changes to the ligand's structure) changes (rotations and translations). Every time the ligand moves within the structural barrier, Total Energy is released. This strategy is more efficient in that it is more susceptible to tolerating ligand flexibility. Because of the significant dissipation of energy for each configuration, this method takes longer to predict the best docked conformer. In shape complementarity method, the interface configuration features of the ligand and target are used to give the binding interactions between them. The molecular surface of the ligand is represented in terms of the surface region of the target that is available to solvents. Searching for ligand in the complementary pocket on the target surface is made easier by the compatibility between two interfaces depending upon shape fitting representation. This method scans tens of thousands of ligands in a matter of seconds, making it fairly rapid (72,73).

Sampling algorithms used for molecular docking, characteristics of the algorithms and the corresponding docking softwares are listed below (Table1).

Table 1. Sampling algorithms, characteristics and softwares for molecular docking (75).

Algorithms	Characteristics	Softwares
Matching algorithms	Geometry-based, suitable to VS and database enrichment for its high speed	DOCK, FLOG, LibDock and SANDOCK
Incremental construction	Fragment-based docking incrementally	DOCK, FlexX, Hammerhead, SLIDE, eHiTS
Monte Carlo	Stochastic search	AutoDock, ICM, QXP, Affinity
Genetic algorithms	Stochastic search	AutoDock, GOLD, DIVALI, DARWIN

2.2 Computational Drug Design

It takes a multidisciplinary effort to create efficient and marketable medications because the drug development process is quite complicated. Finding a molecule that can structurally and chemically fit into a particular region on a protein of interest is the goal of drug discovery and development. This substance becomes a medicine that people can use once it has successfully completed both animal testing and clinical studies on humans. The traditional approaches to medication development involve the secondary inspection of compounds produced in labs or discovered naturally. This approach has issues with a lengthy designing process and high expense. The drug development process has been effectively quickened by modern approaches, such as structure-based drug design, with the aid of informatic resources and computational methodologies (76). A remarkable amount of progress has been accomplished in nearly every area related to drug design and development. A newer version of technology has been created that is simple to use and offers superior computational tools for developing chemically stabilized and effective molecules with refining abilities. These methods can take advantage of cheminformation to accelerate the drug discovery process and reduce costs (77). Traditionally, a nearly blind screening method that was time- and labor-intensive has been the center of the drug creation procedure. Computer-aided drug design (CADD) was born out of a new knowledge of the quantitative link between structural and bioactivity. The expense of development

will be reduced by approximately a 1/3. The design durations are shortened to just 6-8 years from 10-16 years. Also, computer technologies may prevent academic laboratories from following the "unsuitable" leads of molecules to be used as drug target (78).

It is common practice to analyze small therapeutic prospects' characteristics and research drug-receptor combinations in atomic depth using computational chemistry techniques. To organize and manage the massive databases of chemical and biological activity, tools from the statistics and information sciences are becoming highly important. By using tailored structure-based versatile chemistry from the identification of active regions, datasets of derivative molecules are created. A list of the leading probable candidates can be quickly generated by a computer, which can also predict the interaction of all possible variants. Essentially, a computer screens out all ineffective ligands, enabling chemists to concentrate on, produce, and investigate just the top feasible and effective ligands (77,79).

Functions of the computational technologies in drug design can be summarized in four categories. First is archiving and data retrieving. Second is to get statistics on the correlation between structure and toxicity. Third one is to visualize molecules to investigate the similarities or differences and interaction between ligands (drug target) with receptor molecules. Lastly, it is used to estimate motion of molecules and strengths of interactions (79). Ligands are the promising compounds can be used as drug, and they are detecting depending on target protein and binding properties between them. When it comes to investigate protein dynamics, MD simulation is an effective method to detect what properties of molecules are significant and what interactions are in relations with binding activity. To estimate interactions depending on structure of molecule, quick and feasible clustering process based on molecule shape can be done. Also, field-based similarity of a structure is computed. Another implication for investigating interaction based on structure is Flexible Quantitative Structure Activity Relationsips (QSAR) assessment on cluster generated depending on shape of molecules (80).

There are three primary types of programs used in designing drug; scanners, builders, and hybrids. Programs in Scanner category scan the lead molecules and encompass every database search programs. On the other hand, programs in Builders and Hybrids category provides de novo generation of lead molecules. In the database, incomplete compounds are represented by segments or chemical component parts, and weak binding proteins are needed as a spot of connection. By recombination or prodrug from fragments, iteratively introducing small alterations, it generates a pool of derivatives with enhanced receptor compatibility (79,81).

Several examples of softwares, each of which have different properties, commonly used in drug design and development are Affinity, AutoDock comprising AutoGrid, AutoTors, and AutoDoc, Dock, FlexX, GRAMM, HADDOCK (77).

2.3 Antimicrobial Peptides

In past several decades, multidrug-resistant bacteria have been emerging especially where clinical applications are applied, like hospitals. There are several reasons causing this rapid emerging, for instance overuse or improper use of antimicrobial drugs causes bacteria to gain resistance. Resistant bacteria increase nosocomial infections and consequently increase in-hospital morbidity and mortality rates. To overcome this issue, novel, and effective alternatives other than antibiotics are needed to be developed. In this regard, antimicrobial peptides (AMPs) have become very popular option as therapeutic agents such that 36 antimicrobial peptides have undergone preclinical and clinical phase and almost 10,000 papers on AMPs have been published up to 2019 (1). Even though discovered AMPs number reached to around 3000, most of them not convenient to be used as therapeutics or drugs. Only Seven of them have been approved by the US Food and Drug Administration (FDA), they were discovered in Gram-positive soil bacteria (82). These approved small peptides (AMPs) are gramicidin D, daptomycin, vancomycin, oritavancin, dalbavancin and telavancin (83).

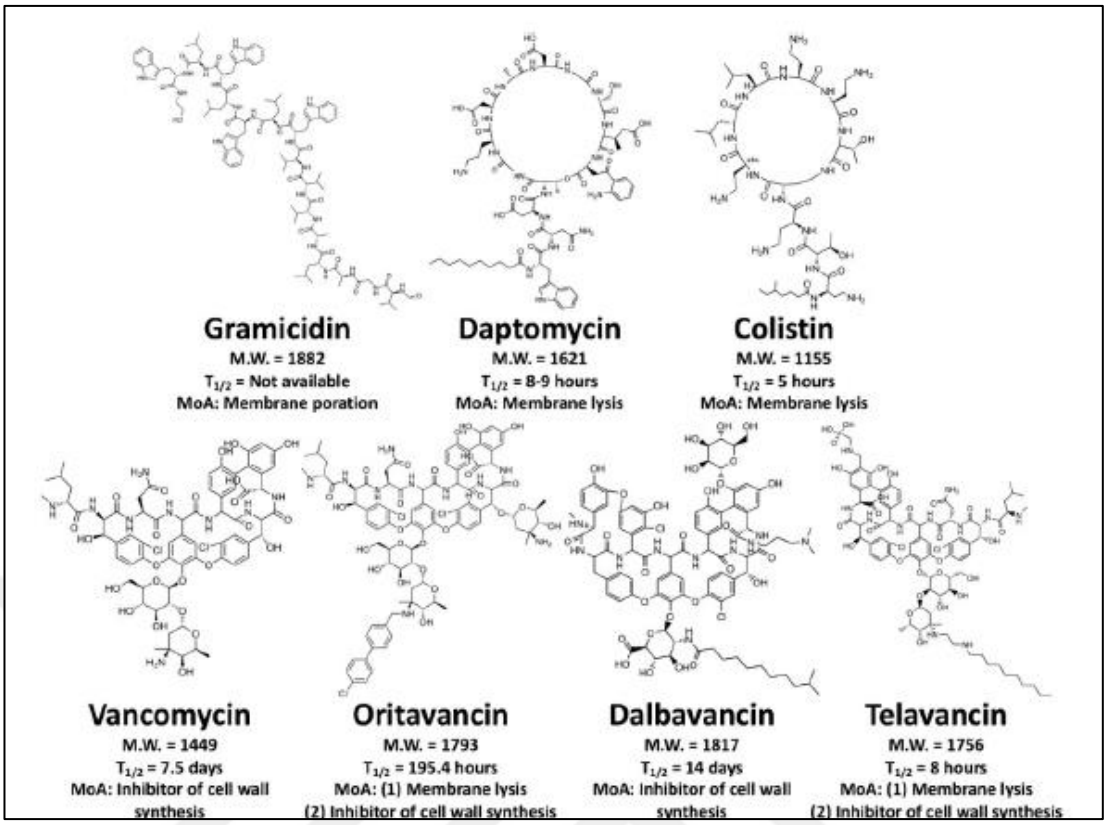

Figure 2. Chemical Structures of seven FDA-approved AMPs (82).

Oritavancin, dalbavancin and telavancin are small lipoglycopeptide that are the derivatives of vancomycin. They are effective against vancomycin-resistant bacteria by inhibiting cell wall formation. Oritavancin and telavancin can also affect membrane permeability and detach cell membrane.

2.3.1 Constituent of the AMPs

Average length of the AMPs is in 10aa – 50aa long range. Average hydrophobic content of peptides is 54%. And the mean peptide net charge is +3. They are generally stated as small cationic hydrophobic peptides thereby they target and disrupt anionic bacterial cell membranes using electrostatic interactions (84).

2.3.2 Mechanisms of action of the peptides:

AMPs or not AMPs, some small peptides functions as therapeutics characterized in receptor-binding peptides which activate or block the specific receptor and cause biological response. Other than that, some peptides functions as inhibitors of biological peptides, some as membrane active peptides (MAPs) and some have other functions (85).

Antimicrobial agents can be categorized based on the antimicrobial activity mechanisms:

- Agents that inhibit cell wall synthesis (vancomycin, oritavancin, dalbavancin and telavancin)
- Depolarize the cell membrane, (membrane active peptides, MAPs)
- Inhibit protein synthesis,
- Inhibit nucleic acid synthesis
- Inhibit metabolic pathways in bacteria, (receptor binding peptides, e.g. cathelicidin and human B defensins)

Table 2. Antimicrobial groups based on mechanism of action [modified according to Reygaert WC. 2018 (86) via Microsoft Word]

Mechanism of Action	Antimicrobial Groups
Inhibit Cell Wall Synthesis	β-Lactams Carbapenems Cephalosporins Monobactams Penicillins Glycopeptides
Depolarize Cell Membrane	Lipopeptides
Inhibit Protein Synthesis	Bind to 30S Ribosomal Subunit Aminoglycosides Tetracyclines Bind to 50S Ribosomal Subunit Chloramphenicol Lincosamides Macrolides Oxazolidinones Streptogramins

Table 2. Antimicrobial groups based on mechanism of action [modified according to Reygaert WC. 2018 (86) via Microsoft Word] (continued)

Mechanism of Action	Antimicrobial Groups
Inhibit Nucleic Acid Synthesis	Quinolones Fluoroquinolones
Inhibit Metabolic Pathways	Sulfonamides Trimethoprim

2.3.3 Resistance mechanisms

To develope effecitive AMPs, we should first look at the resistance mechanisms of bacteria.

The four major groups of antimicrobial resistance mechanisms are as follows (85):

1) restricting a drug's absorption
2) adjusting a target of drug
3) drug inactivation
4) active drug outflow.

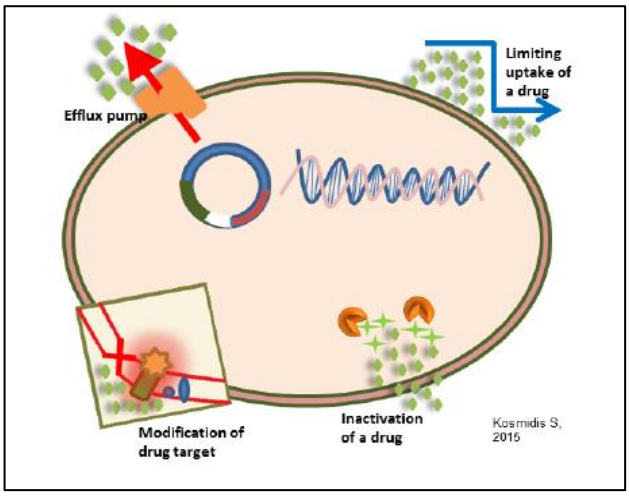

Figure 3. Demonstration of resistance mechanisms of antimicrobials (86).

Levels of resistance may differentiate among the bacterial groups. Susceptibility and resistance are usually measured as a function of inhibitory concentration (MIC)

which is the lowest concentration of an antimicrobials that will inhibit the growth of bacteria.

Resistance mechanisms can be either native or acquired from other organisms.

Natural Resistance may be intrinsic(trait) or induced (naturally present gene in the bacteria but only expressed in resistance levels when exposed to an antibiotic). The most common bacterial mechanisms functioning in intrinsic resistance are reduced permeability of the outer membrane consisting specifically the lipopolysaccharide, LPS, in gram (-) bacteria.

Acquired Resistance's main routes are mutation on chromosomal DNA of the microorganism and Horizontal Gene Transfer (HGT). This process mainly is to gain genetic material by transformation, transposition, and conjugation. One example of the resistance through mutation is *Staphylococcus aureus* gaining resistance to methicillin.

Intrinsic resistance may use limiting uptake, drug inactivation, and drug efflux while acquired resistance mechanisms used may be drug target modification, drug inactivation, and drug efflux. Another crucial resistance mechanism is the biofilm formation.

2.3.4 Biofilm

Biofilm formation is generated along with the bacterial colonization. Microorganism aggregates and attached a surface and surrounded by an extracellular polymer substance (EPS) consisting of polysaccharides, extracellular DNA, proteins, lipids and water makes the biofilm formation. It is actually an adaptation process of bacteria to environmental stress factors for instance antibiotics, host immune system, starvation etc. Bacterial cell in the biofilm prone to have slow metabolism rate and slow cell division so that antimicrobials targeting cell division and growing remain ineffective. Biofilm entity protects its organism from antimicrobial agents and makes it resistant.

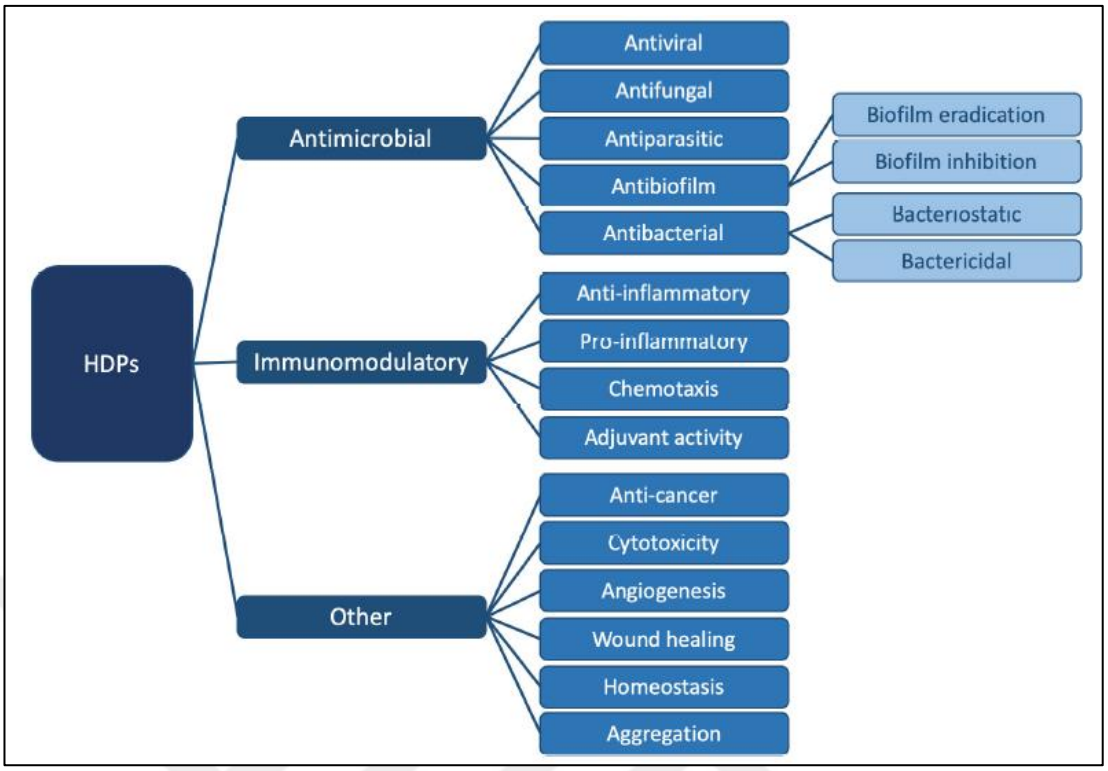

Figure 4. HDPs' known functions' demonstration highlighting antibacterial and antibiofilm functions in particular (83).

In this figure, how different type of functions that AMPs have is demonstrated.

Antimicrobial peptides functions not only as antimicrobials, but they also function as antibiofilm agents, immune modulators, anti-cancer agents and anti-inflammatories. Moreover, they are active against bacteria and pathogens like viruses, fungi and parasites. To emphasize the versatile property of the AMPs, the term of "Host Defense Peptide" have been using.

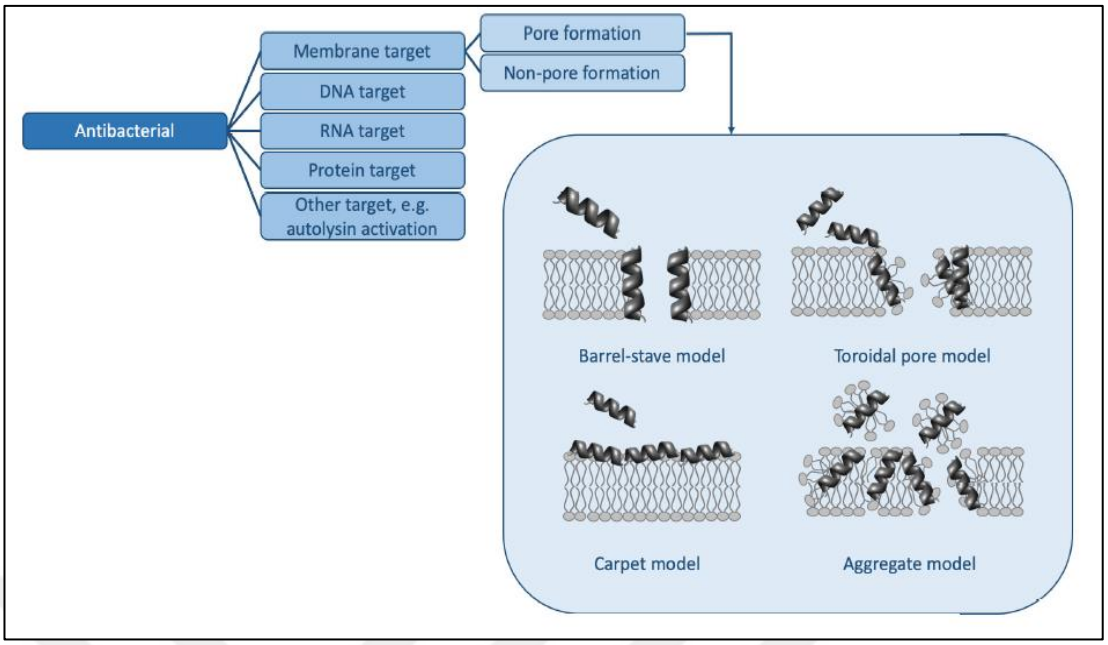

Figure 5. Mechanisms of action for antibacterial HDPs. The pore forming mechanisms demonstrated (83).

AMPs having Antibacterial functions can target membrane, DNA, RNA, protein etc. Commonly seen mode of action of AMPs in membrane penetration is to generate pore formation. Membrane pore-forming AMPs constitute a large subgroup of MAPs (membrane active peptides). These peptides bind to cell membranes and spontaneously assemble in the lipid bilayer as a channel or pore-like structure, though not all are cytolytic. Well-known natural examples are gramicidin, colistin, melittin, maculatin, and alamethicin (82,85).

The two common models for the channel structures are barrel-stave and toroidal, depending on how the peptide interacts with the lipid headgroups.

Membrane-lytic peptides, daptomycin, colistin, LL-37, aurein and piscidin 1 disrupt cell membranes, like detergents. This destruction causes the internal contents of the bacteria to leak out and lowers the membrane potential of the bacterium. As a result, AMPs damage membranes by drastically enhancing their permeability and

weakening the regulated barrier, which is one of the plasma membrane's most essential role (84).

Membrane-active peptides, whose action is restricted to specific cell membranes, are not well-defined, in contrast to receptor-binding peptides or peptide inhibitors that have clearly characterized binding sites. Although precise processes have not yet been identified, their hydrophobic moment and electrostatic interactions typically contribute to their uniqueness. These characteristics rely on the membrane-active peptides' preference for a particular bacterial species (83,84).

Bacterial membranes typically include more negatively charged particles. The benefit of using membrane-active peptides for antibiotics is that there may be a reduced risk of drug resistance in bacteria. AMPs may therefore be likely candidates for utilization as drug delivery vectors and as new antibiotics (87).

2.3.5 Design with molecular modelling approach

AMPs can be developed in 2 ways;

1) Discovering new peptides from natural origin (from extracted predicted antimicrobial sequences from larger and more complex proteins, organisms, tissue samples, and other sources.)
2) Making synthetic variants along with the optimization processes of the antibacterial activity (88).

2.3.5.1 Designing AMPs

Controlling the selectivity, reducing the toxicity, and lowering unexpected side effects are essential to the design of synthetic AMPs. Thus, AMPs are needed to be optimized properly during developing process. Basic steps of optimization are;

(I) Extending the elimination half-lives of peptides by stabilizing their structures and adding non-canonical amino acids to the peptide sequences.

(II) Determining the biochemical characteristics that make antimicrobial substances produced by Gram-positive bacteria in soil appropriate for human use.

(III) Identifying AMPs that have the capacity to affect the immune system.

(IV) Investigating the potential for AMPs to work in combination with other chemicals or enzymes to improve antibacterial action.

(V) Optimizing the development of computational techniques for high throughput screening and peptide therapeutics.

(VI) Providing suitable in vitro models that imitate in vivo environments to assess the allergic effects (88,89).

Computer aided studies has gained significant interest in the past decade. Now, in almost every study, several parts of the experiment are carried out by computer-based techniques which enable studies to be more cost effective and time effective. Also, such computational techniques allow to analyze large amount of data simultaneously (88).

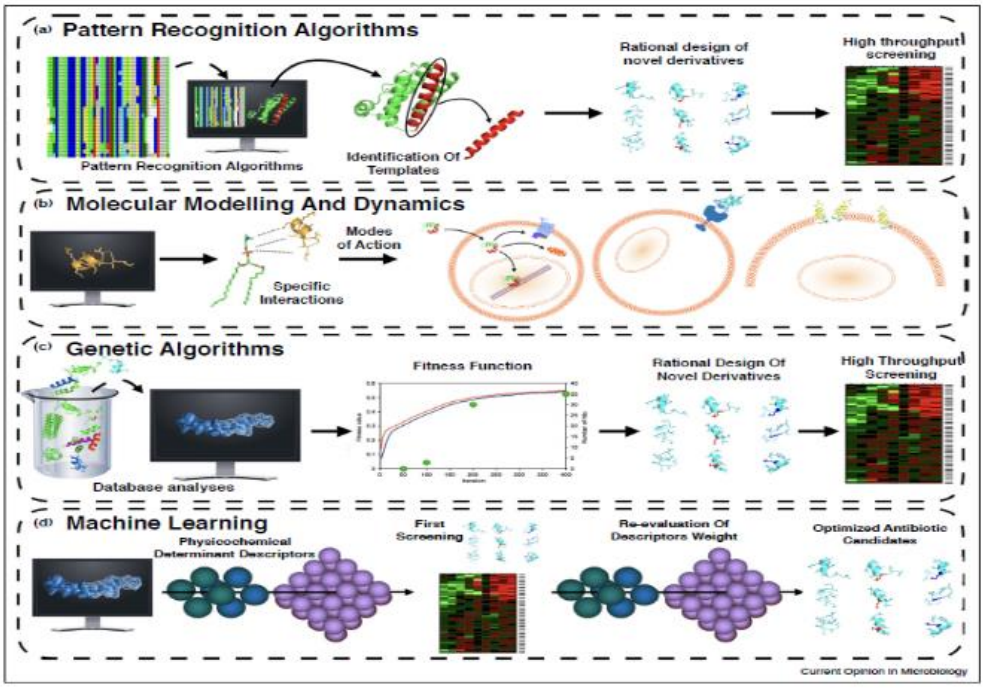

Figure 6. Computational design principles for designing antimicrobial agents (90).

To discover, design, and optimize AMPs, many computational techniques are being applied with the processes represented in Figure 6;

1) Pattern recognition algorithms: used to discover bioactive templates that are encoded into natural biomolecules by comparing them to known bioactive molecules. This tool enables to template based rational design of novel compounds (91).
2) Molecular modelling and Dynamicss: used to analyze structure-activity relationship of the compounds and to investigate mode of action and specific interactions of AMPs (89).
3) Genetic Algorithms: to generate antimicrobial candidates from database using physicochemical properties ranked in a fitness function. Fitness function classifies the novel molecules generated and makes them undergo high-throughput screening.
4) Machine Learning and deep learning: use statistical techniques to make the computer system to be able to learn and improve their performance as far as generating bioactive compounds from physicochemical and biological activity data (88,91).

2.4 Polymers

Any member of the family of natural or manufactured materials known as polymers is made up of very big molecules, or macromolecules, which are combinations of smaller chemical compounds, or monomers. Nearly every aspect of everyday life involves polymer materials in some sort. Rubber tires, foam insulation and cushions, high-performance athletic footwear, clothing, and materials are only a few examples where polymers are the key constituents (92). Polymers also are essential to many new technologies. Examples include "plastic electronics", gene treatment, electric vehicles, and fuel cells etc. A qualified chemist, materials researchers, or chemical engineer must, in short, have a decent understanding of the characteristics of molecular chains and how they contribute to the several favorable characteristics of materials including polymers. Including all living things, human

body too based on polymer backbones such as proteins, nucleic acids, and carbohydrates (93).

Because of versatility of polymers, they are studied in many fields of science such as chemistry, physics, biophysics, molecular biology, biochemistry, material sciences and engineering.

Polymers synthesized by living organisms are named natural polymers or biopolymers while artificially designed and synthesized types of polymers are named synthetic polymers. Polymer synthesizing process is called polymerization that is mainly connecting monomers to form covalent bonding or network. Synthetic polymerization processes mainly fall in to two different concept, chain polymerization and step-growth polymerization (4).

Synthetically designed polymers have been attracting interest for drug designing studies over the years. They are important alternatives for the pharmaceutical industry, as they are versatile, easy to produce, and suitable for designing in accordance with the desired properties. One example of widely use polymer alternatives for studies on drug design and developments are antimicrobial polymers. The utilization of polymers as antimicrobial agents offers a number of benefits because these substances often display long-term efficacy and no residual toxic effects, are chemically inert, non-volatile, and do not penetrate the skin. Three groups of antibacterial polymers can be distinguished depending on the kind of polymeric system. Biocidal polymers, which have inherent antimicrobial effect, are one example. In addition, there are biocide-releasing polymers, that are made up of polymers packed with biocide molecules. Lastly, polymeric biocides are constructed on polymeric backbones with biocidal molecules appended (2–4).

3 MATERIALS AND METHODS

This thesis study comprises of three different project sets. Molecular modelling investigation of the first study with the TÜBİTAK projet number 118Z859, of the second study with the TÜBİTAK projet number 217Z155, and of the third study with the TÜBİTAK projet number 217S060 are explained under the heading 3.1, the heading 3.2 and the heading 3.3, respectively. Focus of the experiments for every three study is to analyze interactions of artificially designed antimicrobial peptides with bacterial-similar membranes and with each other; interactions of artificially designed polymers inspired by antimicrobial peptides with again bacterial-similar membranes and with each other by performing molecular modelling experiments. Detailed information is explained under separate headings for each study.

3.1 Molecular Modelling Experiments on Catelicidin-Like Antimicrobial Peptides and Their Interactions with POPE Membrane

In this study (project number: 118Z859), the conserved sequence of human catelicidins, which also exhibit high similarity with catelicidins of many other livings in nature, served as the basis for the general structure of the catelicidin-like peptides created in this study. Catelicidins' amino acid sequences were retrieved from NCBI. An LL-37 antimicrobial peptide sample was taken from the catelicidin group. This peptide consists of a 19.3 kDa and 18 aa precursor sequence, except for the signal sequence (94). The helix structure gives this peptide antimicrobial properties. Antimicrobial peptides are hydrophobic and positively charged (95). Based on the properties mentioned above, 10-20 amino acid long peptides were designed in both L-form and D-form. Sequences and the properties of the designed peptides in the scope of preliminary study are given in Table 3 (101).

Table 3. Characteristics of designed catelicidin-like peptides.

Peptide Sequence		Amino-acid Content	Hydrophobicity	Net Charge	pI Value	Molecular Weight (g/mol)
P1	RLLLRLLRRLLRLLLR-NH2	D-leucine, L-arginine	62.5%	+7	13.2	2085.75
P2	RLLLRLLRRLLRLLLR-NH2	L-leucine, L-arginine	62.5%	+7	13.2	2085.75
P3	RLLLRLLRRLLRLLLR-NH2	L-leucine, D-arginine	62.5%	+7	13.2	2085.75
P4	RLLLRLLRRLLRLLLR-NH2	D-leucine, D-arginine	62.5%	+7	13.2	2085.75

3.1.1 Molecular modelling

With the molecular modelling and computational method, bilayer lipid membrane with designed peptides system solvated in water were simulated to test antimicrobial property of the peptides based on peptide-membrane interaction. In parallel and consistent with the experimental research required for the peptide design, the results were visualized and analyzed. this sets of study consists of three different sections.

Section 1:

- Molecular dynamics simulations of four designed peptides all in L-form with short (2 ns) simulation duration.
- Molecular dynamics simulations of randomly selected peptides having "model 4" sequence in both D- and L-forms with different combinations (P2 and P4) for relatively long (50 ns) simulations duration. Peptide models are shown in Table 4.

Table 4. Peptide models used in molecular dynamics simulations.

Simulation Duration				
Short			**Long**	
Model No	Aminoacid Sequence	Aminoacid Form	Peptide Code	Aminoacid Form
Model 1	RLKLLLKLLR	L form		
Model 2	RLLRLLLRRLLLRLLR	L form		
Model 3	RLLLRLLRRLLLRLLR	L form L form		
Model 4	RLLLRLLRRLLRLLLR	---	P2 P4	L Form D form

Section 2:

Within the scope of the study, modified peptides were obtained by adding cysteine amino acids to the amide and carboxyl ends of 4 previously designed peptides.

C-P1 and P1-C peptides were designed by adding cysteine amino acids separately to the amide and carboxyl ends of the Model 4-P1 peptide, which has the best biological activity results among the peptides terminated with arginine amino acid. The C-P1 peptide contains the amino acid cysteine at the amide end, and the P1-C peptide at the carboxyl end. Peptides were synthesized as amide-terminated again.

Table 5. Modified peptides and their properties.

	Peptide Sequence	**Amino acid content**	**Hydro-phobicity**	**Net Charge**	**pI Value**	**Molecular Weight (g/mol)**
C-P1	CRLLLRLLRRLLRLLL R-NH2	D-leucine L-arginine	58.82%	+7	13.2	2188.90
P1-C	RLLLRLLRRLLRLLLR C-NH2	D-leucine L-arginine	58.82%	+7	13.2	2188.90

Section 3:

A 100 ns molecular dynamics simulation was performed for this section of the study by positioning the C-P1 peptide formed by adding cystine to the carboxyl end of the P1 sequence peptide in mixed D and L (D-leucine and L-arginine) form, positioned on the POPE (1-palmitoyl-2-oleoyl-sn-glycero-3-phosphoethanolamin) membrane in the same way with the previous peptide-membrane system.

3.1.1.1 Structure Prediction

Section 1:

The 3D structures of the designed peptides were estimated using a de novo called PEP-FOLD3 (96,97). PEP-FOLD3 can estimate only 3D structure of L-form amino acid sequences. On the other hand, D and L forms share mirror images of their structures, therefore D-form amino acids can be obtained by only changing the direction of side chains (R-groups) without changing the locations of the amino acids placed in α-helices.

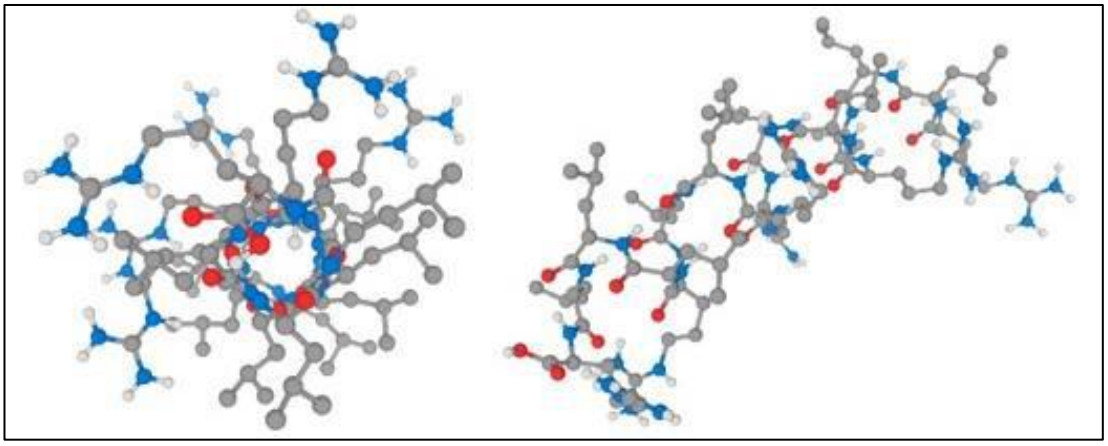

Figure 7. P2 Peptide containing L-leucine and L-arginine in 3D format obtained by PEP-FOLD3.

Section 2:

The errors encountered in the peptides with mixed D and L amino acid forms used in the first section were eliminated, and 3D structures were created by PEP-FOLD3 server for the sequence of the model4-P1 peptide with amino acid forms in the D and L mixed (arginines L and leucines D) forms.

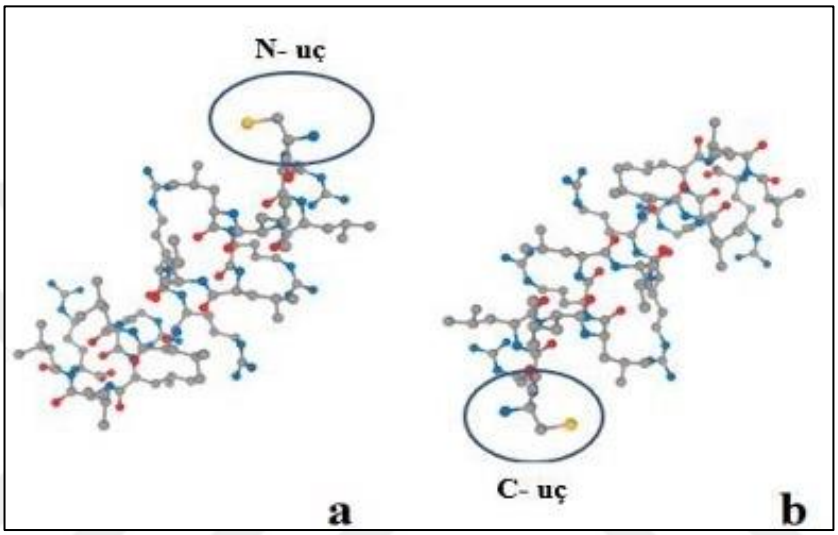

Figure 8. 3D structures of a) C-P1 and b) P1-C by using PEP-FOLD3.

Section 3:

The leucine amino acids in the L form of the C-P1 peptide, whose 3D predictive structure was created with the PEP-FOLD3 server, should be converted to the D form. The conversion from the L form to the D form was performed with plug-in tool in the Discovery Studio 2021 Client software(98), and the final form of the C-P1 peptide was obtained.

3.1.2 Molecular dynamics simulation

Section 1:

For short simulations (2 ns), all L-form peptides with different sequences which are model 1, model 2, model3, and model 4 (P2), were placed on top of the membrane bilayer, then the system was solvated in water.

Also, D-form of model 4 (P4) were simulated with the same kind of peptide-membrane-water system for 2ns long simulation.

For long simulations (50 ns), L-form of model 4 (P2) and D-form of model 4 (P4) were used in the peptide-membrane-water system.

Section 2:

In the previous simulations carried out in section 1 of the study without making the necessary parameterizations, the error has been occurred that amino acids break and disperse in water. New definitions in the bond parameter files were made to ensure that the peptides did not break, and molecular dynamicss simulations of 46 ns were performed.

Section 3:

The peptide (in mixed form D and L) with Model 4 sequences was placed on the POPE membrane surface in the water phase on the C-P1 membrane as 4 identical pieces at a certain distance. A 100 ns long simulation of the peptide-membrane system created was run.

3.1.2.1 System preparation for simulation

Section 1:

3D structure of the model peptides in L-forms were generated by PEP-FOLD3 web server (66,67). CHARMM27 force field parameters were used to run simulations on NAMD 2.11 software (99). To observe the orientation or attachment of the peptides to both each other and to the membrane, 4 identical peptide molecules for every peptide model were positioned with a distance of approximately 10 Å (Angstrom) between them and the distance of the peptides to the bacterial membrane. POPE (phosphatidylethanolamine bilayers) membrane was selected to mimic bacterial membrane. Placing the peptide molecules on the POPE membrane at a certain distance was done using VMD software (100).

Though 3D structure of L-form amino acid sequences can be predicted by PEP-FOLD3, it is unable to generate D-form amino acid structures. Therefore, to generate 3D structure of model 4 peptide (P4) in D-form, a script was written based on the coordinates of alpha helix structure of the model 4 in L-form. Since D-form peptides are identical to L-forms in all respects except for their chirality, the parameters of D-amino acids are nearly the same as their L-structured counterparts. For this reason, molecular dynamicss models were performed based on CHARMM27 force field parameters, as in other peptides. The only difference between the two molecules is the reverse chirality of the methyl side chain and the HA atom at the CA or alpha-carbon atom. For this reason, a new topology file was prepared for the D-form by changing the L-chiral center in the CA atom in the existing topology file for the L-form of the amino acids used and the NAMD 2.11 software was run in parallel, and molecular dynamicss simulations were performed for the peptides designed in the D form.

Section 2:

3D structure of the P1 peptides containing the D and L mixed (arginines L and leucines D) forms were generated by PEP-FOLD3 web server (66,67). CHARMM27

force field parameters were used to run simulations on NAMD 2.11 software (99). Unlike previous peptide simulations, the P1 peptide is positioned at a distance of more than 10 Å from the membrane and each other, as it focuses on eliminating the problem in its parameterization. Placing the peptide molecules on the POPE membrane at a certain distance was done using VMD software (100).

Since PEP-FOLD3 is unable to generate D-forms of amino acid sequences, D-form sequences of P1 peptide were generated based on the same principles mentioned previous section of the study.

Section 3:

The leucine amino acids in the L form of the C-P1 peptide, whose 3D predictive structure was created with the PEP-FOLD3 server, should be converted to the D form. The conversion from the L form to the D form was performed with plug-in tool in the Discovery Studio 2021 Client software(98), and the final form of the C-P1 peptide was obtained.

3D structure of the L form of the C-P1 peptide was generated the PEP-FOLD3 server. Conversion of the leucine amino acids in the L form of the C-P1 peptide was made by plug-in tool in the Discovery Studio 2021 Client software(98), and the final form of the C-P1 peptide was obtained.

Since these D-form molecules are identical in all respects except their chirality, the parameters of D-amino acids are the same as their L-structured counterparts, except for a few different parameters. For this reason, molecular dynamicss models were performed using force field parameters CHARMM27 and CHARMM36 (for both D and L forms) as for other peptides. Molecular dynamicss simulations were performed for the C-P1 peptide designed in mixed form D and L by running NAMD 2.11 software.

3.1.2.2 Steps of molecular dynamics simulation

Section 1:

Minimization: Because the system was put together artificially by VMD membrane plugin, it most likely has many unnatural atomistic positions, which will lead to simulation run to fail due to high velocity movement of the atoms. Thus, minimization run was held for 2 ps timesteps to bring the system to local energy minimum level.

Melting lipid tails: Minimization step was followed by a simulation for 0.5 ns where all the atoms – water, ions, proteins, and lipid headgroups- were fixed except the lipid tails. Since the system has not been equilibrated due to membrane plugin, fixation simulation provides the proper instability.

Minimization and equilibration with protein constrained: Again, a minimization run for 2 ps timesteps and 0.5 ns timesteps simulation, where the water molecules were constrained and the lipids were released, were performed. To do so, it is aimed to be proteins (peptides) surrounded by lipids without interruption of water molecules.

Equilibration with protein released: Later, 0,5 ns timesteps long equilibration run were applied where the whole system was released for further equilibration.

Production run: Finally, the production run was performed since the proteins were equilibrated properly and system was ready.

Short production runs were arranged to take 2 ns timesteps.

Long production runs were arranged to take ~50 ns timesteps.

Outputs of the simulations were visualized and analyzed by using VMD software.

Section 2:

The simulation steps that were performed for MD simulation in section 1, were conducted for section 2, too, except for the simulation duration which is 46ns=~50ns in this section.

Section 3:

Melting lipid tails: Minimization step was followed by a simulation for 0.5 ns where all the atoms – water, ions, proteins, and lipid headgroups- were fixed except the lipid tails. Since the system has not been equilibrated due to membrane plugin, fixation simulation provides the proper instability.

Minimization and equilibration with protein constrained: A minimization run for 0.5 ns timesteps and 0.5 ns timesteps simulation, where the water molecules were constrained and the lipids were released, were performed. To do so, it is aimed to be proteins (peptides) surrounded by lipids without interruption of water molecules.

Equilibration with protein released: Later, 0,5 ns timesteps long equilibration run were applied where the whole system was released for further equilibration.

Production run: Finally, the production run was performed since the proteins were equilibrated properly and system was ready.

The duration of simulation performed for the C-P1 peptide is 100 ns.

Outputs of the simulations were visualized and analyzed by using VMD software.

3.2 Molecular Modelling of Polymer Composed of Mannose-Binding Lectin Protein with POPE Membrane and with Red Blood Cell Membrane-Similar 3D-Membrane

In the second sets of study of this thesis (project number: 217Z155), within the scope of Molecular Modelling studies, it is planned to create model membrane structures belonging to certain species and simulate with synthetically designed polymers (Triphenylphosphonium:mannose 5:2) inspired by antimicrobial peptides designed earlier (101) and a reference peptide (magainin) found in nature.

In this context, besides only the model formed from POPE (1-palmitoyl-2-oleoyl-sn-glycero-3-phosphoethanolamine) and POPG (1-palmitoyl-2-oleoyl-sn-glycero-3-phosphoglycerol) lipids of E. coli, there is also a more complex Top6 membrane model structure consisting of the 6 main lipid species most abundant in E. coli (102).

3.2.1 Molecular modelling

With the molecular modelling and computational method, membrane bilayer that are designed to mimic different natural membranes (bacterial membrane and red blood cell membrane) with designed polymer systems solvated in water were simulated. The results were visualized and analyzed. This sets of study consists of four different sections. In the first section, only the simulation box of Top6 similar membrane were generated and visualized in simulation box. Second section of the study aims to investigate Triphenylphosphonium:Mannose 5:2 polymer's activity on POPE membrane by performing molecular dynamics simulation. Third section is not much different from the section 2, except the simulation duration and property of P atom. Finally, in the fourth section, activity of the Triphenylphosphonium:Mannose 5:2 polymer on red blood cell membrane was investigated.

Section 1:

In the first section of this study, top6 membrane model was created, and also, parameter sets of the antimicrobial similar polymers were generated for further examination of the membrane-polymer activation by molecular dynamics simulation processes. Furthermore, a simulation box made up of model membrane and water were generated.

In order to provide better understanding, antimicrobial peptides which are inspiration of the polymer in this study (101) and magainin protein (reference peptide found in nature) were 3D modeled and compared.

Section 2:

The bilayer lipid membrane (POPE) systems of the polymers designed in the modelling studies of the second part of this project, including water and ion, are also modeled. In molecular modelling studies, firstly, one of the designed polymers, Trifenilphosphosfonium:Mannose 5:2' molecular dynamics simulation and docking methods were performed.

Section 3:

In this section of the study, MD simulation duration of the Triphenylphosphonium:Mannose 5:2 polymer – POPE membrane extended to 200 ns from 100 ns to understand whether the polymer creates a suitable environment for water passage in the membrane. Sama as the previous section, simulation was run twice for each P charge value.

Section 4:

In this part of the project, the Triphenylphosphonium:Mannose 5:2 polymer designed and the bilayer lipid membrane systems containing water and ions were modeled. Firstly, the designed mannose-lectin polymer was simulated with a 3D-formed red blood cell membrane, and then the mannose-lectin and galactose-lectin interactions were examined by docking.

3.2.1.1 Structure prediction

Section 1:

3D structure of peptides proven to have antimicrobial effects using Discovery Studio 2019 software (98); The interpolated charge is visualized according to hydrogen bonds, hydrophobicity, ionizability, and atomic charge. Synthetic polymers synthesized in this study, which are expected to have antimicrobial effects, are visualized, and compared similarly according to the surface distribution of their different properties, as in Table 6.

Table 6. Comparison of the 3D structures of the TN1 peptide, which was designed and modeled and published in the preliminary study of this project, and the reference natural magainin peptide according to different feature distributions (101).

Representation	TN1*	Magainin PDB ID: 2LSA
CPK	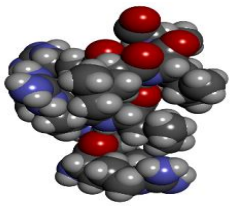	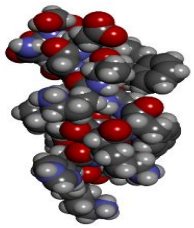
Interpolated Charge 0,100 0,067 0,033 0,000 -0,033 -0,067 -0,100	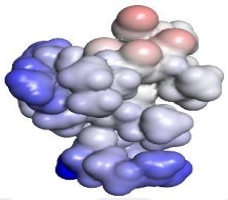	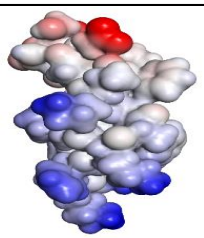
H-Bonds Donor Acceptor	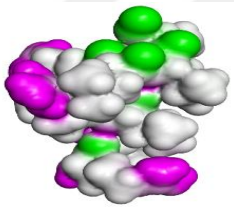	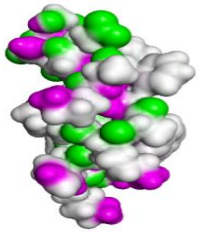
Hydrophobicity 3,00 2,00 1,00 0,00 -1,00 -2,00 -3,00	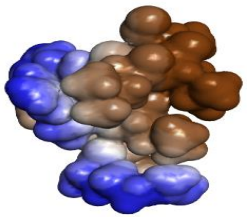	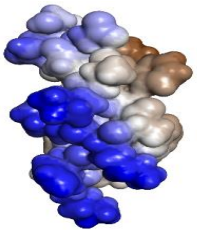
Ionizability Basic Acidic	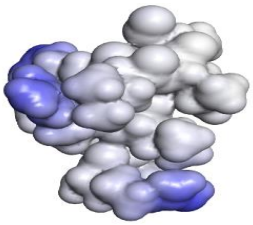	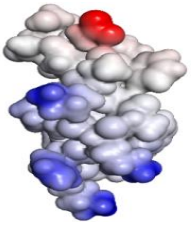
Atom Charge 0,70 0,47 0,23 0,00 -0,23 -0,47 -0,70	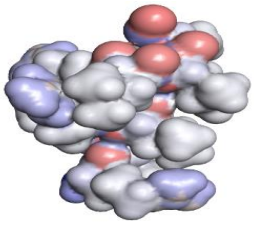	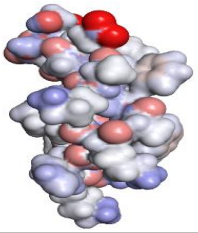

3.2.2 Molecular dynamics simulation

Section 1:

To perform molecular dynamicss simulations and obtain an equilibrated system, Model membrane mimicking the Top6 membrane was generated by using web-based interface, then simulation box with model membrane was visualized. It is aimed to examine the specific interactions by choosing a membrane model specific to the microorganism as the membrane.

Section 2:

MD simulations of Trifenilphosphosfonium:Mannose 5:2 polymer – POPE membrane system were performed twice with different settings; first simulation was set for 100 ns and P atoms' charge in the polymer was set for -0,15095. Second simulation was set for 60 ns and charge of the P atoms in the polymer was given +1.

Section 3:

MD simulations of Trifenilphosphosfonium:Mannose 5:2 polymer – POPE membrane system were performed twice with different settings; first simulation was set for 200 ns and P atoms' charge in the polymer was set for -0,15095. Second simulation was set again for 200 ns and charge of the P atoms in the polymer was given +1.

Section 4:

Trifenilphosphosfonium:Mannose 5:2 polymer – red blood cell membrane system simulation was run with 100 ns simulation duration with 50,000,000 timesteps and 50,000 frames. P charge parameter was set as +1.

3.2.2.1 System preparation for simulation

Section 1:

According to the Top6 structure, a membrane model system simulation box consisting of a total of 42492 atoms, containing the lipid bilayer, water, and ions, was created using the membrane making graphical user interface of CHARMM (103). The simulation box created for this model membrane system was visualized using VMD software.

In order to carry out the molecular dynamics simulation of the designed polymers, it is also necessary to create the parameter files of these new polymers. At this stage, while the parameter sets of the monomers that make up the polymers were created, quantum simulations were made for the atom groups whose parameters are not available in the existing libraries by using the Force Field Toolkit (ffTK), which is an add-on in the VMD software package (104).

In order to run MD simulations, firstly, the 3-dimensional structure files containing each atomic coordinate of the components in the system to be modeled and the force field parameter files used to calculate the interaction forces must be obtained. After these files are obtained in different ways for each component and combined in accordance with the format to be used, they are modeled with a run file in which variables such as temperature, pressure, box size components are also controlled depending on which ensemble (NPT, NVT, etc.) to be modeled. The preparation process of the input files mentioned here varies according to each system and the content of the modelling to be done.

Section 2:

In order to run MD simulations, firstly, 3-dimensional structure files containing each atomic coordinate of the components in the system to be modeled were obtained.

The CACTUS server of the National Cancer Institute (NHI-NCI) in the USA was used for the 3D structures of the newly designed polymers (105).

The force field parameter files used to calculate the interaction forces were obtained. The parameter files of these new polymers were obtained separately for each monomer, and the structure and parameter input file of the whole polymer were created by combining these monomers using VMD commands. While the parameter sets of oxanorbornene monomer part presenting in all monomer types that make up the polymers were created, quantum simulations were made for the atom groups whose parameters are not available in the existing libraries by using the Force Field Toolkit (ffTK), which is an add-on in the VMD software package (104). As a result, CHARMM-compatible force parameter sets were obtained with potential energy surface (PES) scans (106). In the quantum calculations here, this toolkit used 6-31G* as the standard (default) base set and MP2 as the theory method. TRUBA computational resources are used for the Gaussian software required for these quantum calculations (107).

The necessary parameters for the mannose portion of monomer were obtained from the CHARMM force field libraries. For Triphenylphosphonium, first of all, the structure files of the structure with the ID number 59474155 were downloaded from the Zinc database, and a psf template was created with the Molfacture tool of VMD and modified on this template. The first simulation was performed with the parameter sets of the Triphenylphosphonium cation used in the article published by Firaha et al. in 2017 (108).

In the first simulation, the electronic charge on the P atom is set to -0.15095. Then, a second simulation was made by changing the charge on the P atom to +1 within these parameter sets.

After obtaining the parameter sets required for the polymers in both simulations, molecular dynamicss (MD) models were made by combining these polymers with the membrane system that we created at first, including water and ions. The double-layer

model POPE membrane system, which is generally used for bacteria, was created with water on both sides. Designed Triphenylphosphonium:Mannose 5:2 polymer molecules were located diagonally in the water layer on the bacterial membrane with a distance of 12.5 Å. For these MD simulations, the NAMD software was run in parallel on a workstation with high performance computing capacity.

Section 3:

Exact same polymer-membrane system used in Section 2 was used in this section, too. Only difference is the duration of the simulation which was increased to 200 ns.

Section 4:

Arrangements of the previously designed polymer were made using VMD software, and CHARMM 27 and CHARMM 36 force-field libraries were used for simulation (103). The double-layer membrane surface in the structure of the red blood cell membrane, on which the polymer will be positioned, was created with the CHARMM-GUI membrane creation tool, which is a web-based graphical interface (109–111). The component ratios of the designed membrane were created by considering the literature (112). Accordingly, for both the inner and outer lipid layer, 50% 1,2-Dimyristoyl-sn-glycero-3-phosphocholine (DMPC) and 50% 1,2-Dipalmitoyl-rac-glycero-3-phosphocholine (DPPC) lipids were used. The water thickness on the membrane surfaces is 15 Å and the X and Y axis widths are set as 75 Å.

The positioning of the polymer on the membrane was done using the VMD program, and a distance of approximately 15 Å was left between the polymer and the membrane lipid surface. After the positioning process, the water molecules on the membrane surfaces were removed.

In the last stage of the whole system, before the molecular dynamicss stage, the membrane-polymer system was placed in the water box using the "Solvation Box" tool

located in the VMD interface. In this process, the boundaries of the water box are determined in accordance with the dimensions of the system.

3.2.2.2 Steps of molecular dynamics simulation

Section 2:

Melting lipid tails: Since the lipid system provided by the membrane plug-in of the VMD is not in equilibrium, a simulation was first performed in which everything (water, ions, polymer, lipid headgroups) was fixed except the lipid tails. After this simulation lasting 0.5 ns, the lipid ends became irregular.

Minimization and equilibration with protein constrained: Since we have put the system together artificially in the computer environment, there are many unnatural atom positions which do not have minimum energy and maximum entropy, that is, prevent the system from being stable. For this reason, a minimization simulation lasting 0.5 ns was performed to bring the system to its minimum local energy before operating it with full dynamicss.

Equilibration with protein released: Later, 0,5 ns lasting equilibration run were applied where the whole system was released with constrained polymers for further equilibration.

Production run: Finally, the production run was performed since the polymers were equilibrated properly and system was ready.

Outputs of the simulations were visualized and analyzed by using VMD software.

First simulations of Trifenilphosphosfonium:Mannose 5:2 polymer – POPE membrane system with charge of P atoms as -0,15095 lasted 100 ns.

Second simulation of the same system lasted 60 ns and charge of the P atoms in the polymer set to +1.

Section 3:

Exact same steps applied in Section 2 were followed for this section, except for the simulation duration. Simulation durations were increased up to 200 ns.

Section 4:

Exact same steps applied in Section 2 were followed for this section, except for the simulation duration. However, unlike other simulation runs, the production step is designed to last 100 ns, with 50,000,000 timesteps and 50,000 frames.

3.2.3 Docking

Section 2:

Interactions of the mannose part of the designed Triphenylphosphonium:Mannose 5:2 polymer molecule with the lectin protein, the binding energies and binding positions of the molecules were calculated and examined using the method called molecular docking and MGLTools software (113). For this, the structure of the lectin protein in the pdb database was used. The binding site of the mannose group to the lectin protein using Discovery Studio 2019 software (98).

Section 4:

In order to examine the interactions of the mannose part of the designed Triphenylphosphonium:Mannose 5:2 polymer molecule with the lectin protein, which is thought to have metabolic importance for the cell, the binding energies and binding positions of the molecules were calculated and examined using the method called molecular docking and AUTODOCK software. For this, the structure of the lectin

protein “4xoc” PDB file (114) was used obtained from RCSB PDB database (115). The lectin protein was separated from this complex structure using the Discovery Studio 2021 program and brought into a monomer structure that does not contain ligands and water. While mannose was in complex with a different structure obtained from the RCSB database, it was abbreviated to its monomer structure using Discovery Studio 2021 (98). After obtaining the 3D structural data of Lectin and Mannose separately, the docking study of the interactions of the two molecules with each other was carried out using AutoDock Tool and Autodock Vine (116). In addition, a docking study of the lectin-galactose interaction was carried out.

3.3 Molecular Modelling Experiments of Antimicrobial Peptides and Polymers Mimicking Antimicrobial Peptides Inspired from Nature

Last sets of study (project number: 217S060) in this thesis comprises three different parts. In the first part of the study, original antimicrobial peptides produced from natural amino acids, and in the second part, natural antimicrobial peptide-like polymers were designed in the preliminary study (101), and molecular dynamicss simulations were made. The aim of this third part of the study is to produce synthetic derivatives inspired by the structure of these molecules that previously designed and investigate of their antimicrobial activity in terms of resistance, efficiency and determine whether they are wort for further studies.

3.3.1 Molecular modelling

Section 1:

Most active peptides, TN1 and TN3, were investigated by locating them on doble-layered POPE membrane in water with different placements and different amounts. TN6 and D-TN6 peptides were also simulated.

Section 2:

For second part of this study, MD simulation of polymers were made and analyzed. As regard to polymer used for experiments, DABCO-based (double cationic charged) polymer was simulated locating above double-layered POPE membrane structure.

Section 3:

In this last part of the study, modelling studies were continued with the D-TN6 peptide selected in line with previous modelling studies in Section 1. The simulation created with the D-TN6 peptide was extended to 600 ns.

3.3.1.1 Structure prediction

Section 1:

The peptide predicted 3D structures were acquired with PEP-FOLD3 web server during the previously conducted study mentioned before. Nevertheless, since 3D structure of D-TN6 couldn't be estimated by PEP-FOLD3, D-TN6 structure was generated by using the code created for d-form amino acids, which were also used in the previous sections.

Section 2:

3-dimensional structure files of polymer to be used in this study containing each atomic coordinate of the components in the system to be modeled were generated by the CACTUS server of the National Cancer Institute (NHI-NCI) in the USA (105). 3D structures of peptides proven to have antimicrobial effects and polymer designed expected to have antimicrobial effects are compared and visualized depending on their interpolated charge, hydrogen bonds, hydrophobicity, ionizability, and atomic charge using Discovery Studio 2019 software, as in Table 7 (98).

Table 7. Comparison between designed DABCO-based polymer, the 3D structures of the TN1 peptide, which was designed and modeled and published in the preliminary study of this project, and the reference natural magainin peptide according to different feature distributions (101).

Representation	TN1*	Magainin PDB ID: 2LSA	Synthesized Polymer
CPK	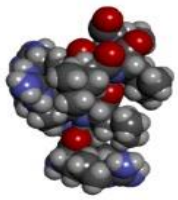		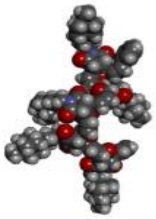
Interpolated Charge 0,100 0,067 0,033 0,000 -0,033 -0,067 -0,100	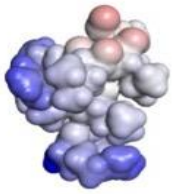	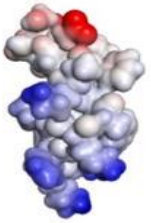	
H-Bonds Donor Acceptor	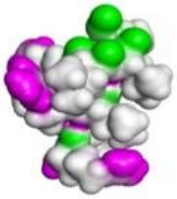	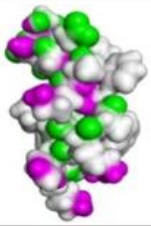	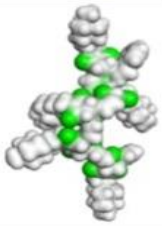
Hydrophobicity 3,00 2,00 1,00 0,00 -1,00 -2,00 -3,00		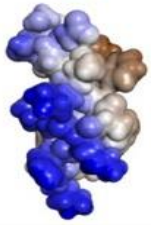	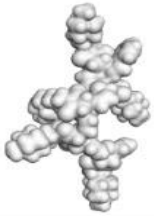
Ionizability Basic Acidic		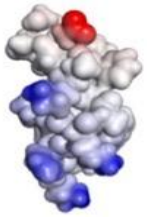	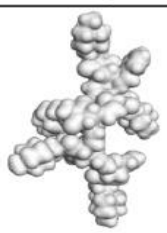
Atom Charge 0,70 0,47 0,23 0,00 -0,23 -0,47 -0,70			

Section 3:

Structure prediction of D-TN6 has been made before.

3.3.2 Molecular dynamics simulation

Section 1:

In the first section, using multi-core high-performance computers, the double-layered lipid membrane (POPE) systems of the designed peptides in water were modeled and it was investigated whether they have antimicrobial properties by affecting the membranes of microorganisms. Molecular dynamics simulations with different settings using TN1, TN3, TN6 and D-TN6 are listed under the system preparation part below.

Section 2:

Simulation system composed of DABCO-based polymer and double-layered POPE membrane in water was simulated to investigate whether the designed polymer has antimicrobial effects.

Section 3:

MD Simulation of D-TN6 peptide was proceeded up to 600 ns to observe how D-TN6 peptide would behave if it could be simulated for longer period.

3.3.2.1 System preparation for simulation

Section 1:

For molecular dynamics simulation of antimicrobial peptides, respectively; TN3-rectangular (12-pack), TN3-ring (12-pack), TN3-isoleucine (4-pack), TN3-valine (4-

pack), TN1-isoleucine (4-pack), TN1-valine (4-pack), TN6 (4-pack), D-TN6 (4-pack) peptide membrane systems were prepared.

Molecular dynamics simulations were performed by running CHARMM27 force field parameters and NAMD 2.11 software in parallel. Placing the peptide molecules on the POPE membrane at a certain distance was done using VMD software.

- TN3 peptides were placed on POPE membrane with 10 Å distance to membrane and to each other as 12 identical peptides in a rectangular shape. Simulation duration was set to 100 ns.
- TN3 peptides were placed on POPE membrane with 10 Å distance to membrane and to each other as 12 identical peptides in circular shape. Simulation duration was set to 100 ns.
- TN3 peptides containing isoleucine instead of leucine were placed on POPE membrane with 10 Å distance to membrane and to each other as 4 identical peptides. Simulation duration was set to 10 ns.
- TN3 peptides containing valine instead of leucine were placed on POPE membrane with 10 Å distance to membrane and to each other as 4 identical peptides. Simulation duration was set to 10 ns.
- TN1 peptides containing isoleucine instead of leucine were placed on POPE membrane with 10 Å distance to membrane and to each other as 4 identical peptides. Simulation duration was set to 10 ns.
- TN1 peptides containing valine instead of leucine were placed on POPE membrane with 10 Å distance to membrane and to each other as 4 identical peptides. Simulation duration was set to 10 ns.
- TN6 peptides were placed on POPE membrane with 10 Å distance to membrane and to each other as 4 identical peptides. Simulation duration was set to 100 ns.
- D-TN6 peptides were placed on POPE membrane with 10 Å distance to membrane and to each other as 4 identical peptides. Simulation duration was set to 100 ns, then to 300 ns.

Section 2:

Firstly, 3-dimensional structure files containing each atomic coordinate of the components in the system to be modeled and force field parameter files used to calculate interaction forces were obtained. After these files are obtained in different ways for each component and combined in accordance with the format to be used, they are modeled with a run (*.conf) file in which variables such as temperature, pressure, box size components are also controlled depending on which ensemble (NPT, NVT, etc.) will be modeled.

To carry out the MD simulation of the designed sample polymer, the parameter files of this new polymer were obtained for a single monomer, and the structure and parameter input file of the whole polymer were created by combining these monomers using VMD commands. At this stage, the parameter sets of the oxanorbornene monomer part in all monomer types, using the Force Field Toolkit (ffTK) which is an add-on in the VMD software package, quantum simulations were made for the atom groups whose parameters are not available in the existing libraries. As a result, CHARMM-compatible force parameter sets were obtained with potential energy surface (PES) scans (106).

In the quantum calculations here, ffTK used 6-31G* as the standard (default) base set and MP2 as the theory method. TRUBA computational resources are used for the Gaussian software required for these quantum calculations (107). Parameters for other parts of the monomer were obtained from existing CHARMM force field libraries.

After obtaining the necessary parameter sets for the polymers, molecular dynamicss models were carried out by combining the parameters in the CHARMM27 force field libraries, literature, and quantum optimization by running the NAMD 2.11 software in parallel. Placing the polymer molecules on the POPE membrane at a certain distance was done using VMD software. To observe the orientation or behavior of the polymers to both each other and to the membrane, 4 identical polymer molecules

were positioned at a distance of approximately 10 Å from each other and the bacterial membrane.

Section 3:

Four identical D-TN6 peptide molecules were positioned above the POPE membrane in water with a distance of approximately 10 Å between them and to the bacterial membrane.

3.3.2.2 Steps of molecular dynamics simulation

Section 1:

Melting lipid tails: Since the lipid system provided by the membrane plug-in of the VMD is not in equilibrium, a simulation was first performed in which everything (water, ions, polymer, lipid headgroups) was fixed except the lipid tails. After this simulation lasting 0.5 ns, the lipid ends became irregular.

Minimization and equilibration with protein constrained: Since we have put the system together artificially in the computer environment, there are many unnatural atom positions which do not have minimum energy and maximum entropy, that is, prevent the system from being stable. For this reason, a minimization simulation lasting 0.5 ns was performed to bring the system to its minimum local energy before operating it with full dynamicss.

Equilibration with protein released: Later, 0,5 ns lasting equilibration run were applied where the whole system was released with constrained polymers for further equilibration.

Production Run: Finally, the production run was performed since the polymers were equilibrated properly and system was ready.

Outputs of the simulations were visualized and analyzed by using VMD software.

Section 2:

Same simulation steps as in previous part were followed. Only difference from the previous modelling experiment is the simulation duration which is set to 150 ns for this section's MD simulations.

Section 3:

Same simulation procedure with the simulations made in previous sections was followed through. Only the simulation duration was increased to 600 ns.

4 RESULTS

4.1 Molecular Modelling Experiments on Catelicidin-Like Antimicrobial Peptides and Their Interactions with POPE Membrane

4.1.1 Molecular dynamics simulation

Section 1:

Short (2 ns) simulations: During the design of antimicrobial peptide molecules, it was aimed to calculate the interactions of peptides with microorganism membranes by using molecular modelling and computational methods, and the analysis of the results was performed simultaneously with the experimental studies required for the peptide design, in a simultaneous and feedback manner.

By making short simulations of the designed 4 peptide models (all of them in L-form), their tendency towards the membrane from the water phase was investigated.

Model 1 Peptide – RLKLLLKLLR

The Model 1 sequence peptide structure was first placed on the membrane place in the water phase, as shown in Figure 9, in 4 pieces, with a distance of approximately 10 Å to the membrane and to each other.

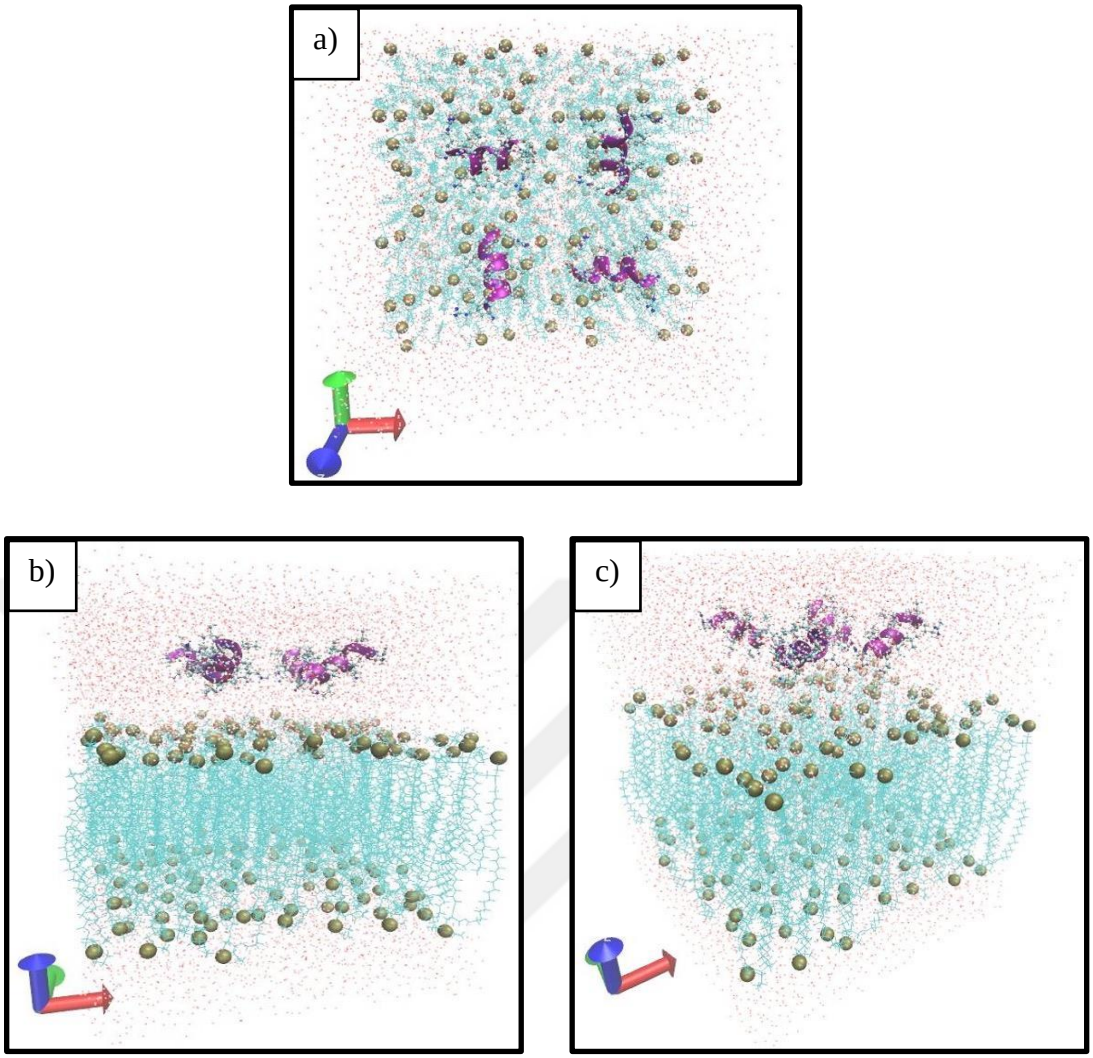

Figure 9. Rectangular positioning of the Model 1 peptide molecule on the bacterial membrane and in water, a) top view, b) side view, c) corner view. Water molecules are shown with red dots, phosphate molecules with green VDW balls, membrane lipids with light blue lines, peptides with purple alpha helix structure, New Cartoon/Secondary Structure, and atoms with CPK notation.

After the simulation system shown in the figure above was prepared, it was used as the initial input and a short (2ns) MD simulation was performed primarily for the model 1 sequence peptide-membrane system. In Figure 10, this simulation result of the model 1 peptide is visualized from the side. As visualized in this way, it has been observed that model 1 molecules tend to move towards the membrane and enter the membrane during this simulation period.

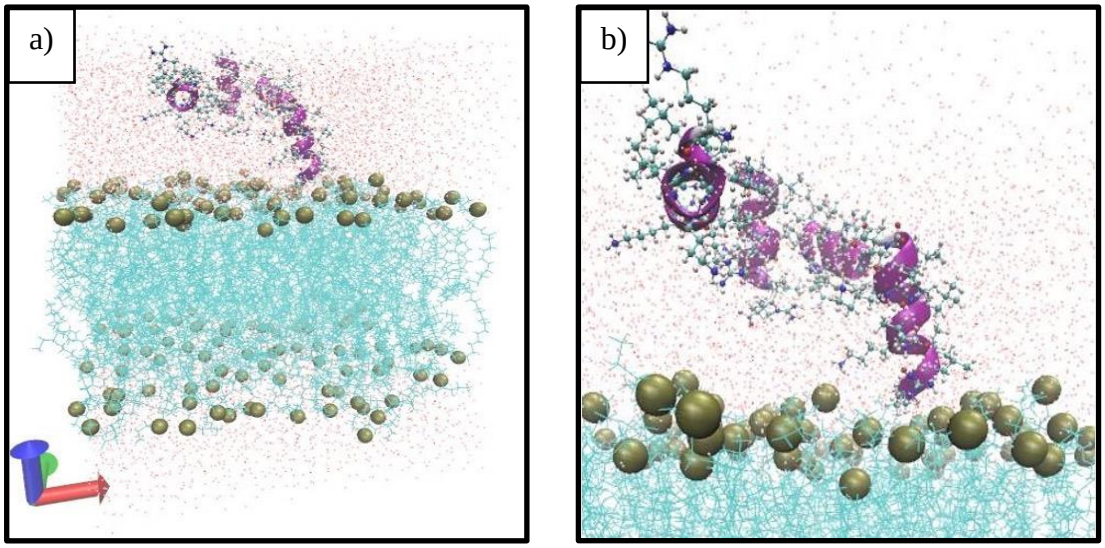

Figure 10. Short molecular simulation result after positioning the Model 1 peptide molecule on the bacterial membrane and in water, a) side view, b) zoomed-in view. Water molecules are shown in red-white, phosphate molecules in green balls, membrane lipids in light blue, alpha helix structure of peptides and atoms in purple.

It is observed in Figure 10 that 4 peptides with Model 1 sequence, all in L form, are directed to the membrane and one of the peptides is very close to the membrane. The graph of the distance (Å) of a converging atom of the Model 1 peptide to a P atom on the membrane according to the time step is given in Figure 11.

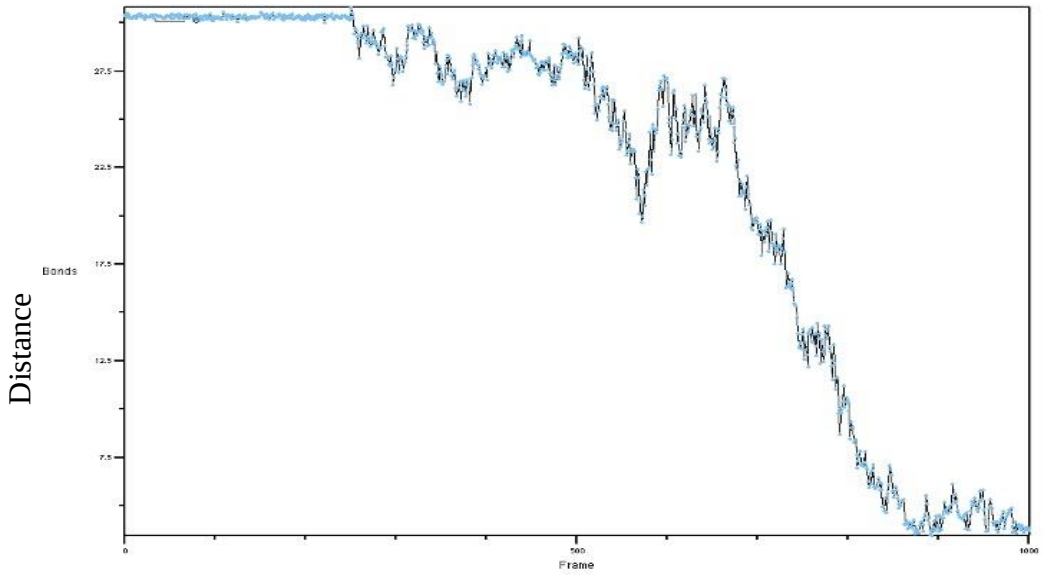

Figure 11. Graph of the distance (Å) of the Model 1 peptide (ARG1:NH2) to the membrane (POPE28:P) versus time step.

Model 2 Peptide – RLLRLLLRRLLLRLLR

The Model 2 sequence peptide structure was first placed on the membrane place in the water phase, as shown in Figure 12, in 4 pieces, with a distance of approximately 10 Å to the membrane and to each other.

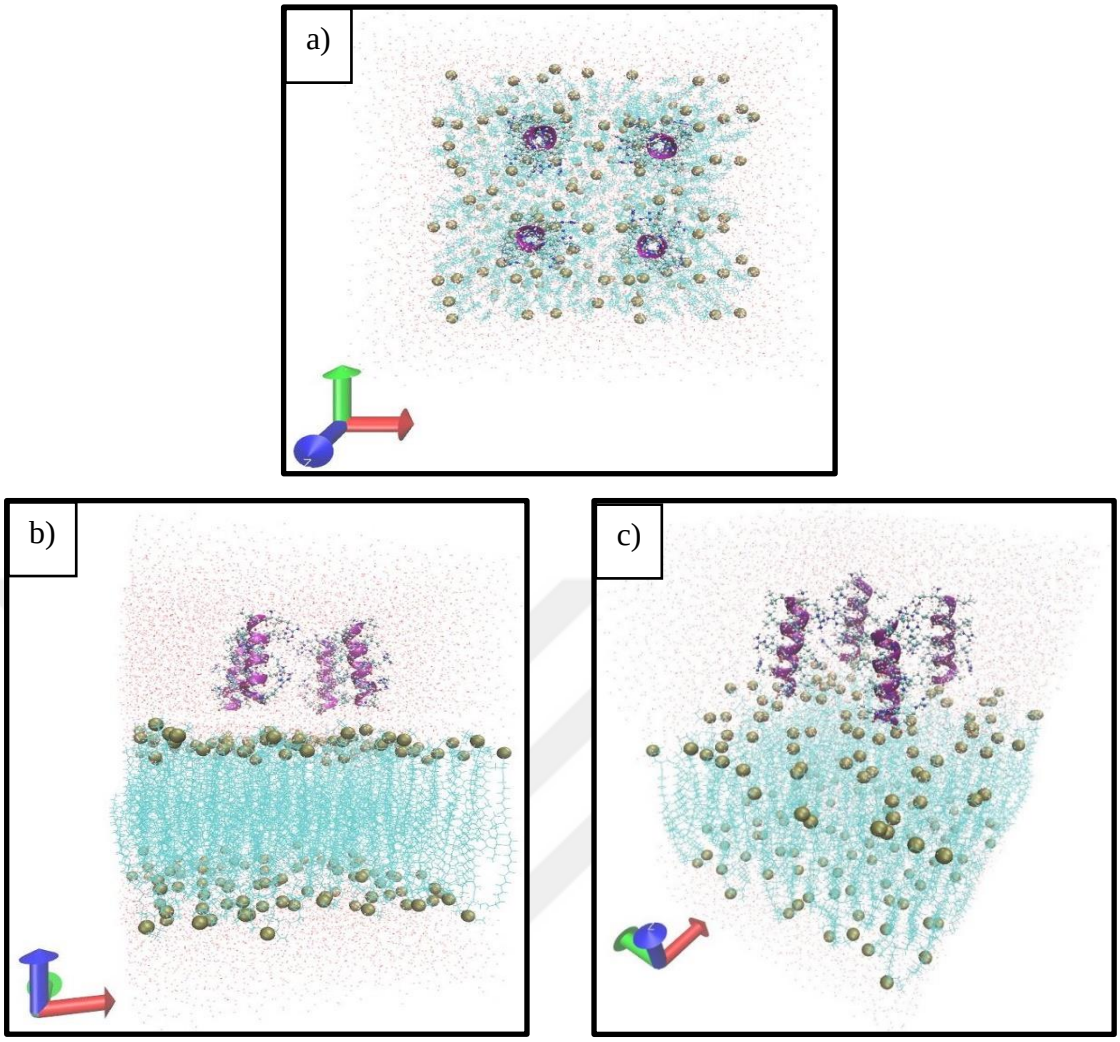

Figure 12. Circular positioning of the Model 2 peptide molecule on the bacterial membrane and in water, a) top view, b) side view, c) corner view. Water molecules are shown with red dots, phosphate molecules with green VDW balls, membrane lipids with light blue lines, peptides with purple alpha helix structure, New Cartoon/Secondary Structure, and atoms with CPK notation.

After the simulation system shown in the figure above was prepared, it was used as the initial input and a 2 ns MD simulation was performed. In Figure 13, this simulation result of the model 2 peptide is visualized from the top and the side. As visualized in this way, it was observed that the Model 2 peptide molecules tended towards the membrane and penetrated into the membrane during this simulation time, which lasted for 2 ns.

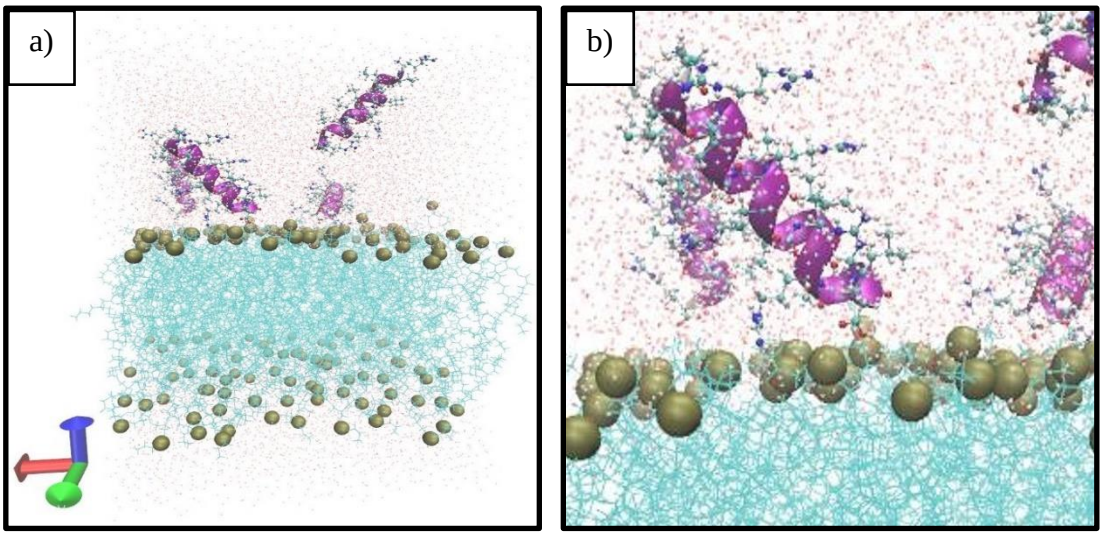

Figure 13. Molecular simulation lasting 2 ns after positioning the Model 2 peptide molecule on the bacterial membrane and in water, a) side view, b) zoomed-in view. Water molecules are shown in red-white, phosphate molecules in green balls, membrane lipids in light blue, alpha helix structure of peptides and atoms in purple.

The graph of the distance (Å) of a converging atom of the Model 2 peptide to a P atom on the membrane according to the time step is given in Figure 14.

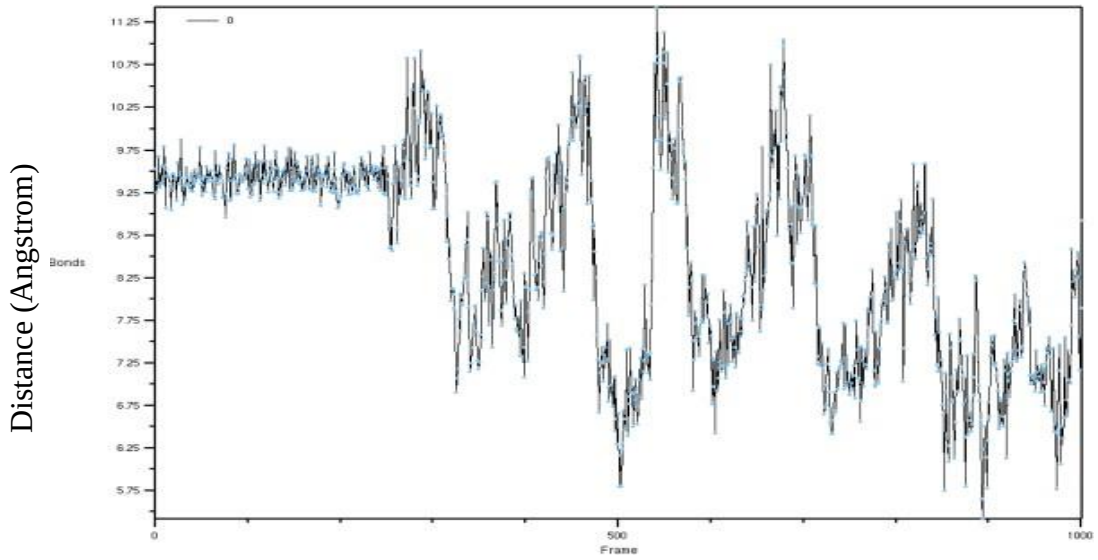

Figure 14. Graph of the distance (Å) of the Model 2 peptide (ARG16:CA) to the membrane (POPE3:P) versus time step

Model 3 Peptide – RLLLRLLRRLLLRLLR

The Model 3 sequence peptide structure was first placed on the membrane place in the water phase, as shown in Figure 15, in 4 pieces, with a distance of approximately 10 Å to the membrane and to each other.

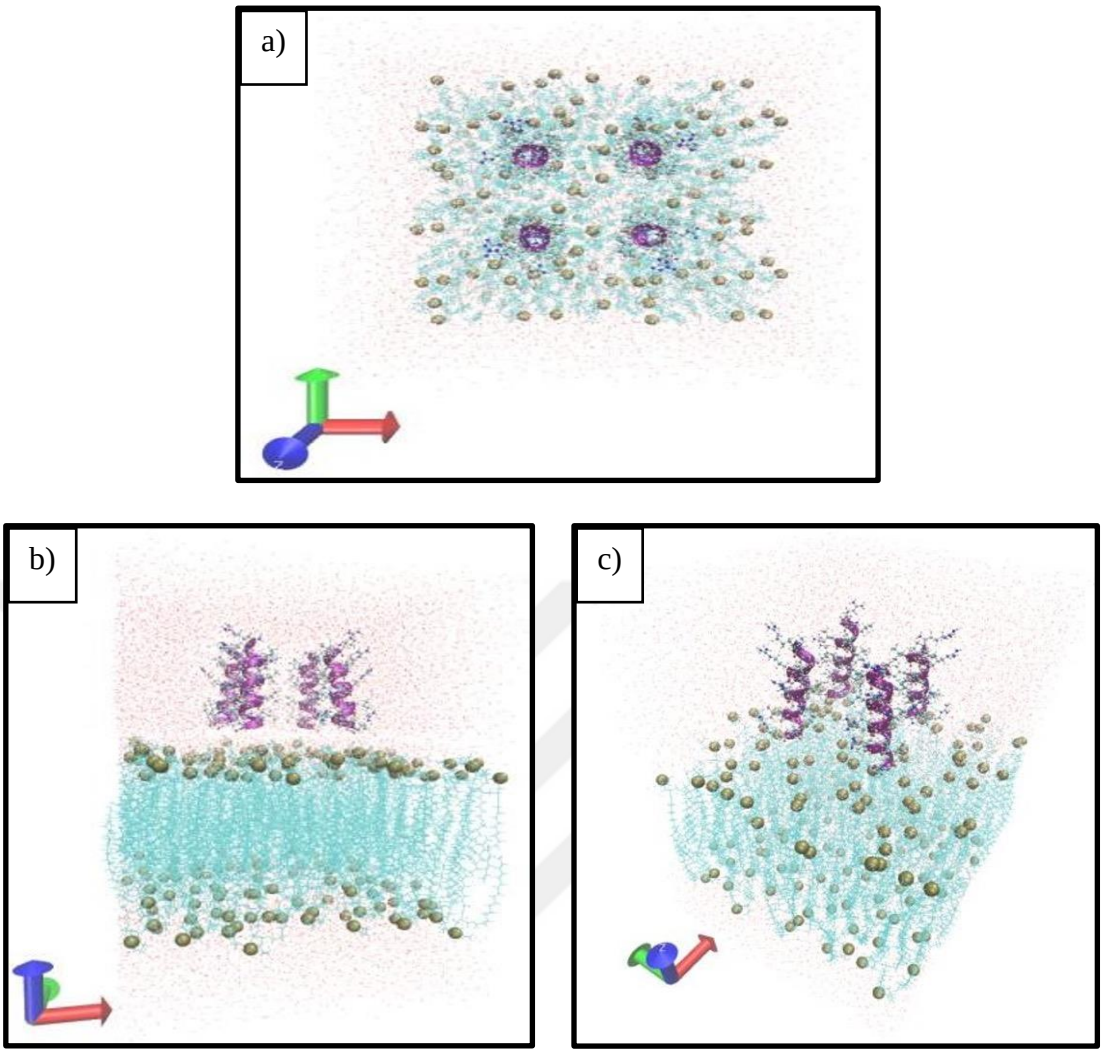

Figure 15. Positioning of the Model 3 peptide molecule on the bacterial membrane and in water, a) top view, b) side view, c) corner view. Water molecules are shown with red dots, phosphate molecules with green VDW balls, membrane lipids with light blue lines, peptides with purple alpha helix structure, New Cartoon/Secondary Structure and atoms with CPK notation.

After the simulation system shown in the figure above was prepared, it was used as the initial input and a 2 ns MD simulation was performed. This simulation result of the Model 3 peptide is visualized in Figure 16. As seen in this figure, it was observed that the Model 3 molecules tended towards the membrane during this short simulation time of 2 ns.

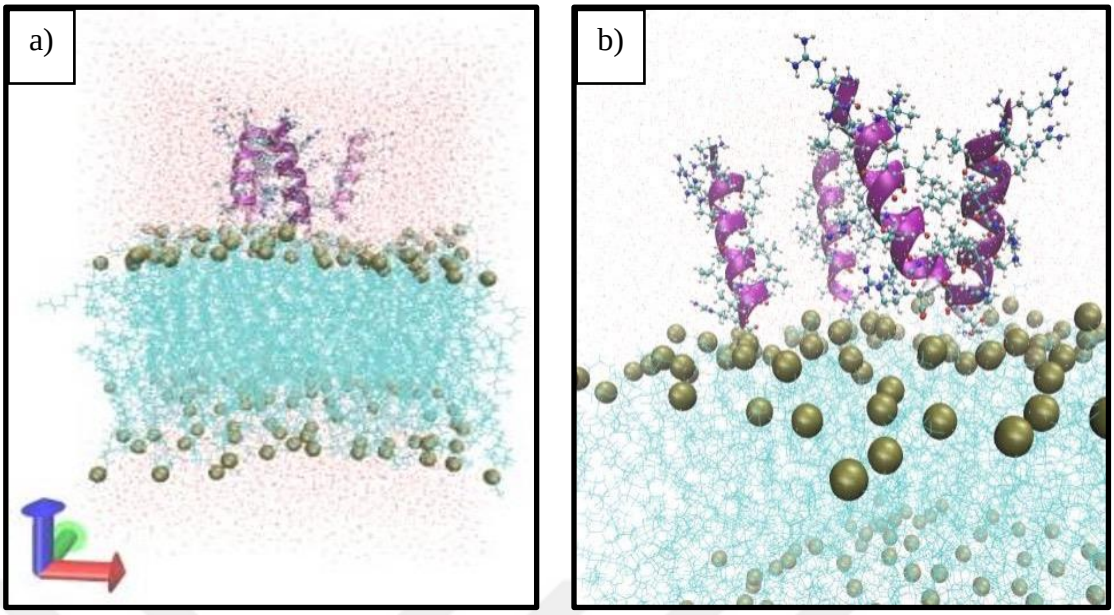

Figure 16. Molecular simulation lasting 2 ns after positioning the Model 3 peptide molecule on the bacterial membrane and in water, a) side view, b) zoomed-in view. Water molecules are shown in red-white, phosphate molecules in green balls, membrane lipids in light blue, alpha helix structure of peptides and atoms in purple.

The graph of the distance (Å) of a converging atom of the Model 3 peptide to a P atom on the membrane according to the time step is given in Figure 17.

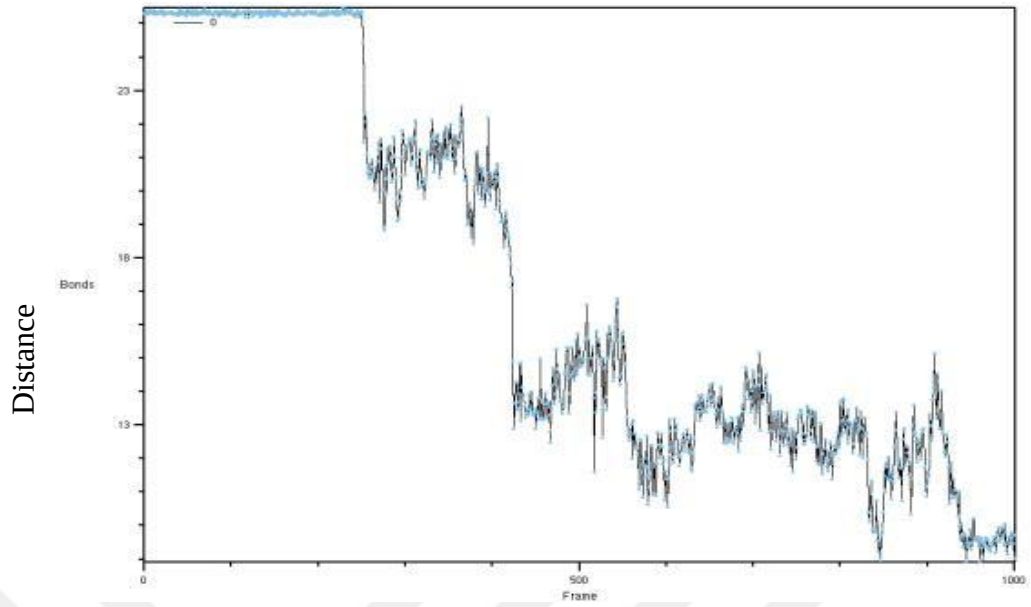

Figure 17. Graph of the distance (Å) of the Model 3 peptide (ARG16:NH1) to the membrane (POPE30:H1) versus time step

Model 4 Peptide – RLLLRLLRRLLRLLLR

The Model 4 sequence, all in L-form, peptide structure (P2) was first placed on the membrane place in the water phase, as shown in Figure 18, in 4 pieces, with a distance of approximately 10 Å to the membrane and to each other.

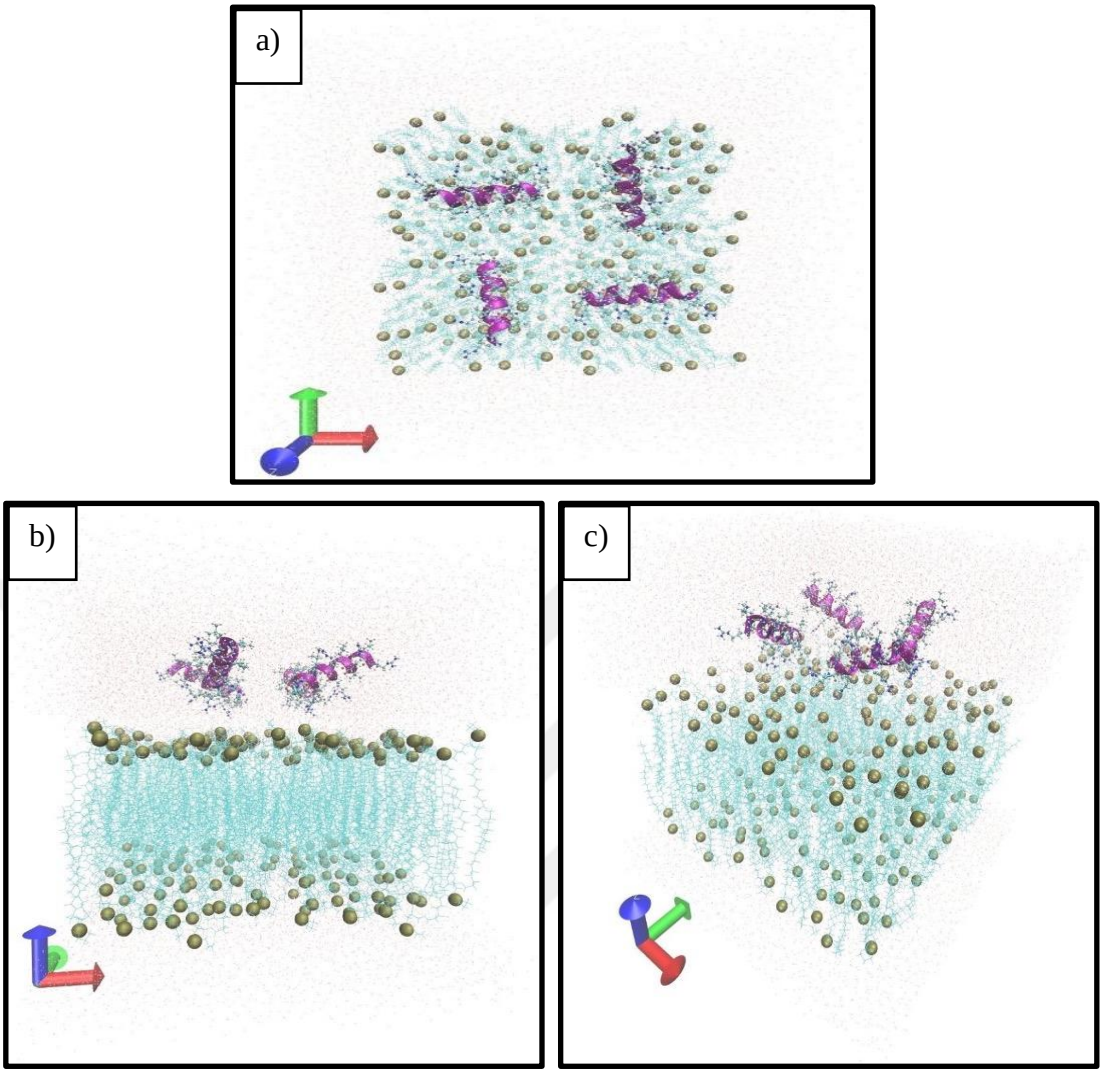

Figure 18. Positioning of the Model 4 (P2) peptide on the bacterial membrane and in water, a) top view, b) side view, c) corner view. Water molecules are shown with red dots, phosphate molecules with green VDW balls, membrane lipids with light blue lines, peptides with purple alpha helix structure, New Cartoon/Secondary Structure and atoms with CPK notation.

After the simulation system shown in the figure above was prepared, it was used as the initial input and a total of 2 ns MD simulation was carried out. This simulation result of Model 4 (P2) peptide is visualized in Figure 19. As visualized in this way, it was observed that the Model 4 peptide molecules tended towards the membrane during this short simulation time of 2 ns.

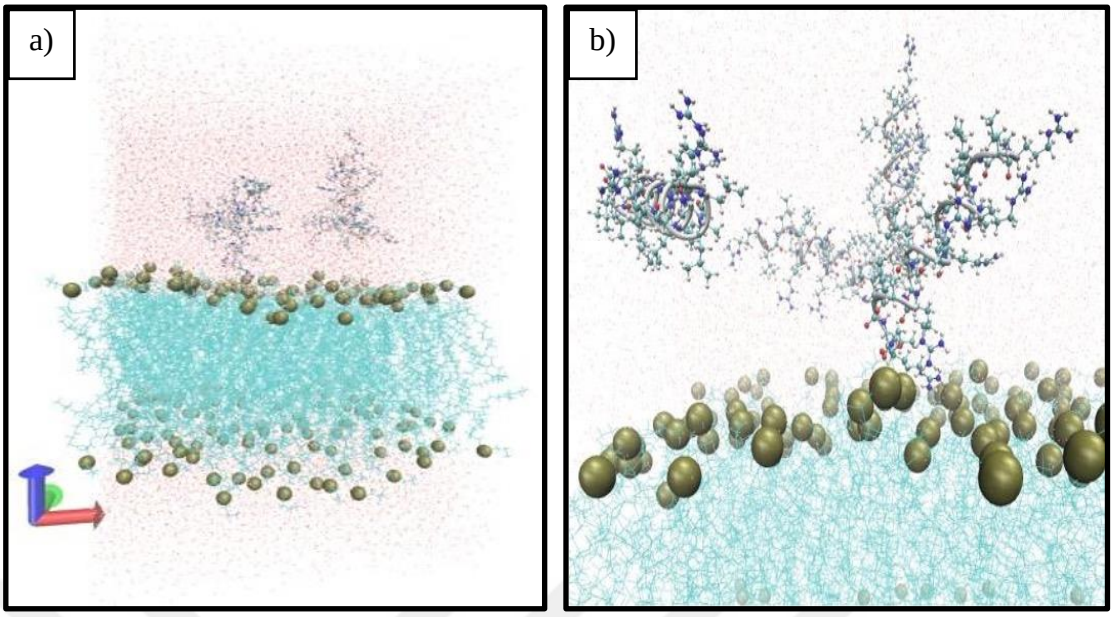

Figure 19. Molecular simulation lasting 2 ns after positioning the Model 4 (P2) peptide molecule on the bacterial membrane and in water, a) side view, b) zoomed-in view. Water molecules are shown in red-white, phosphate molecules in green balls, membrane lipids in light blue, alpha helix structure of peptides and atoms in purple.

The graph of the distance (Å) of an approaching atom of the Model 4 (P2) peptide to a P atom on the membrane according to the time step is given in Figure 20.

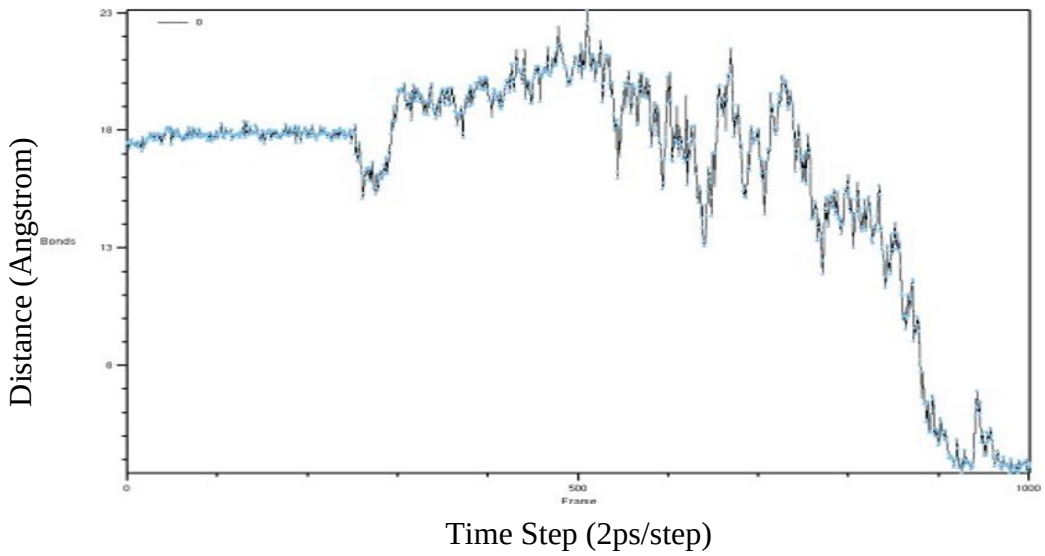

Figure 20. Graph of the distance (Å) of the Model 4 peptide (ARG16:NH2) to the membrane (POPE29:P) versus time steps.

Long (~50 ns) Simulations:

In this section, as a result of short (2ns) simulations for elimination, long (~50 ns) simulations of L and D form peptides belonging to the model 4 peptide sequences selected for experimental studies among four models were performed, and the results were visualized and presented.

Model 4 Sequence all in L-form: Peptide P2

Since the initial structure of the P2 peptide is the same as the t=0 initial structure of the model 4 in the short simulation, 4 identical pieces of P2 were placed on the membrane in the water phase with a distance of approximately 10 Å to the membrane and to each other. After the short simulation stages, the simulation time was extended to 50 ns, and a long simulation to be used for detailed analysis was carried out.

In Figure 21, this simulation result of the P2 (all L-form model with 4 sequences) peptide is visualized. It was observed that during this long simulation period of ~50ns, the P2 peptide molecules were directed towards the membrane and the atoms at their ends began to enter between the membrane P atoms.

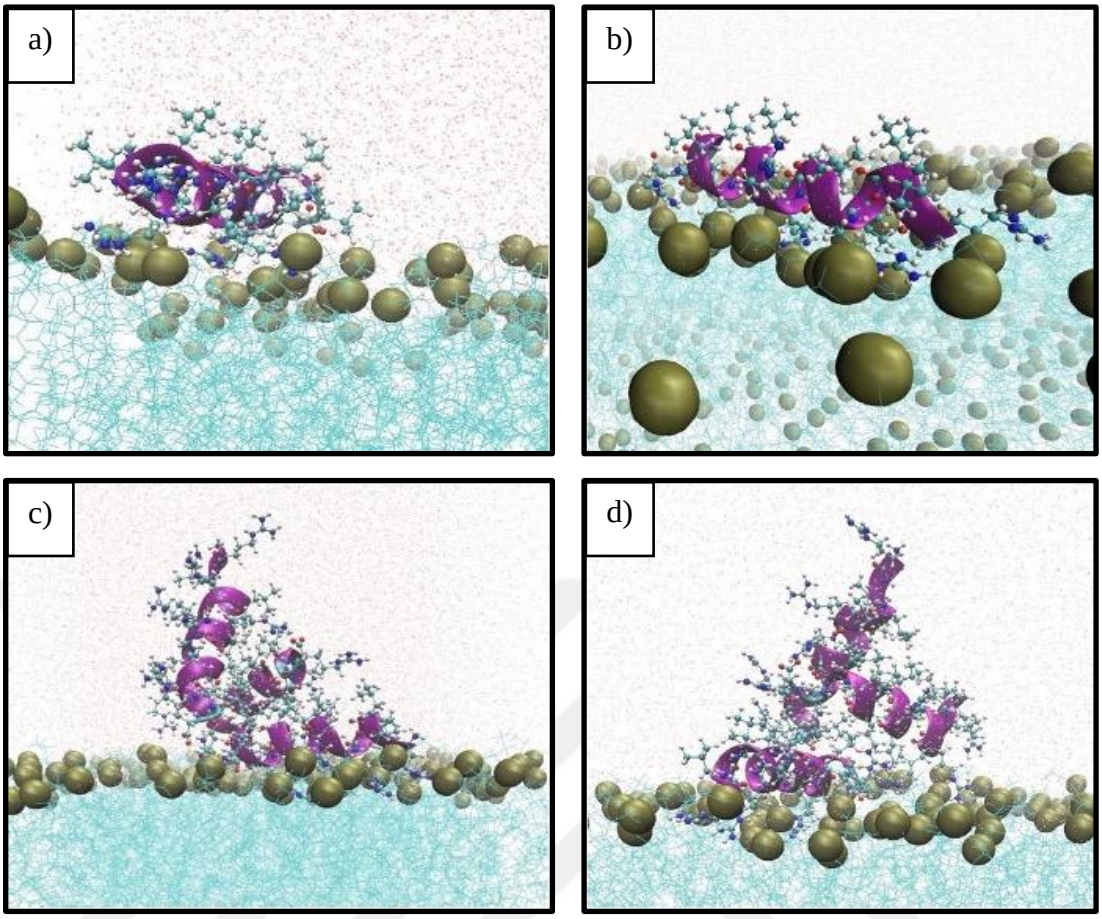

Figure 21. 50ns molecular simulation carried out after the P2 peptide molecule is positioned on the bacterial membrane and in water. a) and b) the appearance of the single conjugated peptide, c) and d) the triple converged peptide. Water molecules are shown in red-white, phosphate molecules in green balls, membrane lipids in light blue, alpha helix structure and atoms of peptides in purple.

The graph of the distances (Å) of the two approaching atoms of the P2 peptide to two of the P atoms on the membrane according to the time step is given in Figure 22.

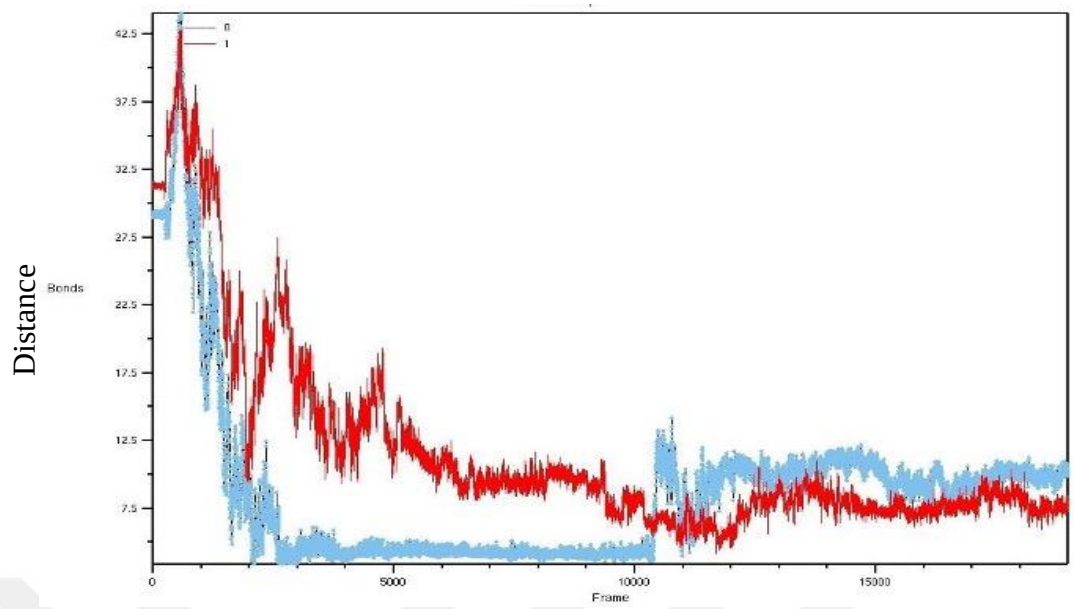

Time Step (2ps/step)

Figure 22. Graph of the distances (Å) of the P2 peptide to the membrane (between ARG1:NH2-POPE3:P and ARG5:NH2-POP11:P atom pairs) versus time step.

Model 4 Sequence all in D-form: Peptide P4

The four identical P4 peptide structures were first placed in the water phase on the membrane as shown in Figure 23, with a distance of approximately 10 Å to the membrane and to each other.

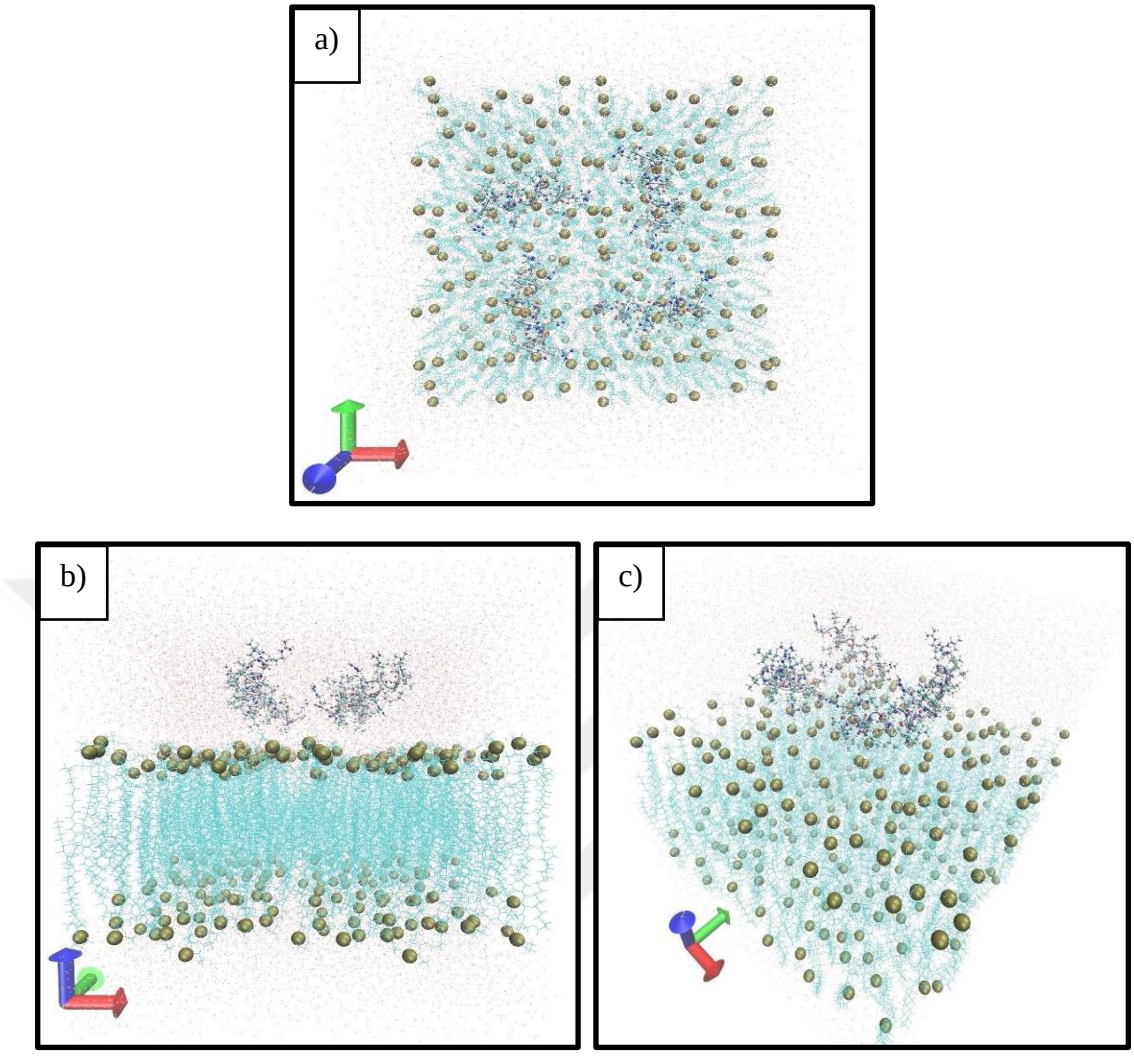

Figure 23. Positioning of the P4 peptide molecule on the bacterial membrane and in water, a) top view, b) side view, c) corner view. Water molecules are shown with red dots, phosphate molecules with green VDW balls, membrane lipids with light blue lines, peptides' structure is shown with New Cartoon/Secondary Structure and atoms are with CPK notation.

After the simulation system shown in the figure above was prepared, it was used as the initial input and a 50ns MD simulation was carried out. This simulation result of the P4 peptide is visualized in Figure 24. It was observed that during this long simulation period of 50ns, P4 molecules tended to the membrane and began to enter between the P atoms on the membrane, causing deformation on the membrane surface.

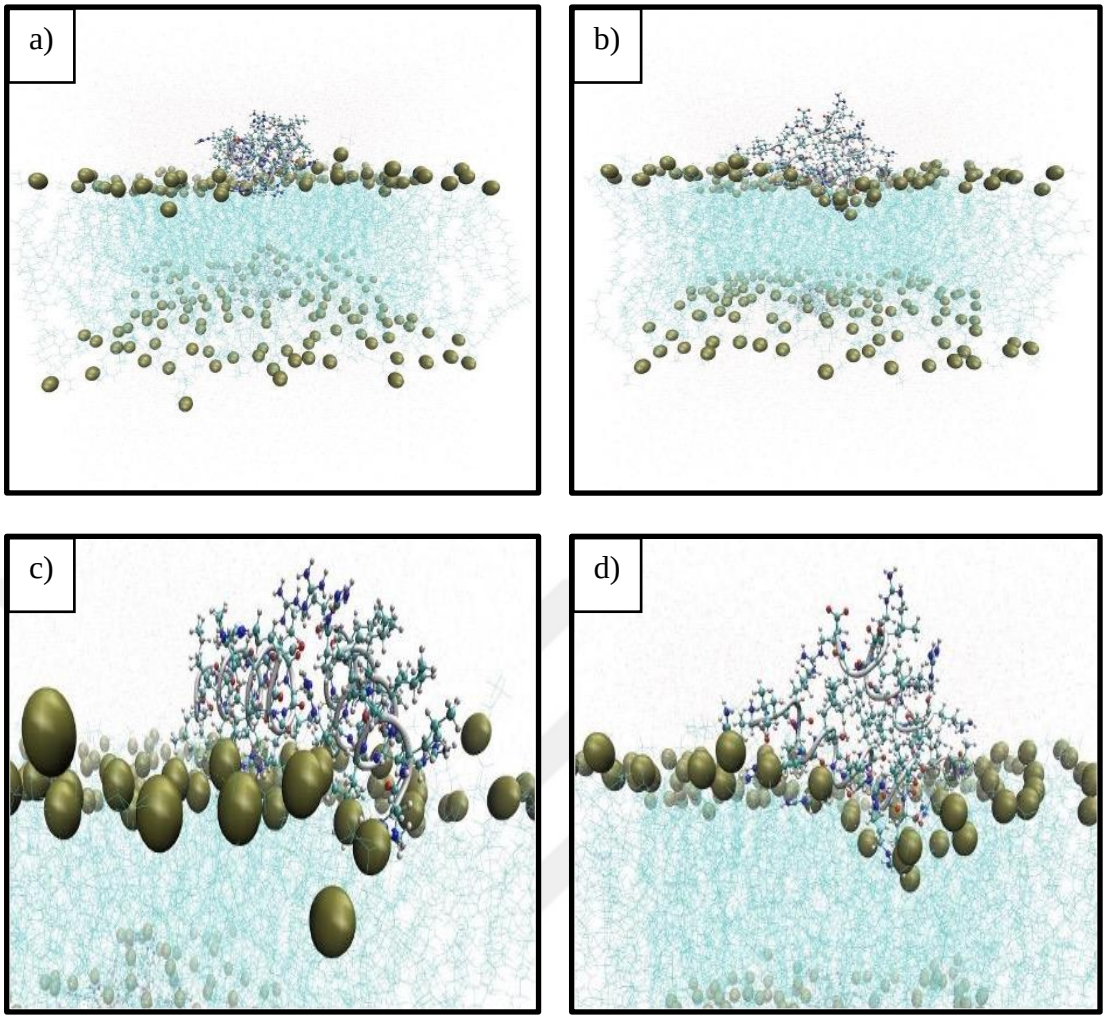

Figure 24. 50ns molecular simulation carried out after the P4 peptide molecule is positioned on the bacterial membrane and in water. a) and b) side view from different angles, c) and d) close-up view of the initiation of the membrane entry. Phosphate molecules are shown as green balls, lipids as light blue lines, atoms of peptides as CPK.

The graph of the distance (Å) of an approaching atom of the P4 peptide to one of the P atoms on the membrane according to the time step is given in Figure 25.

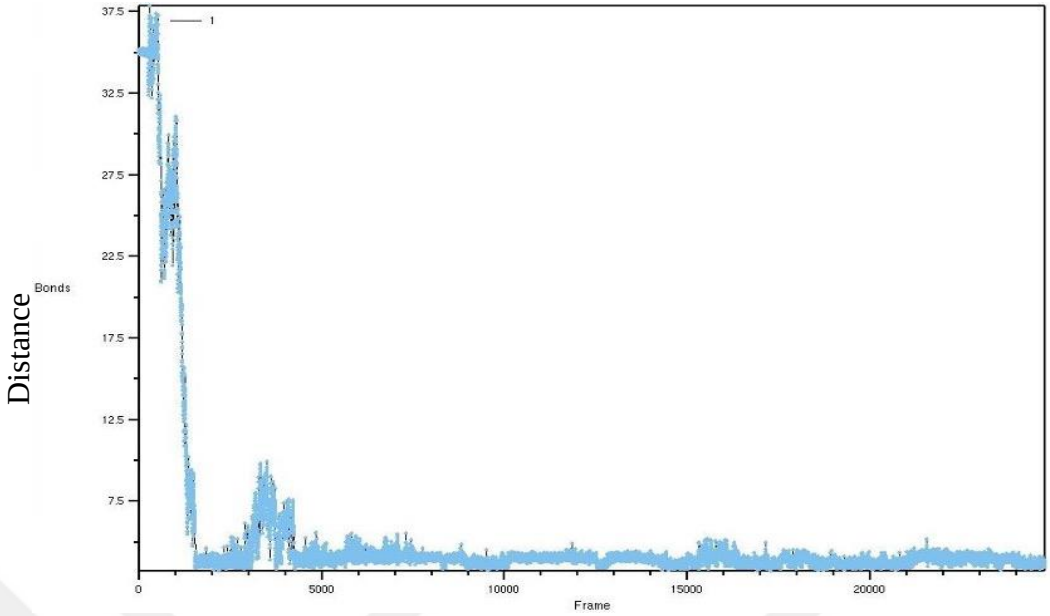

Figure 25. Graph of the distance (Angstrom) of the P4 peptide (DAR16:NH2) to the membrane (POPE5:P) versus time step.

When the molecular modelling results were examined, it was seen that all 4 peptides belonging to the model sequences that were emphasized during the design phase were directed to the membrane as a result of short-term (2 ns) simulations. The simulation time was extended (to 50 ns) for L and D form peptides from model 4 sequences, which were found to have good MIC values in experimental results. As a result of long simulations, it was observed in the simulations that both the L (P2) and D forms (P4) of the model 4-sequence peptide began to penetrate into the membrane.

Section 2:

Model4-P1 Peptide

(Arginine L- form and Leucine D-form RLLLRLLRRLLRLLLR)

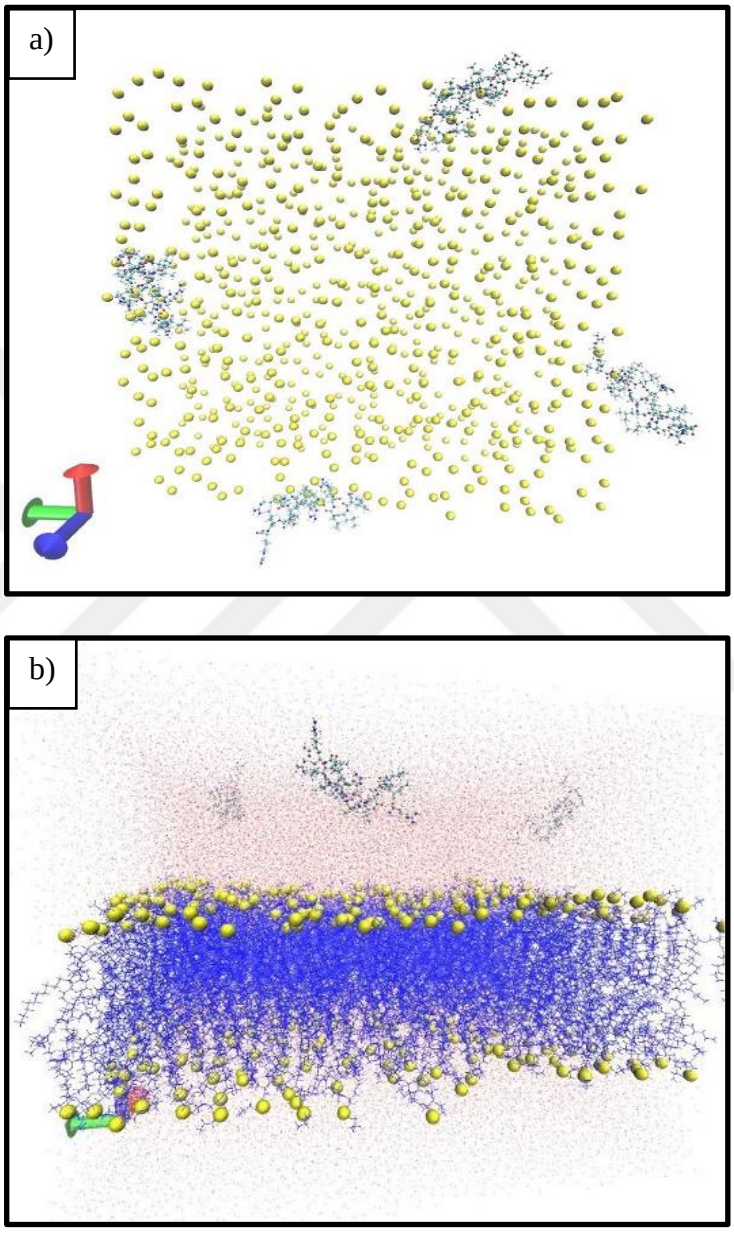

Figure 26. Positioning of the Model4-P1 peptide molecule on the bacterial membrane and in water, a) top view water and lipids closed, b) side view, c) side lipids closed view, d) lipids and water closed view. Water molecules are shown as red dots, phosphate molecules collect pure VDW, membrane lipids are shown as blue lines, atoms of peptides are shown as CPK notation.

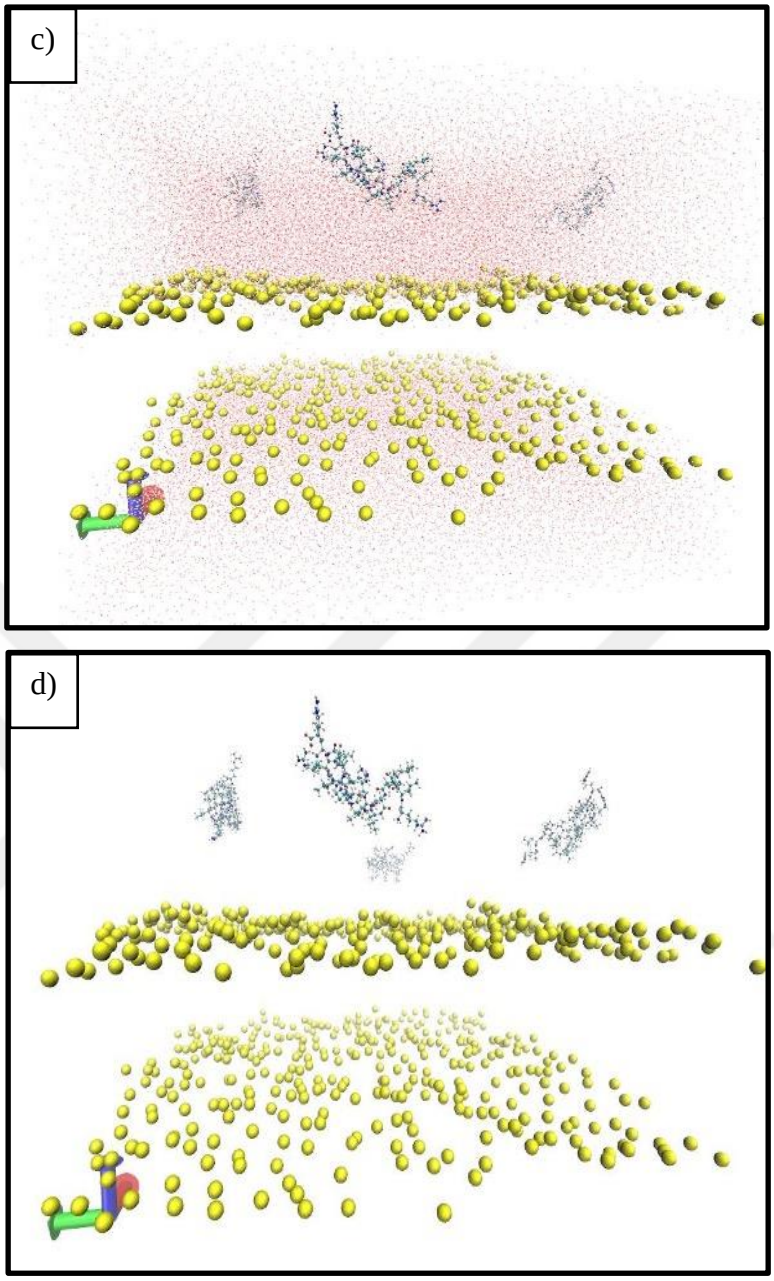

Figure 26. Positioning of the Model4-P1 peptide molecule on the bacterial membrane and in water, a) top view water and lipids closed, b) side view, c) side lipids closed view, d) lipids and water closed view. Water molecules are shown as red dots, phosphate molecules collect pure VDW, membrane lipids are shown as blue lines, atoms of peptides are shown as CPK notation (continued).

After the simulation system shown in the figure above was prepared, it was used as the initial input and a total of ~46 ns MD simulation was performed. This simulation result of Model4-P1 peptide is visualized in Figure 27. It was observed that the

Model4-P1 peptide molecules tended to stick to the membrane during the simulation period.

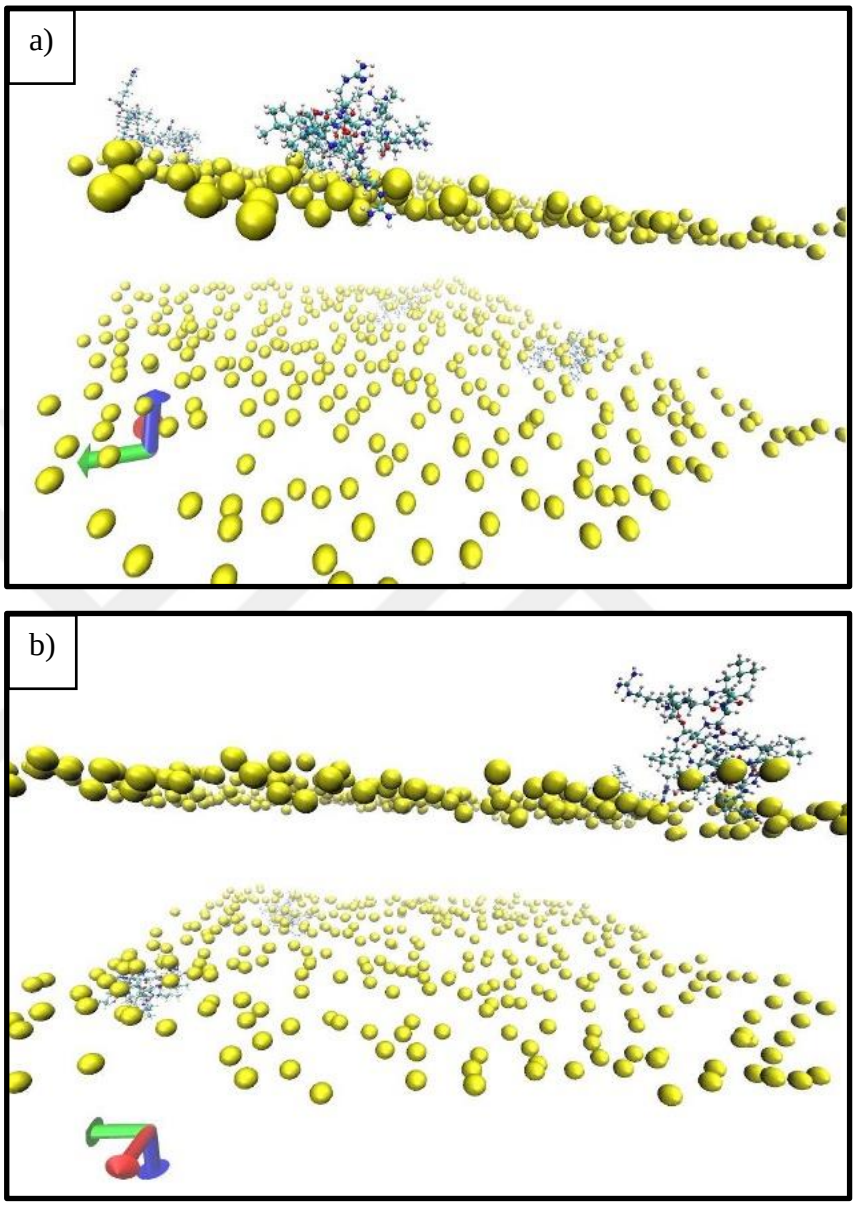

Figure 27. Molecular simulation with ~46 ns duration after positioning the Model4-P1 peptide molecule on the bacterial membrane and in water, a) side view, b) view from a different angle. Water molecules and lipids are closed when visualizing, phosphate molecules collect yellow VDW, peptides are shown with CPK atoms.

Section 3:

Model 4 Peptid

C-P1 form (Cystine - Arginine in L- and Leucine in D-form C-RLLLRLLRRLLRLLLR)

The peptide (C-P1) structure (in mixed form D and L) with Model 4 sequences was first placed on the membrane as 4 identical pieces in the water phase on the POPE membrane as seen in Figure 28. A simulation box of approximately 80x80x112 Angstrom dimensions was created and modeled.

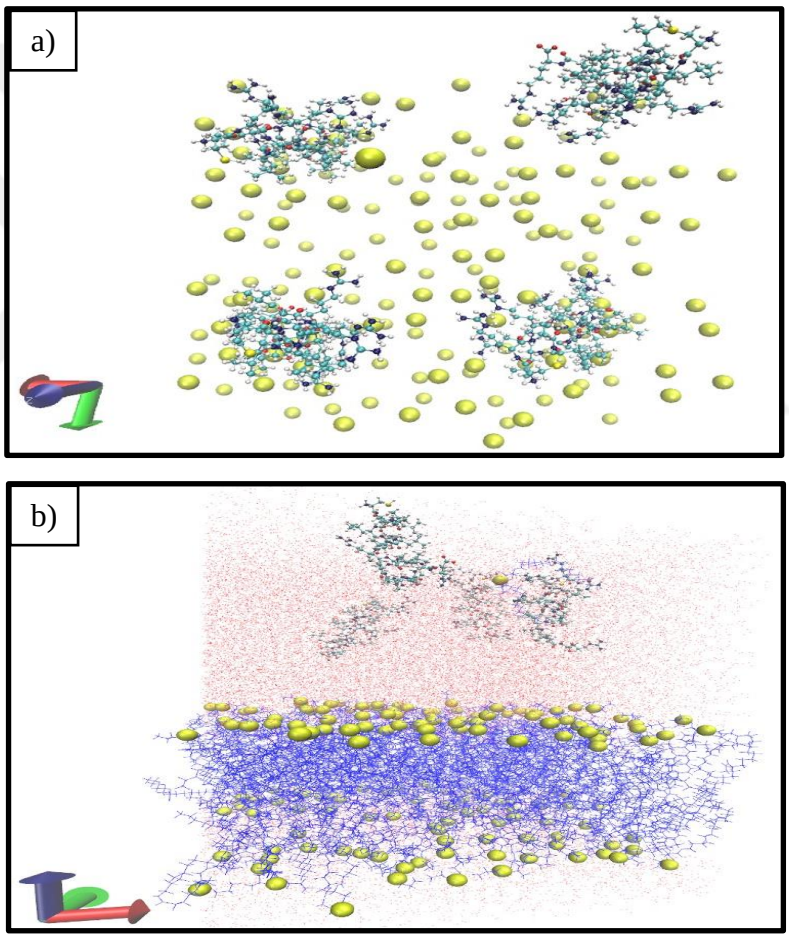

Figure 28. Positioning of the Model4 C-P1 peptide molecule on the bacterial membrane and in water, a) top view water and lipids closed, b) side view, c) side lipids closed view, d) lipids and water closed view. Water molecules are shown as red dots, phosphate molecules collect pure VDW, membrane lipids are shown as blue lines, atoms of peptides are shown as CPK notation.

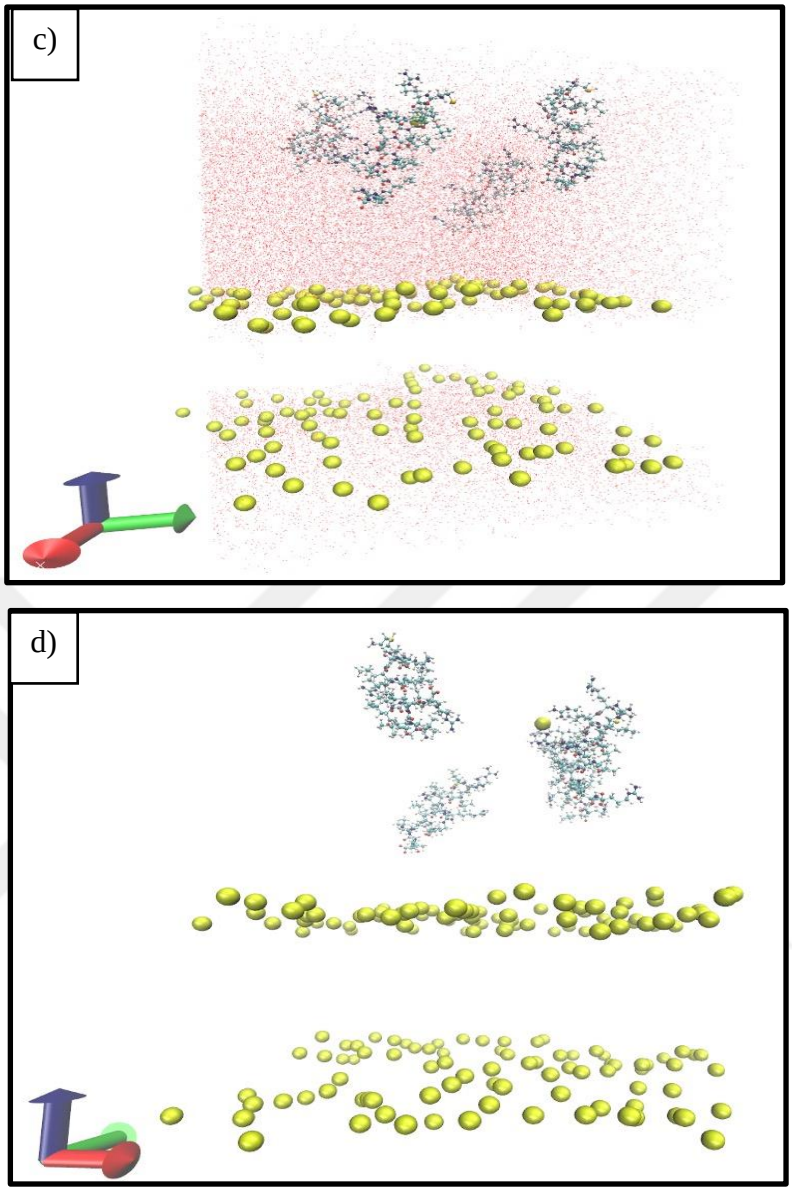

Figure 28. Positioning of the Model4 C-P1 peptide molecule on the bacterial membrane and in water, a) top view water and lipids closed, b) side view, c) side lipids closed view, d) lipids and water closed view. Water molecules are shown as red dots, phosphate molecules collect pure VDW, membrane lipids are shown as blue lines, atoms of peptides are shown as CPK notation (continued).

After the simulation system shown in the figure above was prepared, it was used as the initial input and a total of 100 ns MD simulation was carried out. This simulation result of Model4 C-P1 peptide is visualized in Figure 29. It was observed that the

Model4 C-P1 peptides tended to be directed and adhered to the membrane during the simulation.

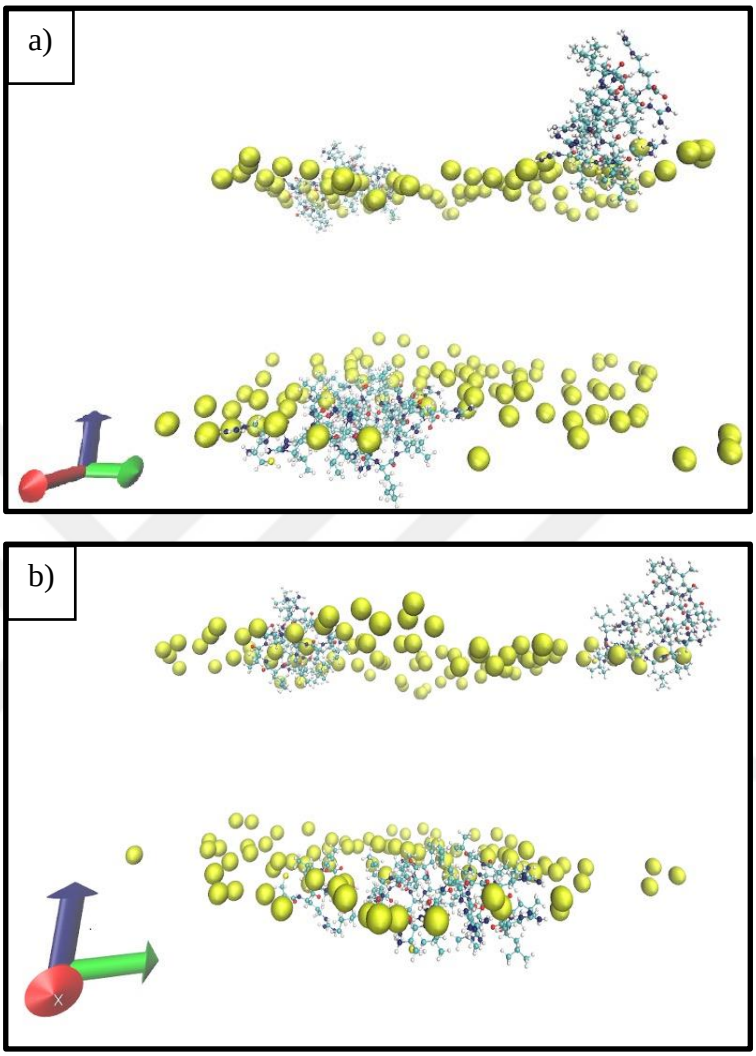

Figure 29. Molecular simulation of 100 ns duration after positioning the Model4 C-P1 peptide molecule on the bacterial membrane and in water, a) side view, b) view from a different angle. Water molecules and lipids are closed when visualizing, phosphate molecules collect yellow VDW, peptides are shown with CPK atoms.

4.2 Molecular Modelling of Polymer Composed of Mannose-Binding Lectin Protein with POPE Membrane and with Red Blood Cell Membrane-Similar 3D-Membrane

4.2.1 Molecular dynamics simulations

Section 1:

According to the Top6 structure, a membrane model system simulation box consisting of a total of 42492 atoms, containing the lipid bilayer, water, and ions, was created, and visualized using VMD software.

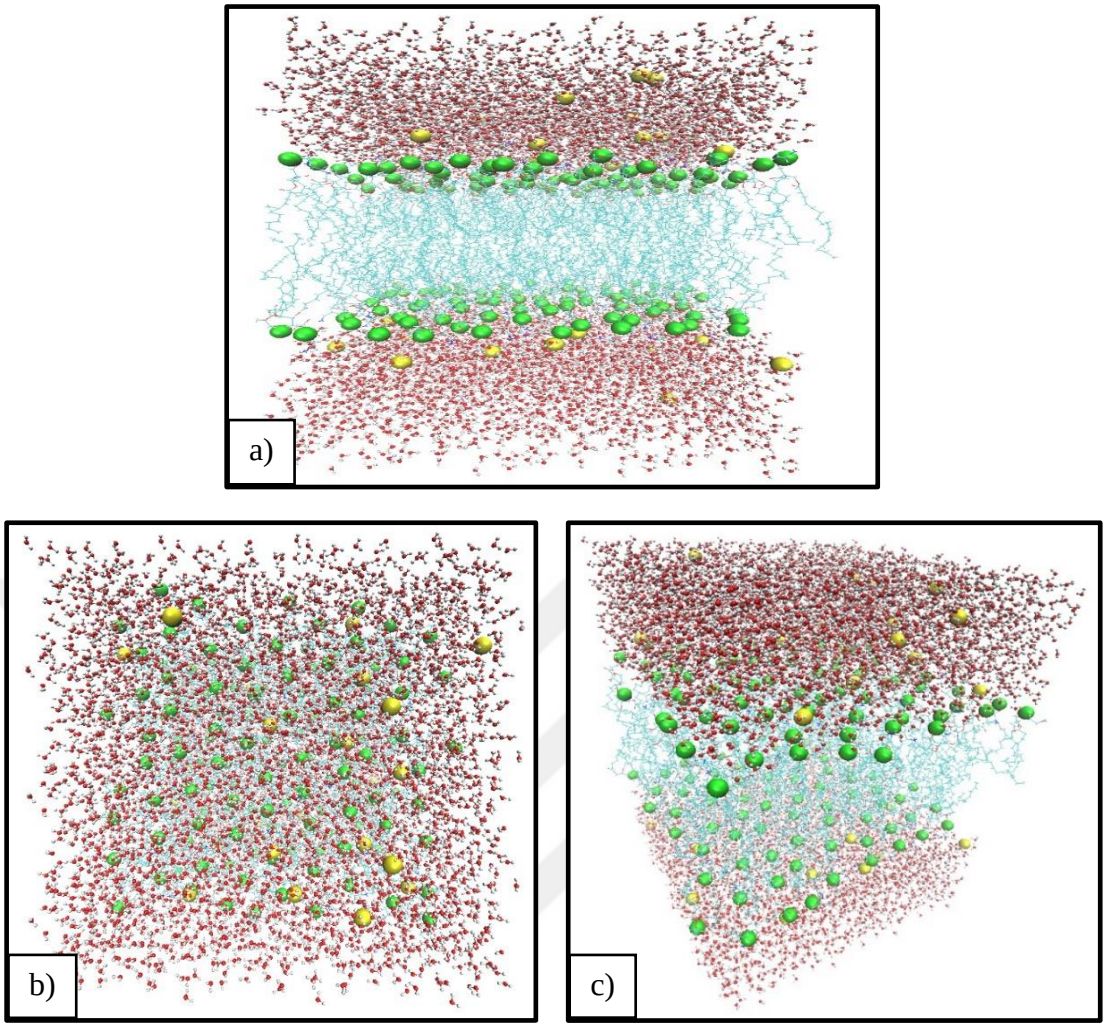

Figure 30. The simulation box designed within the scope of the project with the Top6 membrane by molecular modelling methods, from different angles; a) from the front b) from the top, and c) View from the side corner. Red oxygen, white hydrogen, with water molecules CPK notation; turquoise with line representation of lipid molecules; P atoms of the lipid heads are green with vdW notation; and ions are shown in yellow with vdW notation.

Section 2:

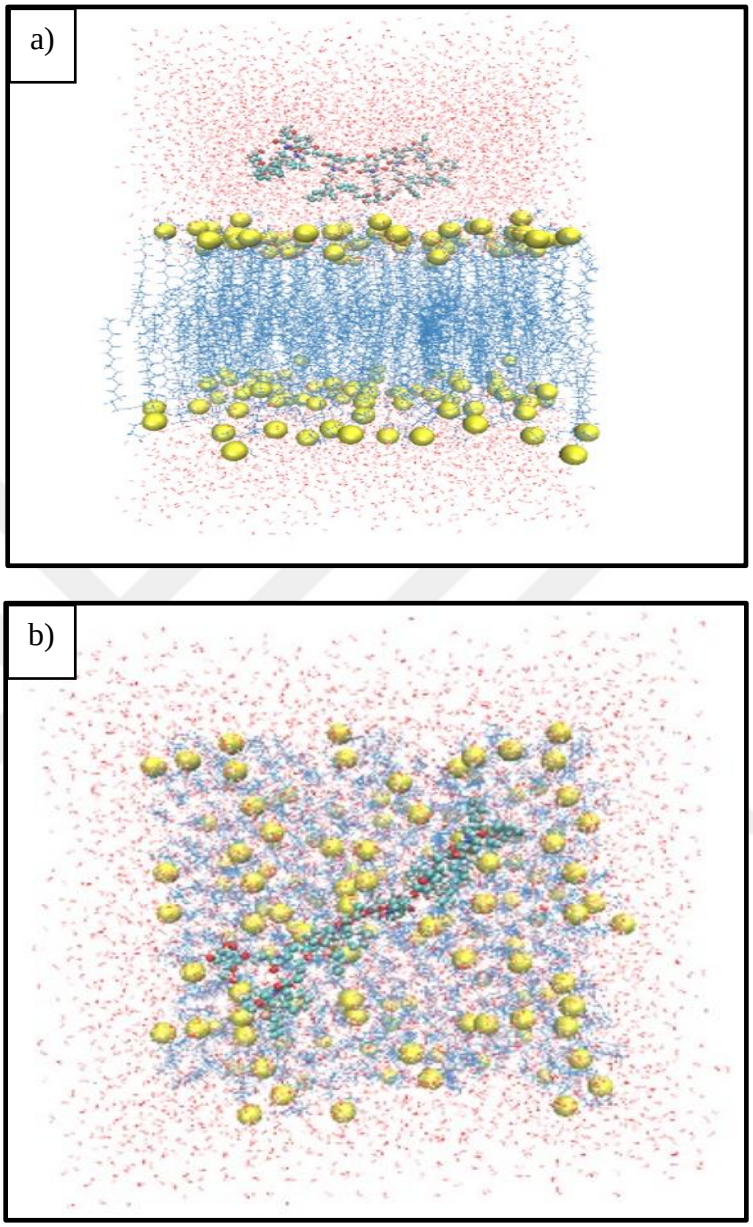

Figure 31. Positioning the designed Triphenylphosphonium:Mannose 5:2 polymer molecule on the bacterial membrane and in water. Water molecules are shown in red-white, phosphate molecules in yellow balls, membrane lipids in blue, polymer CPK notation. a) Cross-sectional view of the membrane and polymer. b) View of the membrane and polymer from above.

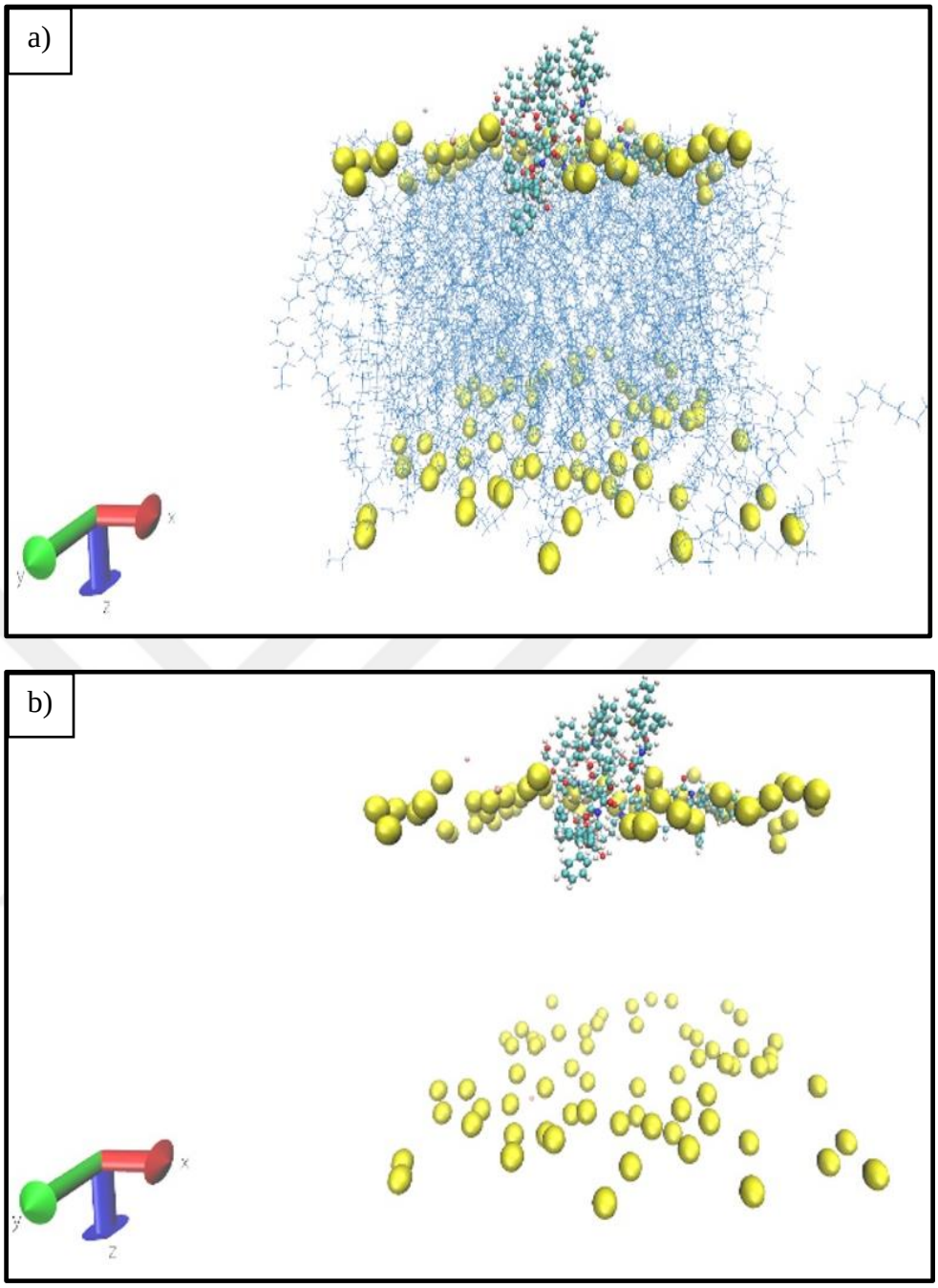

Figure 32. Molecular simulation result lasting 100ns after positioning the designed Triphenylphosphonium:Mannose 5:2 polymer molecule (P charge: -0.15095) in bacterial membrane and water. a) Phosphate molecules are shown as yellow balls, membrane lipids in blue, polymer CPK notation. b) Lipid ends are not shown in order to better see the interaction between the polymer and the membrane.

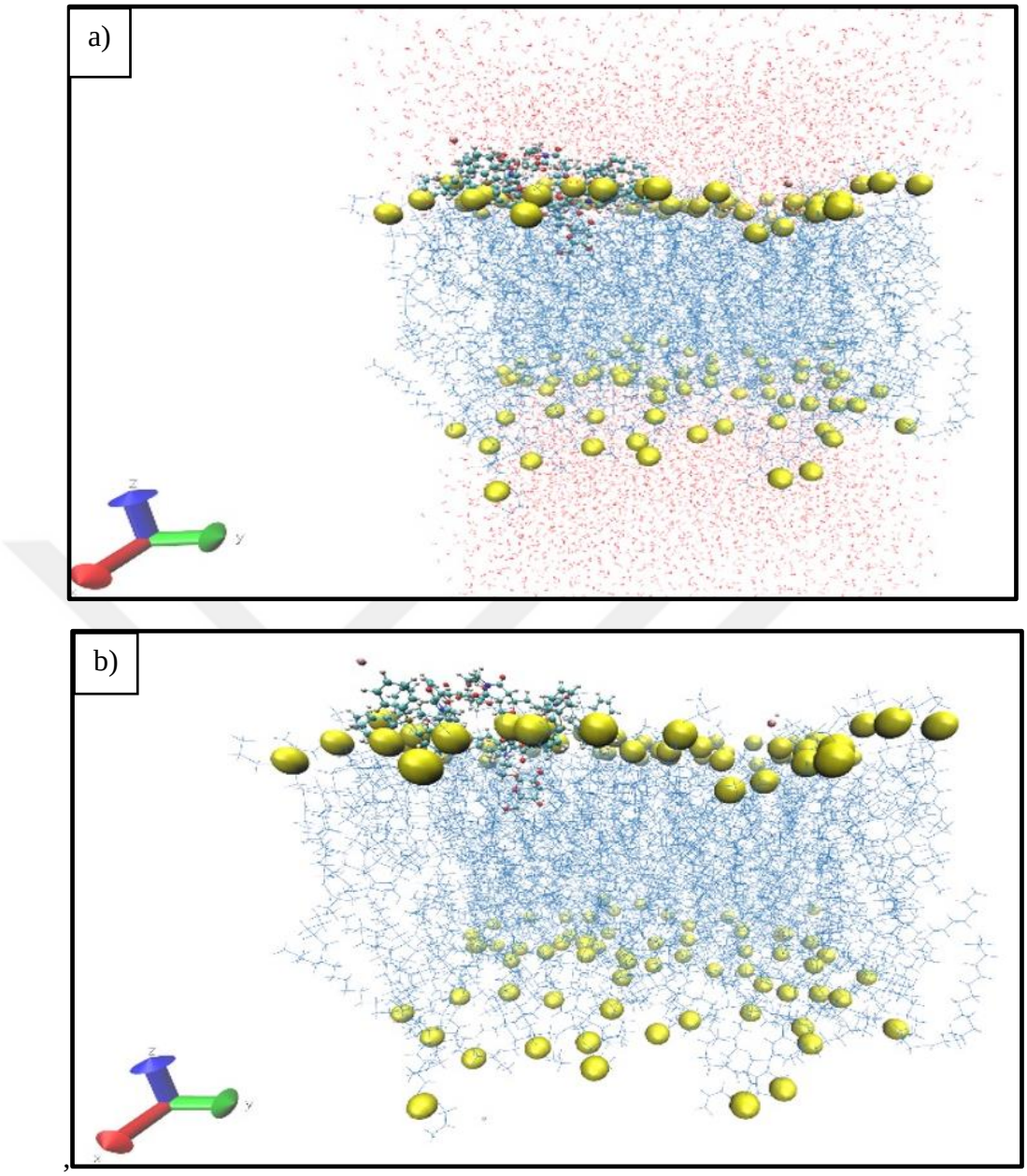

Figure 33. Molecular simulation lasting 60 ns after the positioning of the designed Triphenylphosphonium:Mannose 5:2 polymer molecule (P charge: +1) in the bacterial membrane and water. a) Water molecules are shown in red-white, phosphate molecules in yellow balls, membrane lipids in blue, polymer CPK notation. b) The view of the water being closed in order to better see the interaction between the polymer and the membrane. c) The image of the lipid ends being closed in order to better see the interaction between the polymer and the membrane. d) Another view of the end where the polymer enters the membrane.

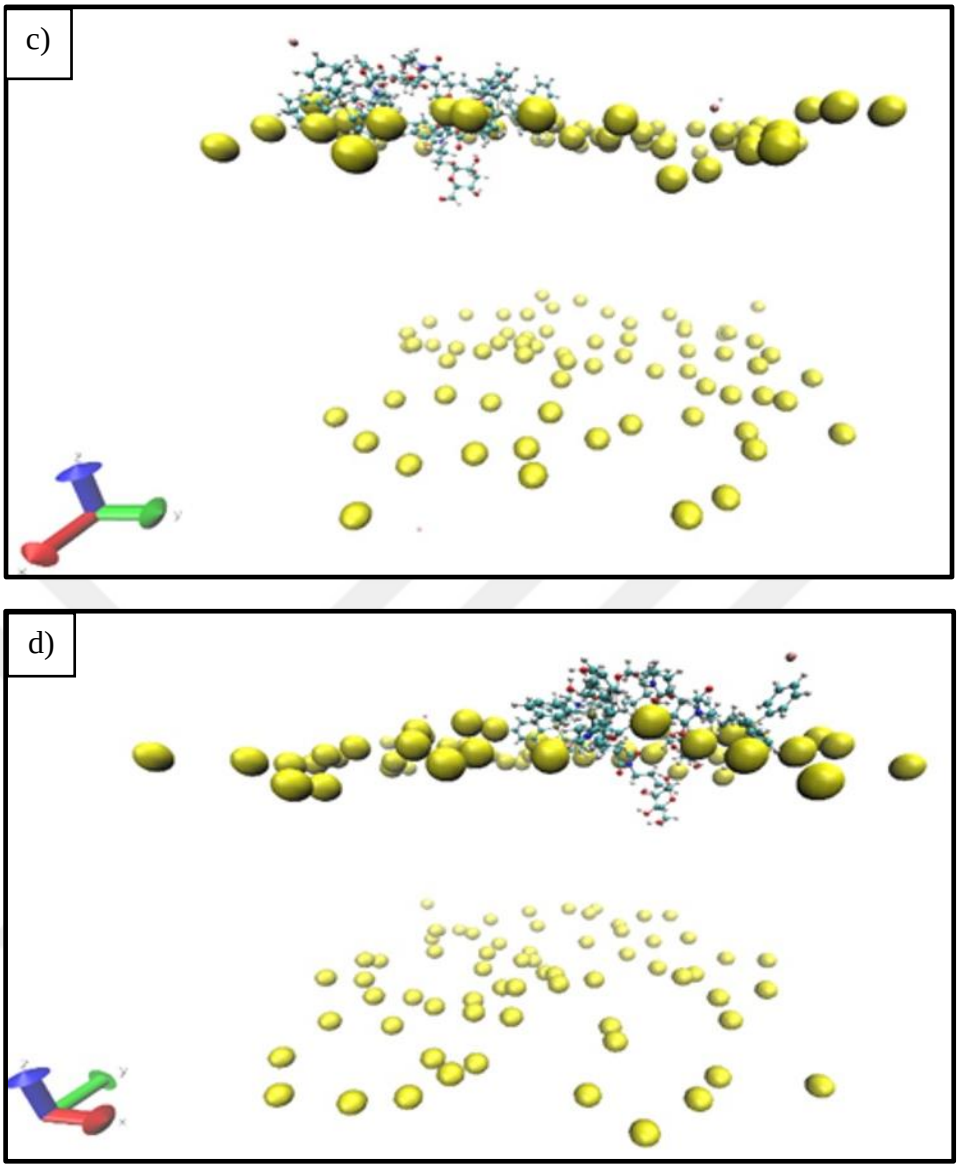

Figure 33. Molecular simulation lasting 60 ns after the positioning of the designed Triphenylphosphonium:Mannose 5:2 polymer molecule (P charge: +1) in the bacterial membrane and water. a) Water molecules are shown in red-white, phosphate molecules in yellow balls, membrane lipids in blue, polymer CPK notation. b) The view of the water being closed in order to better see the interaction between the polymer and the membrane. c) The image of the lipid ends being closed in order to better see the interaction between the polymer and the membrane. d) Another view of the end where the polymer enters the membrane (continued.

When the simulations were examined, it was observed in both simulations that the polymer moved towards the membrane and eventually penetrated into the membrane

so that the mannose group remained in the membrane. Meanwhile, it is visualized in Figure 34 that the root-mean-square-deviation graph of the polymer molecule, which was initially positioned linearly, also converges depending on the time step, that is, the polymer forms a stable conformation.

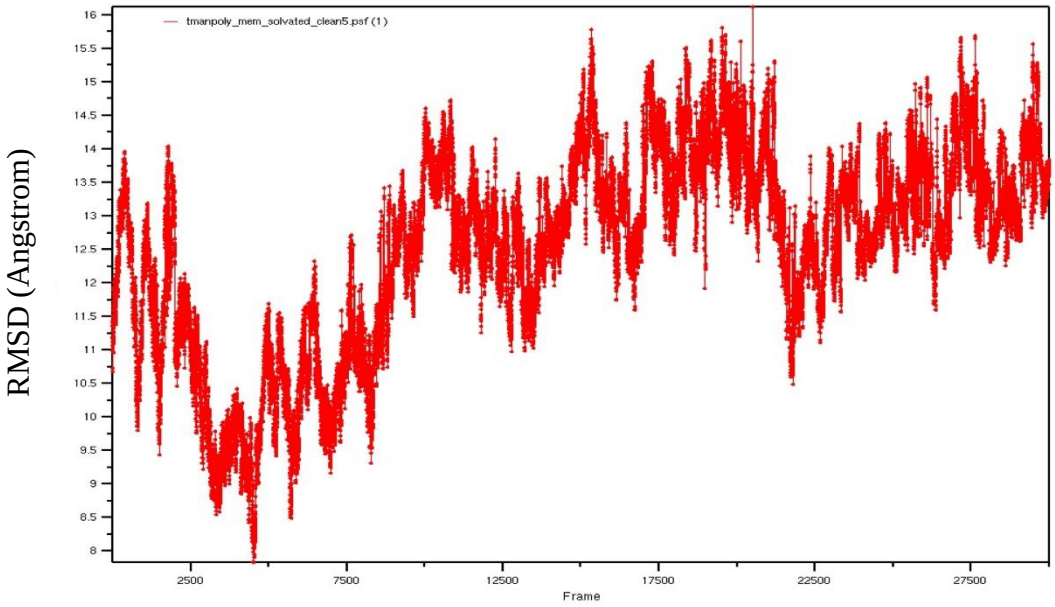

Figure 34. Time step root mean square deviation plot of the designed Triphenylphosphonium:Mannose 5:2 polymer molecule.

The graph of the distance (Angstrom) of the Triphenylphosphonium:Mannose 5:2 polymer from the membrane in the second 60 ns simulation according to the time step is given as distance-time graph in Figure 35. When this graph is examined, it is seen that the polymer molecule, which was first deployed at a distance of 12.5 Angstrom, converges to the membrane with back-and-forth movements, and the distance between the polymer and the membrane is 0 in the 16000th step, each of which is 2 fs, in about 32 ns. When the simulation was examined, it was observed that the triphenylphosphonium group first entered the membrane after adhering to the membrane, but then left, and the mannose group remained there during the simulation period after entering the membrane.

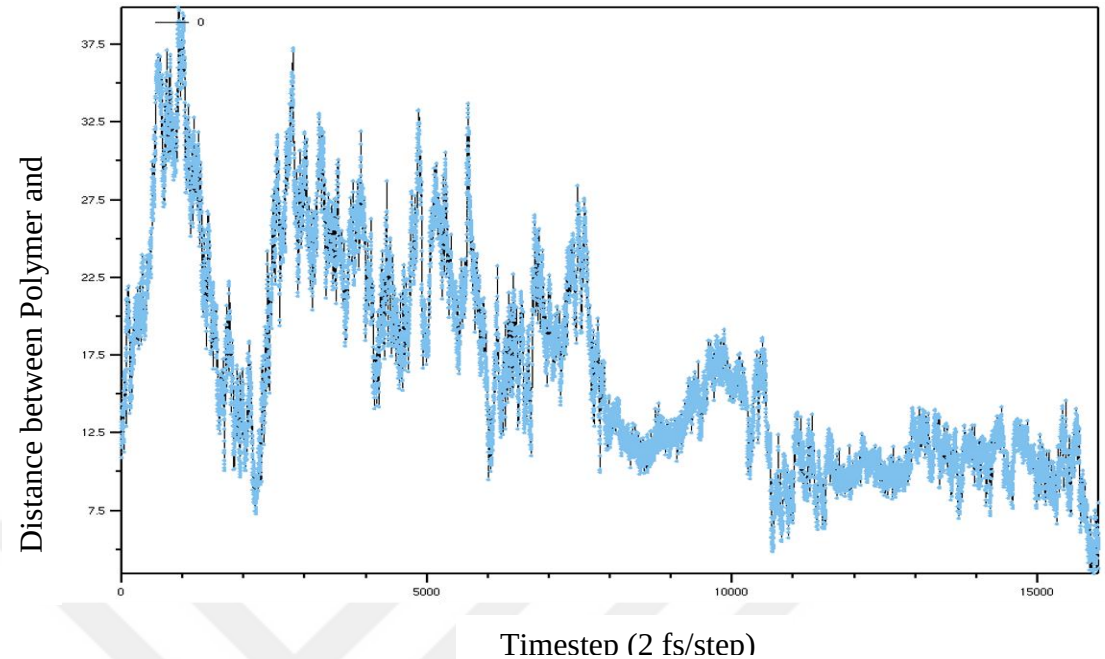

Figure 35. Graph of the distance (Angstrom) of Triphenylphosphonium:Mannose 5:2 polymer from the membrane versus time step (2fs/step)

Section 3:

Molecular simulation results lasting 200 ns after the positioning of the designed Triphenylphosphonium:Mannose 5:2 polymer molecule in the bacterial membrane and water are shown in Figure 36 and Figure 37.

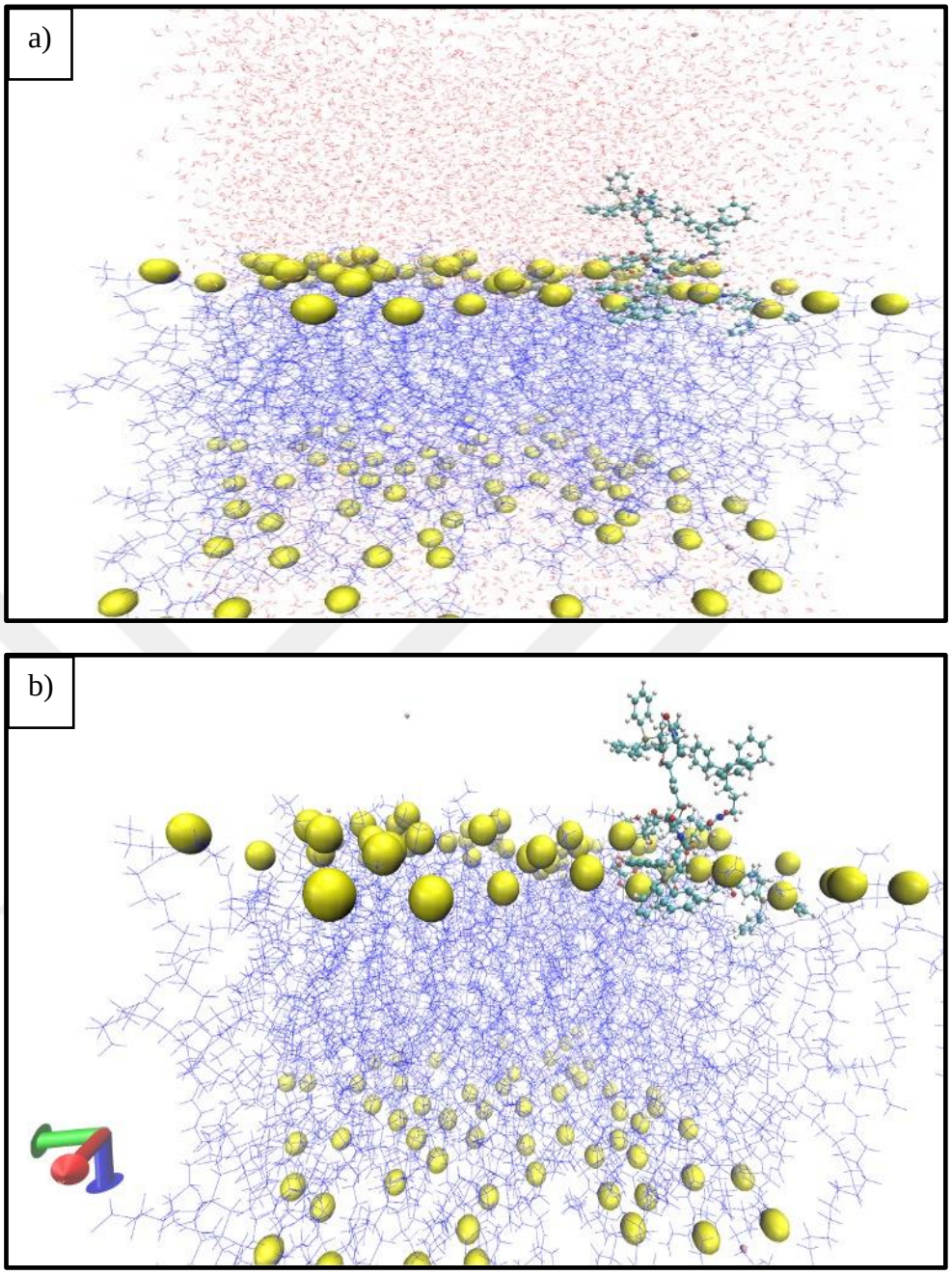

Figure 36. Molecular simulation lasting 200ns after positioning the polymer molecule (P charge: -0.15095) in bacterial membrane and water. a) Water molecules are red-white, phosphate molecules collect yellow VDW, membrane lipids are shown with blue lines, polymer CPK notation. b) The view of the water being closed in order to better see the interaction between the polymer and the membrane. c) The image of the lipid ends being closed in order to better see the interaction between the polymer and the membrane. d) Another view of the end where the polymer enters the membrane.

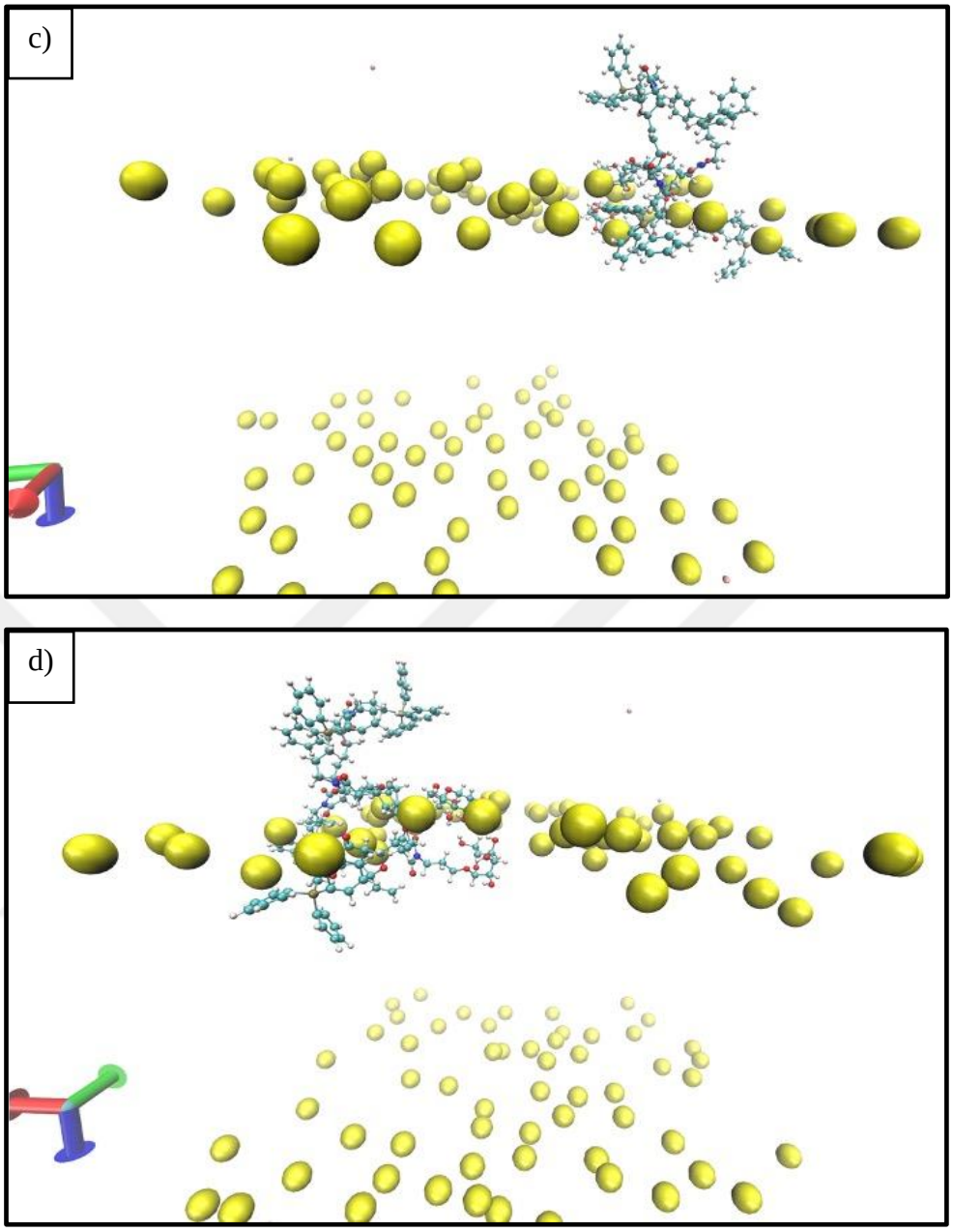

Figure 36. Molecular simulation lasting 200ns after positioning the polymer molecule (P charge: -0.15095) in bacterial membrane and water. a) Water molecules are red-white, phosphate molecules collect yellow VDW, membrane lipids are shown with blue lines, polymer CPK notation. b) The view of the water being closed in order to better see the interaction between the polymer and the membrane. c) The image of the lipid ends being closed in order to better see the interaction between the polymer and the membrane. d) Another view of the end where the polymer enters the membrane (continued).

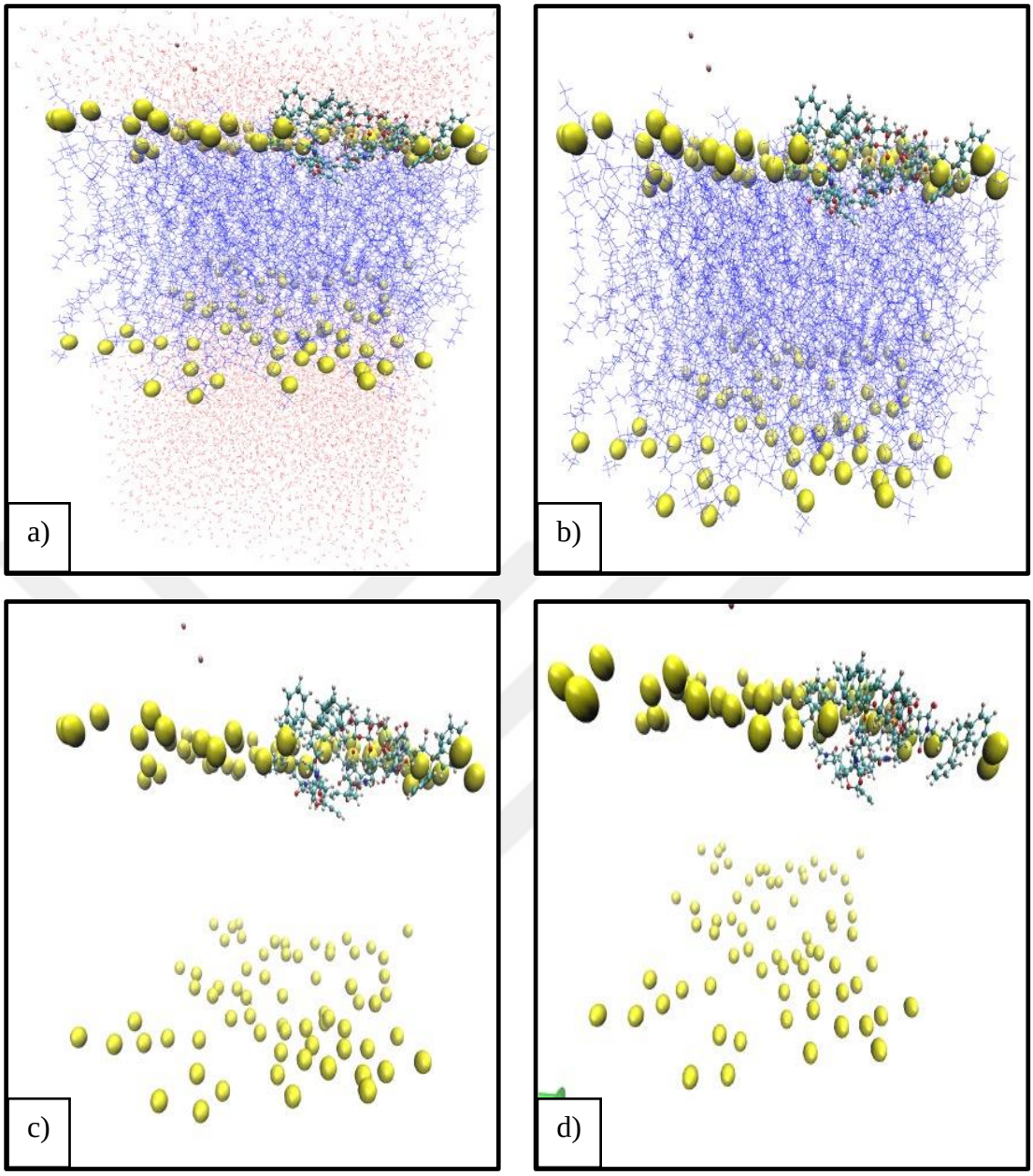

Figure 37. Molecular simulation lasting 200ns after the positioning of the polymer molecule (P charge: +1) in the bacterial membrane and water. a) Water molecules are red-white, phosphate molecules collect yellow VDW, membrane lipids are shown with blue lines, polymer CPK notation. b) The view of the water being closed in order to better see the interaction between the polymer and the membrane. c) The image of the lipid ends being closed in order to better see the interaction between the polymer and the membrane. d) Another view of the end where the polymer enters the membrane.

When the simulations are examined, in both simulations, the polymers observed in the second section of the second study, where the polymer moves towards the membrane and eventually begins to enter the membrane so that the mannose group remains in the membrane, during the simulation period between 100-200ns presented in this third section of the study, the polymers partially enter and exit the membrane, similar to the first 100ns. It was observed that it did not enter the membrane and take a vertical position.

Section 4:

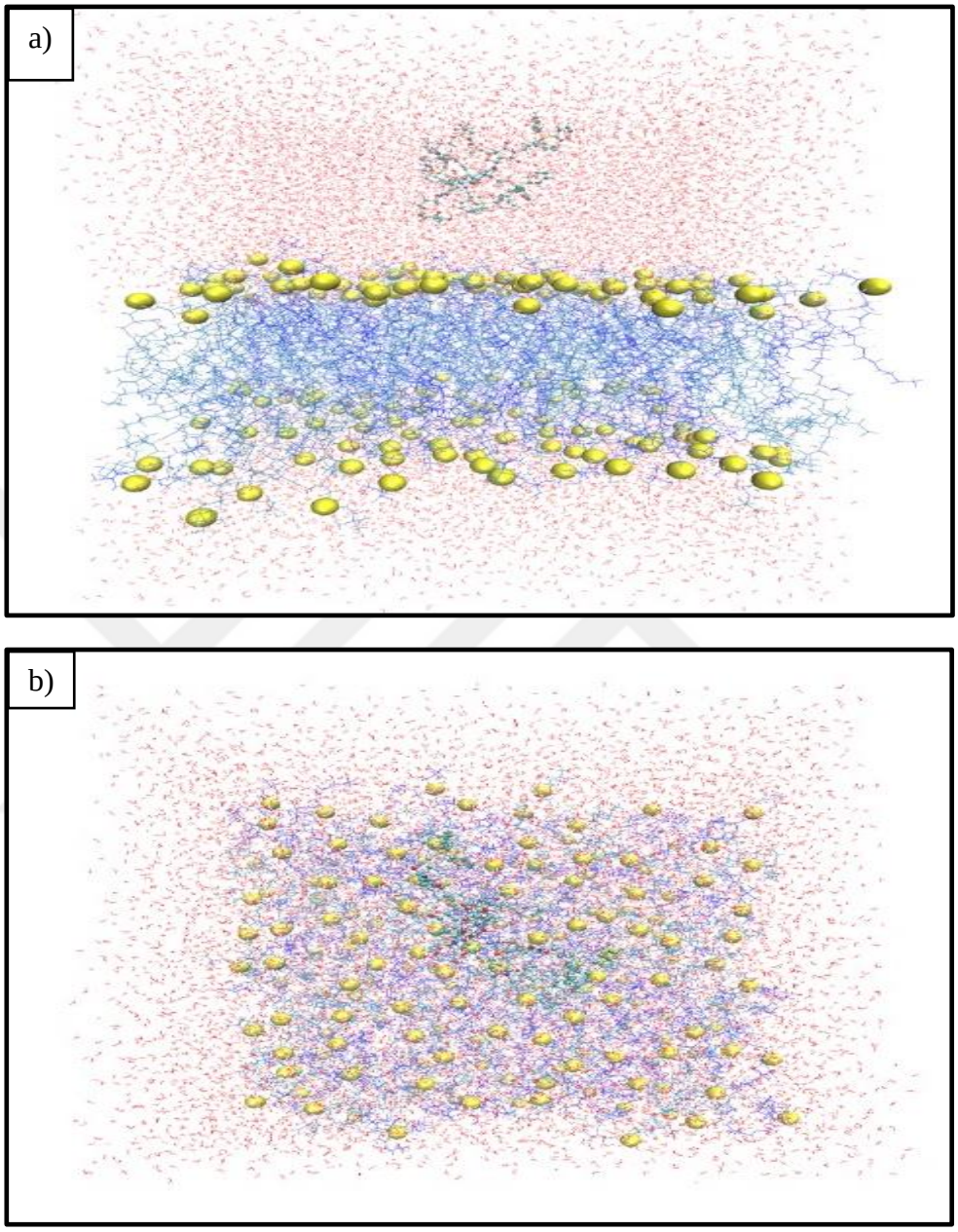

Figure 38. Positioning the designed Triphenylphosphonium:Mannose 5:2 polymer molecule on the bacterial membrane and in water. Water molecules are shown in red-white, phosphate molecules in yellow balls, membrane lipids in blue, polymer CPK notation. a) Cross-sectional view of the membrane and polymer. b) View of the membrane and polymer from above.

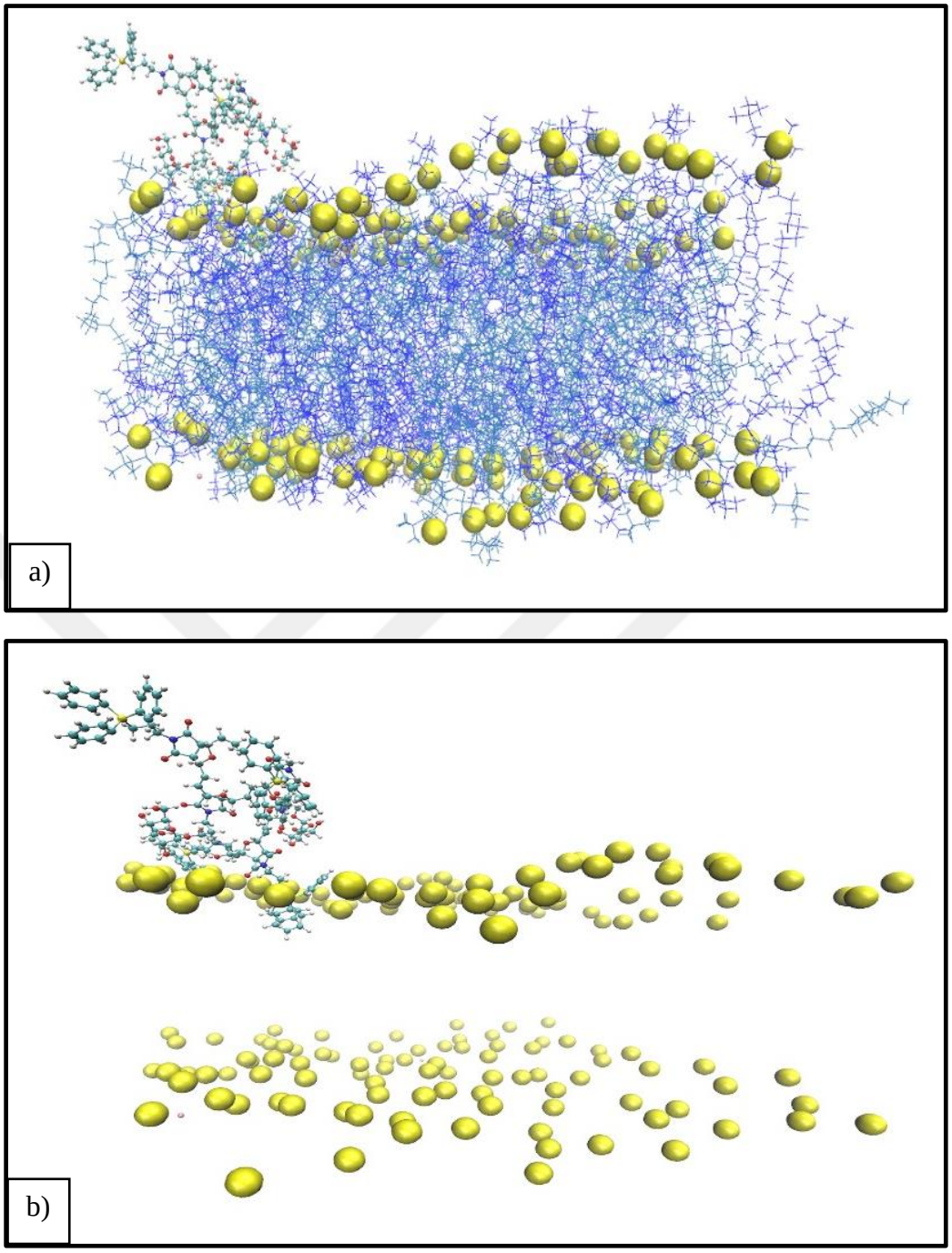

Figure 39. Molecular simulation result lasting 100ns after positioning the designed Triphenylphosphonium:Mannose 5:2 polymer molecule (P charge: +1) in bacterial membrane and water. a) Phosphate molecules are shown as yellow balls, membrane lipids in blue, polymer CPK notation. b) Lipid ends are not shown to see the interaction between the polymer and the membrane better.

When the simulation was examined, it was observed that the polymer oriented towards the membrane and eventually penetrated the membrane so that the mannose group remained in the membrane. Meanwhile, it is visualized in Figure 40 that the root-mean square deviation graph of the polymer molecule, which was initially positioned linearly, also converges to the time step, that is, the polymer forms a stable conformation.

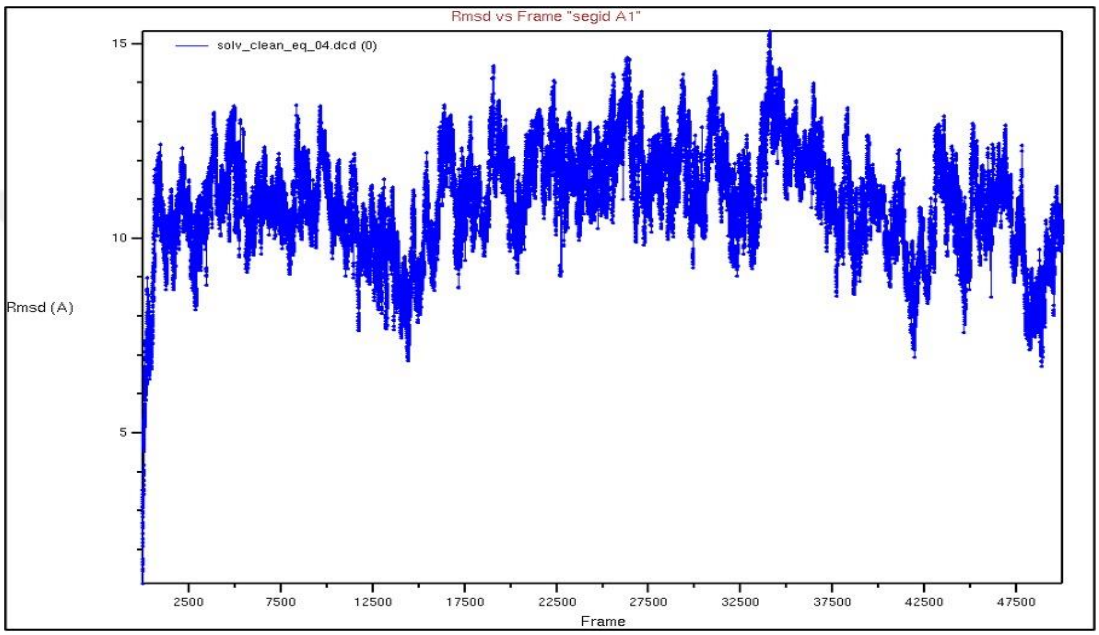

Figure 40. Time step root mean square deviation plot of the designed Triphenylphosphonium:Mannose 5:2 polymer molecule.

The graph of the distance (Å) of the Triphenylphosphonium:Mannose 5:2 polymer from the membrane in the second 100ns simulation according to the time step is given in Figure 41.

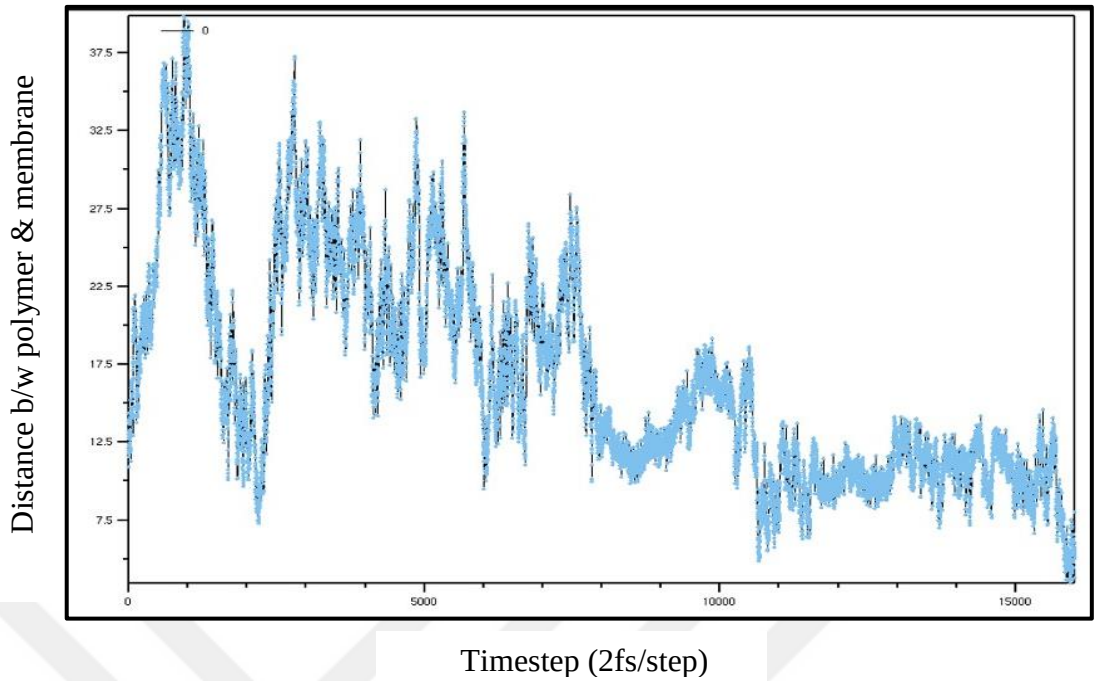

Figure 41. Graph of the distance (Å) of Triphenylphosphonium:Mannose 5:2 polymer from the membrane versus time step (2fs/step).

When this graph is examined, it is seen that the polymer molecule, which was first positioned at a distance of about 15 Å, converges to the membrane with back-and-forth movements, and after the 30000th step, the distance between the polymer and the membrane becomes 0 in 2 fs steps, that is, in approximately 60 ns. When the simulation was examined, it was observed that the triphenylphosphonium group first entered the membrane after adhering to the membrane, but then came out, while the mannose group remained there during the simulation period after entering the membrane.

4.2.2 Docking

Section 2:

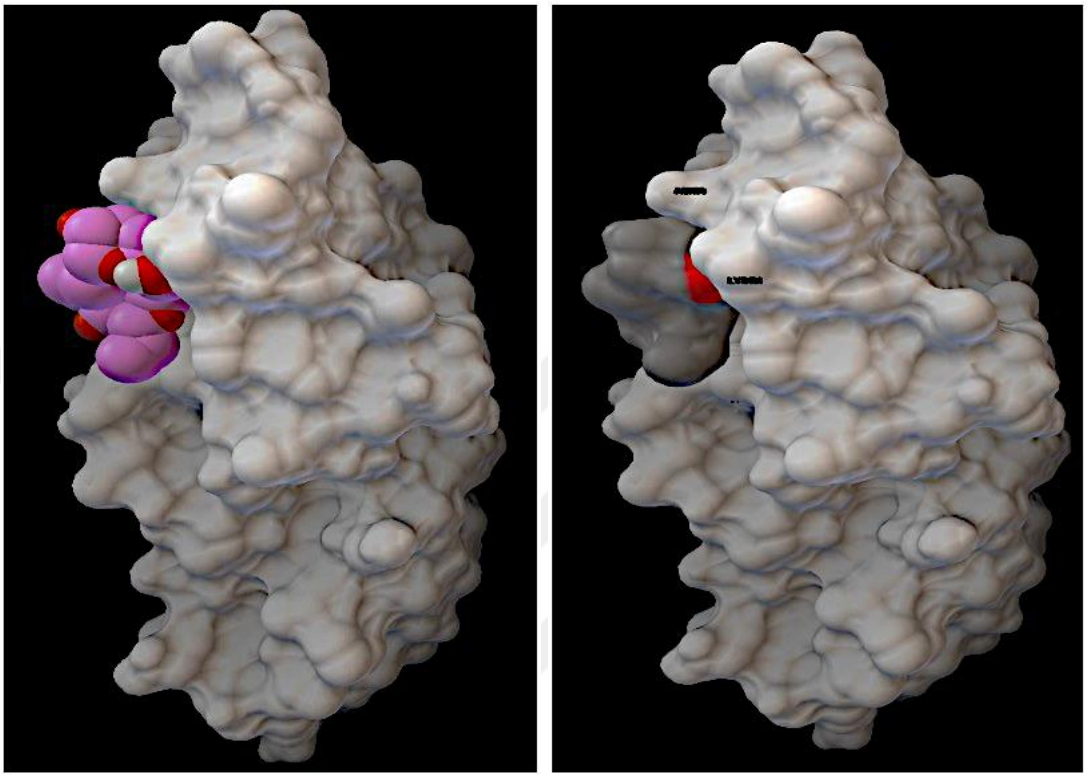

Figure 42. Investigation of the interaction of lectin protein and mannose group with MGLTools software (113). The lectin protein is shown in light gray, and the monomer part of the polymer containing the mannose group is shown in pink and dark gray by choosing the molecular surface representation.

When the shape and docking results were examined, it was found that the docking binding score was -1.14, where mannose binds to the lectin protein from a binding site containing LYS and ARG amino acids.

Section 4:

Using the AutoDock Tool and Autodock Vine, the docking investigation of the interactions between the two molecules was conducted after acquiring the 3D structural data of Lectin and Mannose independently.

The binding score (affinity) for lectin- mannose was discovered to be -6.4. A docking analysis of the lectin-galactose interaction was also conducted. It is intended to compare how mannose and galactose interact through this process. The results showed that the lectin-galactose docking interaction score was -6.5. The data showed that mannose and galactose showed a negligible difference when interacting with the lectin protein.

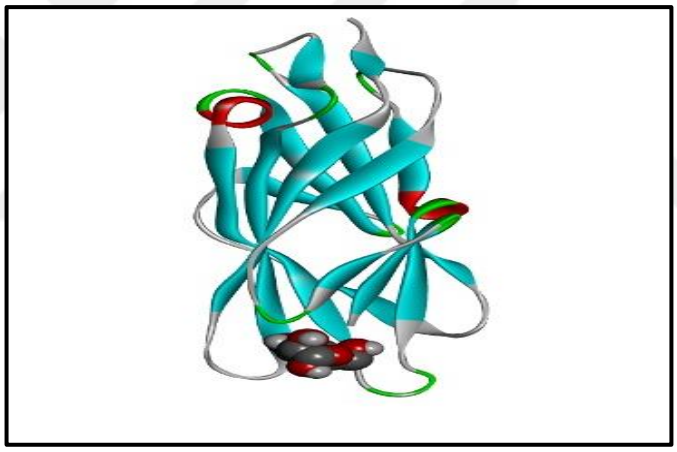

Figure 43. Investigation of the interaction of lectin protein and mannose group with Discovery Studio (2021) software. Lectin protein is shown in “solid ribbon” format in turquoise, red and green, Mannose monomer is shown in CPK format in black and red.

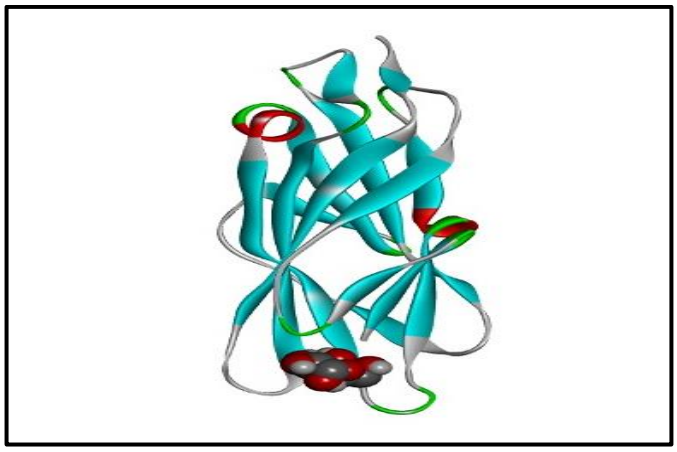

Figure 44. Investigation of the interaction of lectin protein and galactose group with Discovery Studio (2021) software. Lectin protein is shown in “solid ribbon” format in turquoise, red and green, Mannose monomer is shown in CPK format in black and red.

4.3 Molecular Modelling Experiments of Antimicrobial Peptides and Polymers Mimicking Antimicrobial Peptides Inspired from Nature

Here, the visualizations of the initial input and output positions obtained as a result of the modelling for the peptide membrane systems simulated, the distances of the peptides from the P atoms of the membrane depending on the time step, and the root mean square deviation graphs are given. In addition, the comparison of the contact times of each amino acid and the phosphate ends of the bacterial membrane in percentage terms for the L and D forms of the selected TN6 peptide is shown in the Table 8 and Table 9:

4.3.1 Molecular dynamics simulation

Section 1:

TN3 Peptide – 12 pack in rectangular shape

The TN3 peptide structure was first placed in the water phase on the membrane, as seen in Figure 45 with 12 peptides at a distance of approximately 10 Å to the membrane and to each other.

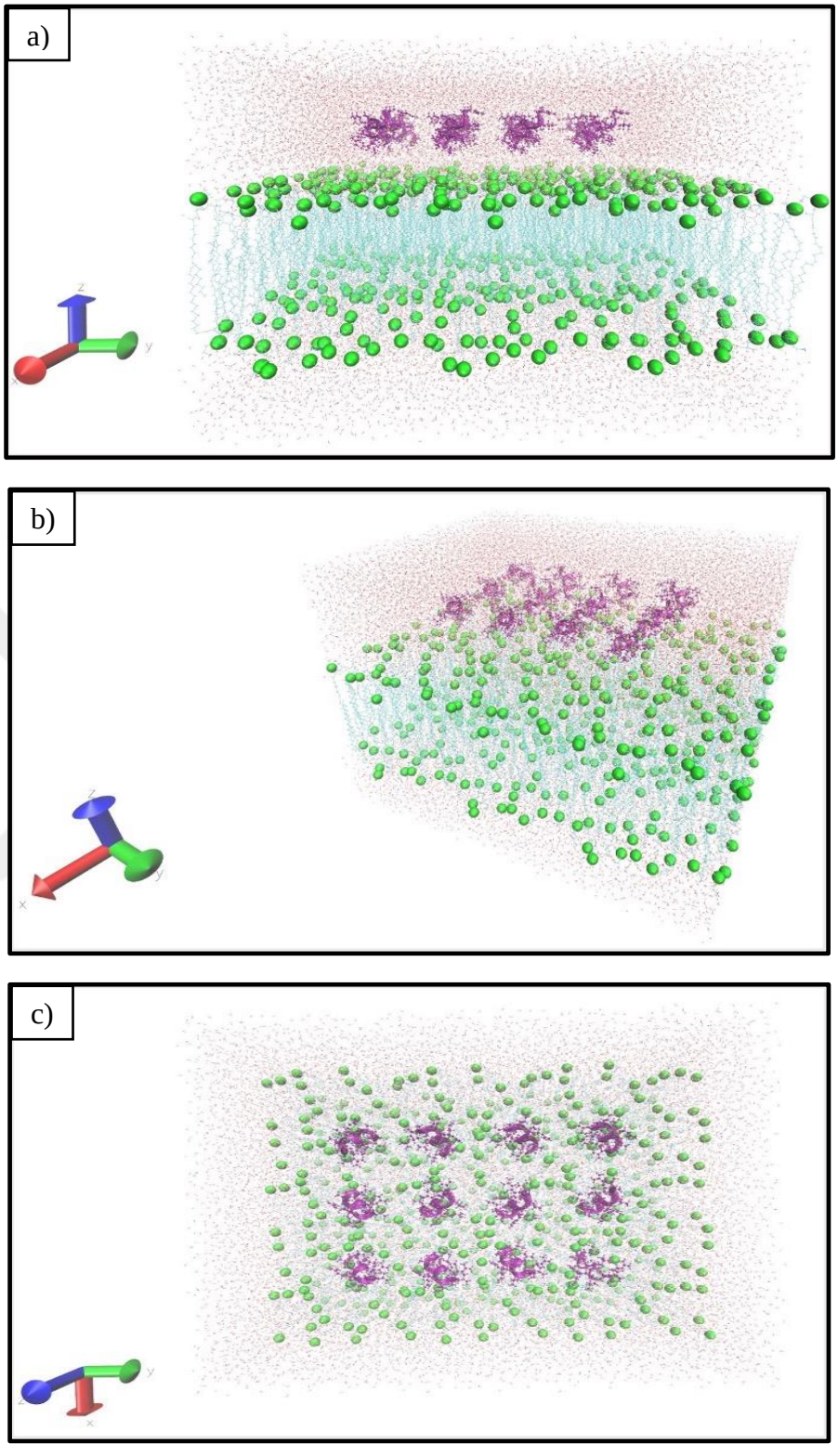

Figure 45. Rectangular positioning of the TN3 peptide on the bacterial membrane and in water, a) side view, b) side cross view, c) top view. Water molecules are shown in red-white, phosphate molecules in green balls, membrane lipids in light blue, alpha helix structure of peptides and atoms in purple.

After the simulation system shown in the figure above was prepared, it was used as the initial input and a 100ns MD simulation was carried out. In Figure 46, this simulation result of the TN3 peptide is visualized from the top and the side. It has been observed that TN3 molecules tend to move towards the membrane and enter the membrane during this simulation period of 100ns.

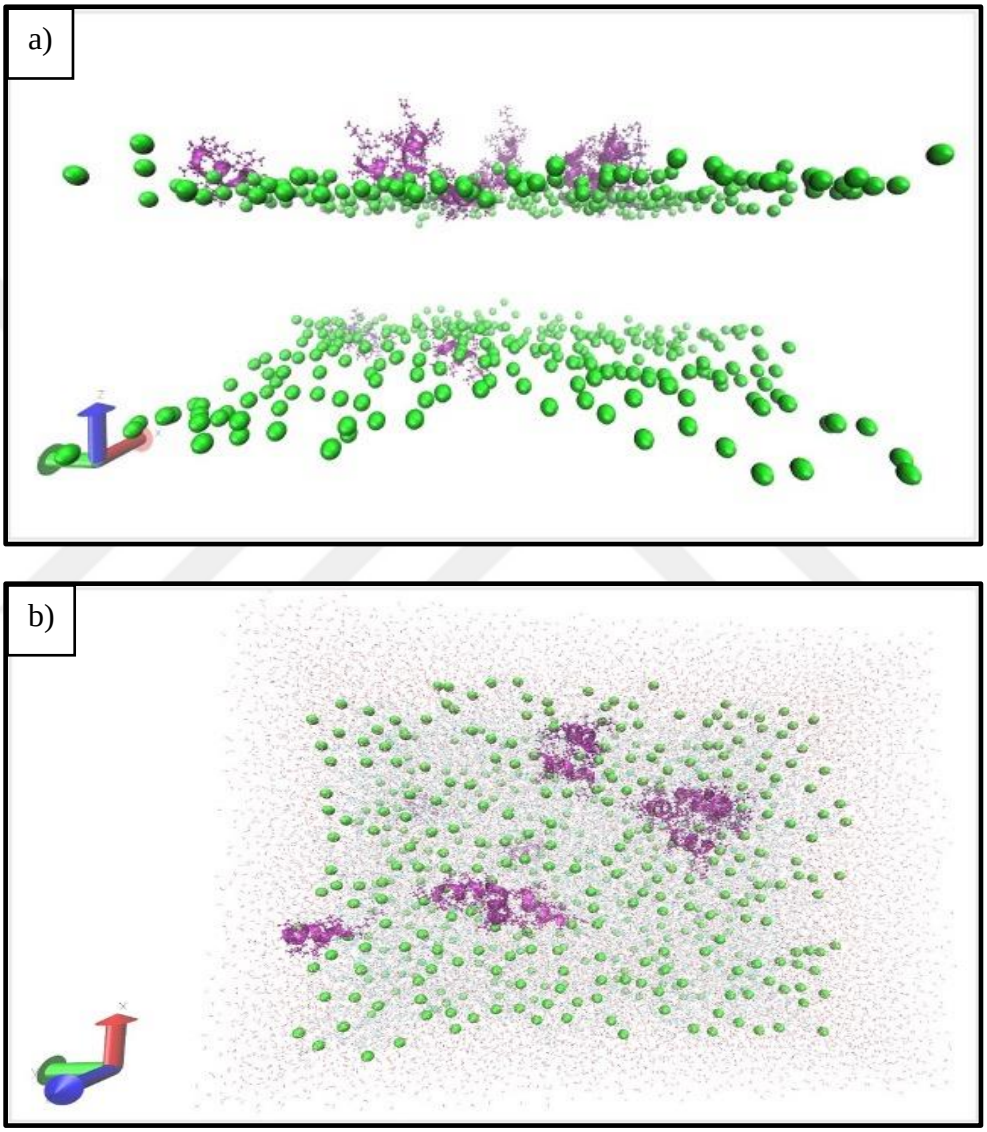

Figure 46. Molecular simulation lasting 100 ns after the TN3 peptide is positioned on the bacterial membrane and in water, a) side view (lipid ends and water molecules are closed for better observation of membrane entry), b) top view. Water molecules are shown in red-white, phosphate molecules in green balls, membrane lipids in light blue, alpha helix structure of peptides and atoms in purple.

The graph of the distance (Angstrom) of the TN3 (rectangularly positioned) peptide to the membrane is given in Figure 47, and the root mean square deviation graph is given in Figure 48.

It is observed in Figure 46 that the peptides positioned as 12 and rectangular shape are grouped in a maximum of 4 peptide pack. For this reason, peptides continued to be positioned as 4 to save time and computer power.

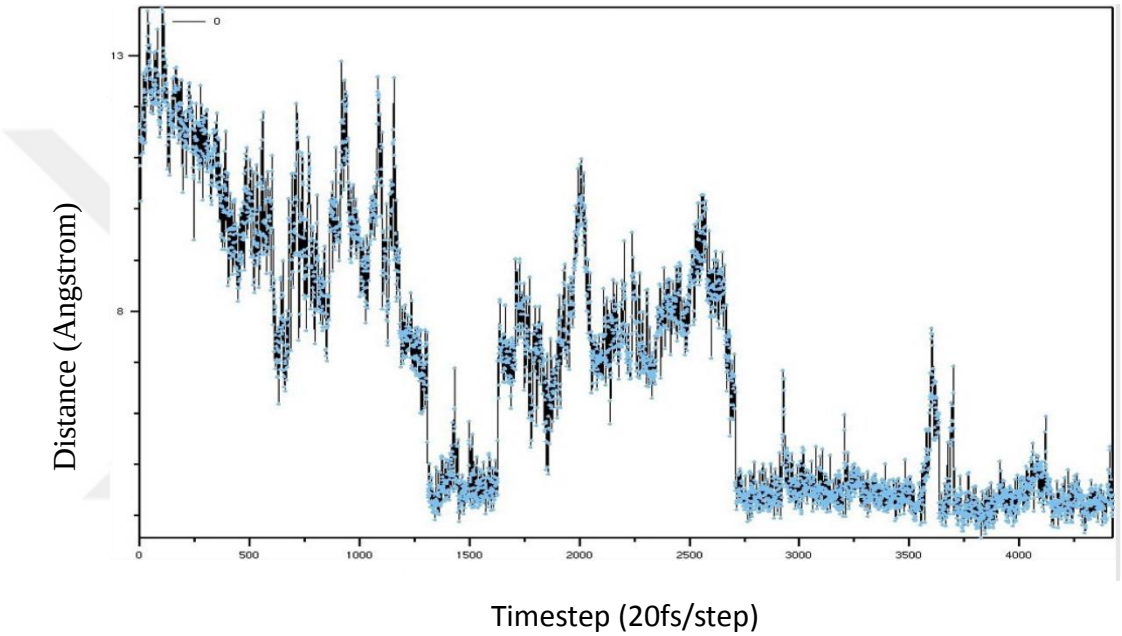

Figure 47. Graph of TN3 peptide's distance from the membrane (Angstrom) versus time step.

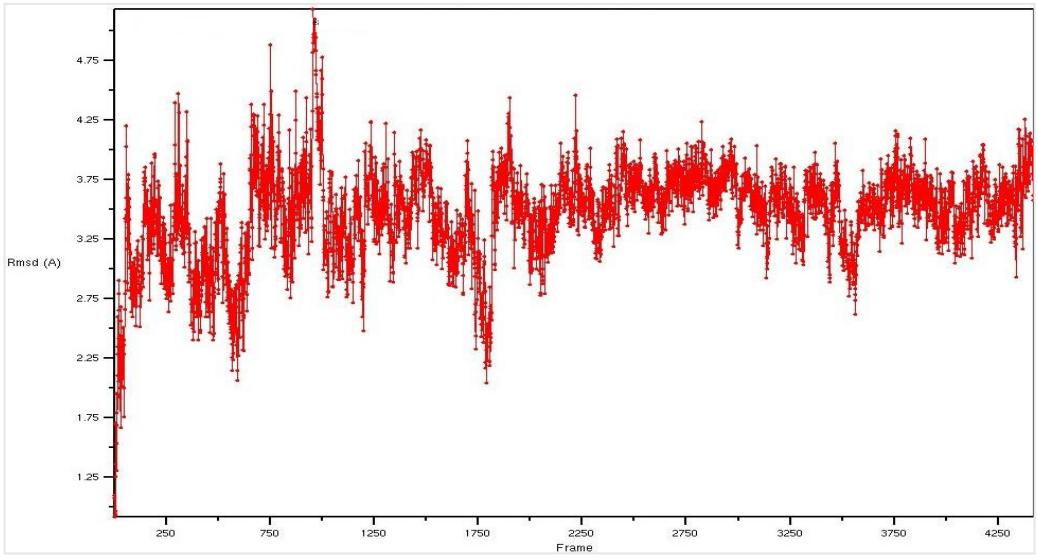

Figure 48. Graph of root mean square deviation of TN3 peptide with respect to timestep

TN3 Peptide – 12 pack in circular shape

As seen in Figure 49, the TN3 peptide structure was first placed in 12 pieces in the water phase on the membrane, with a distance of approximately 10 Å to the membrane and to each other.

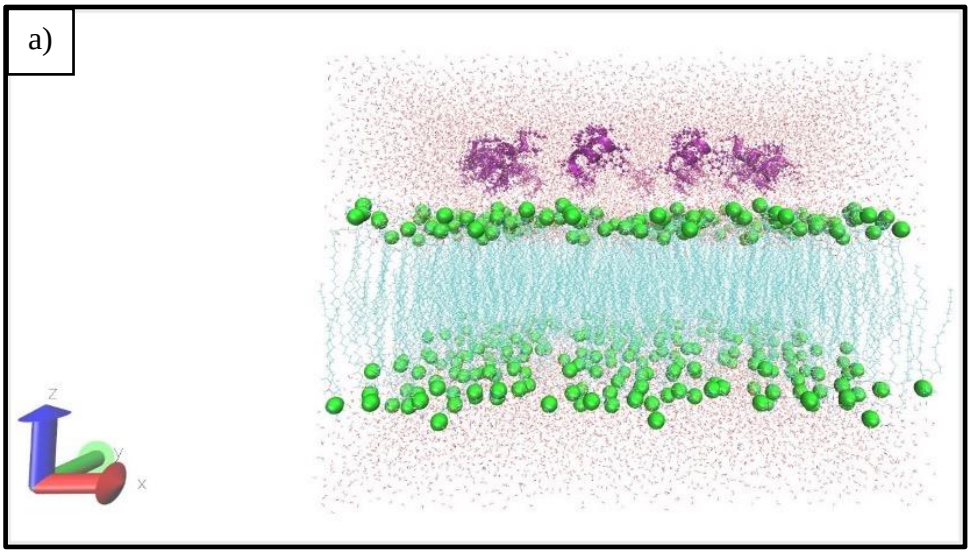

Figure 49. Circular positioning of the TN3 peptide on the bacterial membrane and in water, a) side view, b) side cross view, c) top view. Water molecules are shown in red-white, phosphate molecules in green balls, membrane lipids in light blue, alpha helix structure of peptides and atoms in purple.

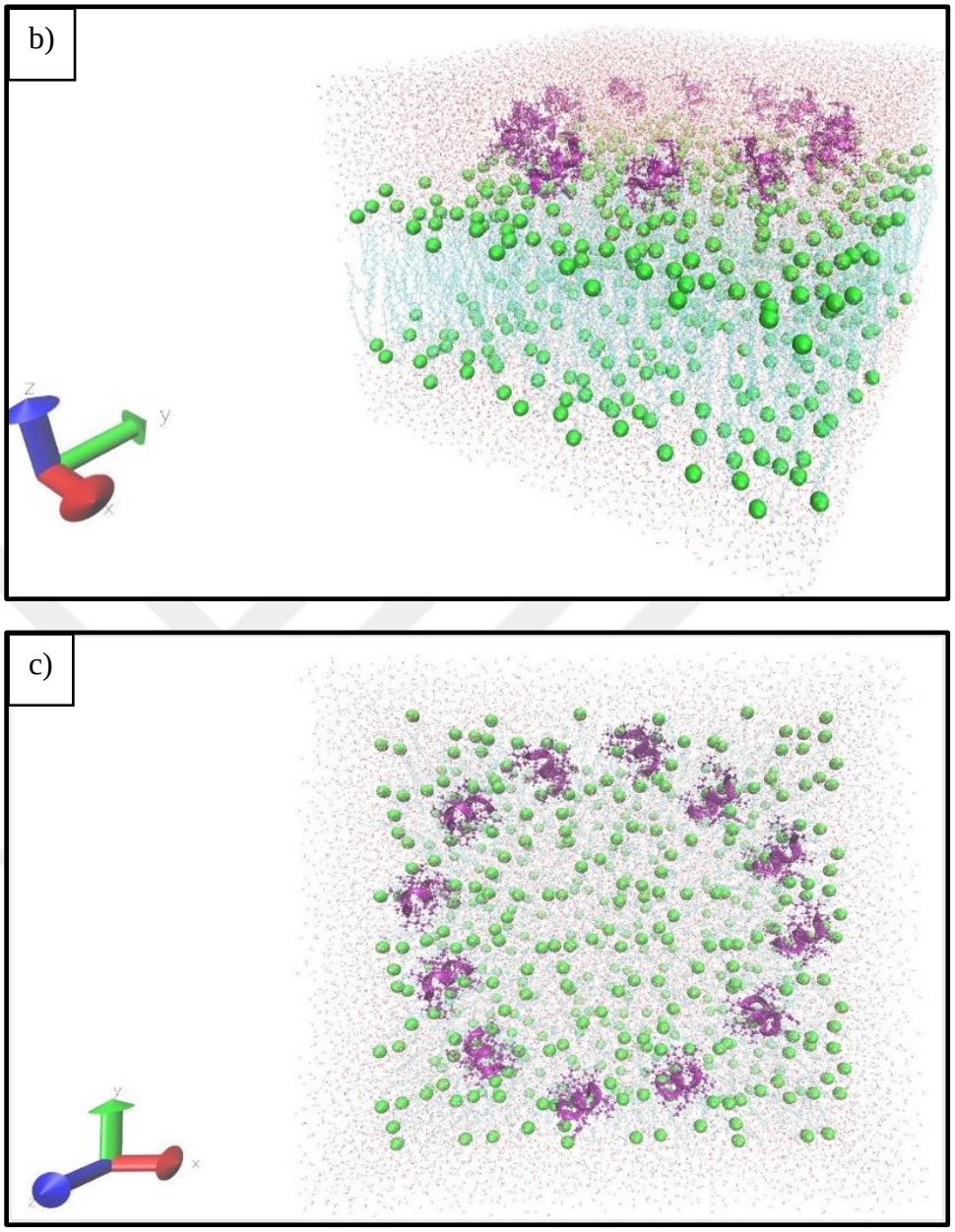

Figure 49. Circular positioning of the TN3 peptide on the bacterial membrane and in water, a) side view, b) side cross view, c) top view. Water molecules are shown in red-white, phosphate molecules in green balls, membrane lipids in light blue, alpha helix structure of peptides and atoms in purple (continued).

After the simulation system shown in the figure above was prepared, it was used as the initial input and a 100ns MD simulation was carried out. In Figure 50, this simulation result of the TN3 peptide is visualized from the top and the side. It has been

observed that TN3 molecules tend to move towards the membrane and enter the membrane during this simulation period of 100ns.

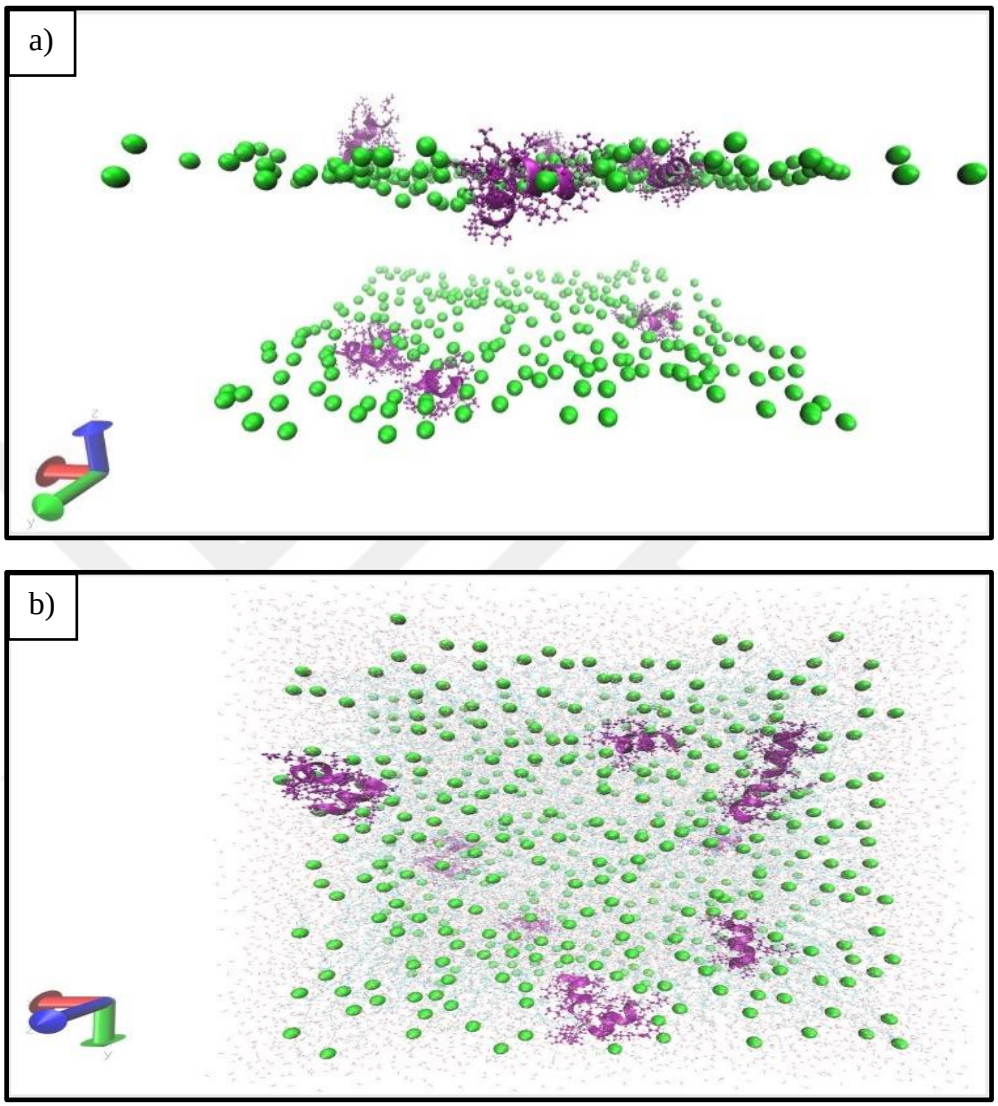

Figure 50. TN3 molecule positioned on the bacterial membrane and in water, a) side view (lipid ends and water molecules are eliminated for better observation of membrane entry), b) top view. Water molecules are shown in red-white, phosphate molecules in green balls, membrane lipids in light blue, alpha helix structure of peptides and atoms in purple.

The graph of the distance (Angstrom) of the TN3 (located in the circular) peptide to the membrane is given in Figure 51, and the root mean square deviation graph is given in in Figure 52.

It is observed in Figure 50 that the peptides positioned as 12 and ring shape are grouped in maximum of 4 peptide pack. For this reason, peptides continued to be positioned as 4 to save time and computer power.

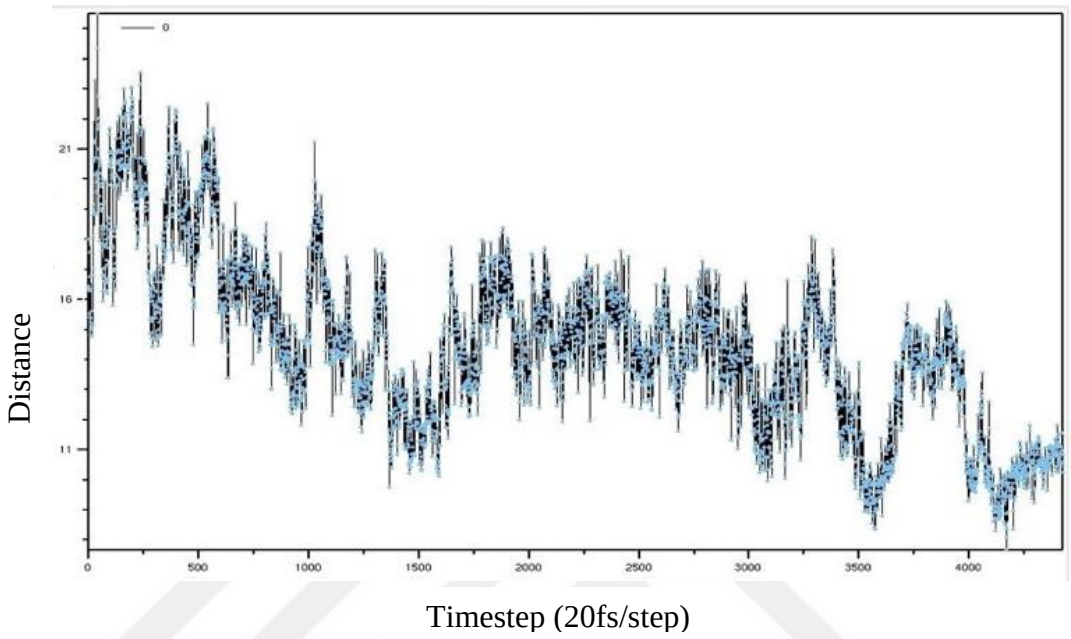

Figure 51. Graph of TN3 peptide's distance from the membrane (Angstrom) versus time step.

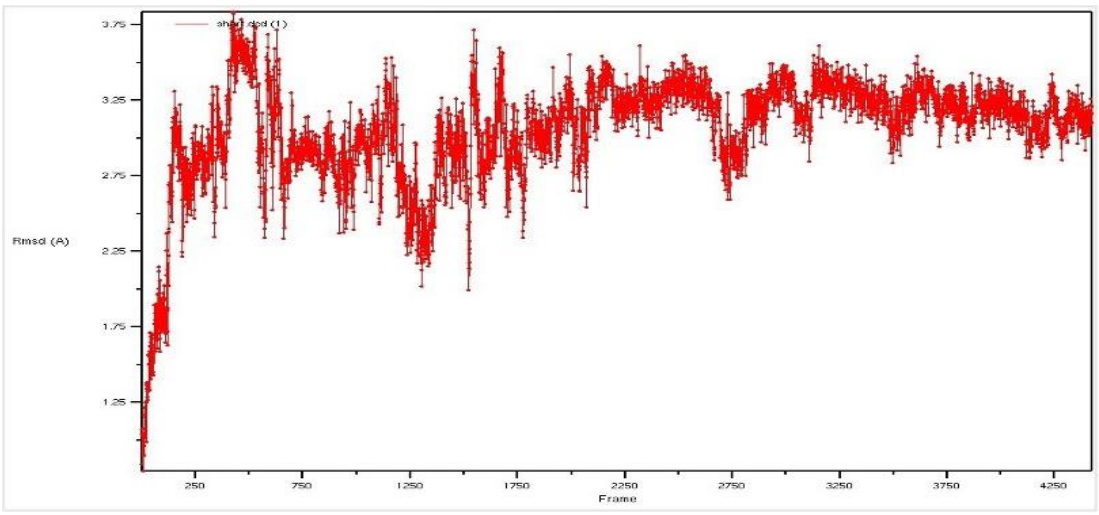

Figure 52. Graph of root mean square deviation of TN3 peptide with respect to time step.

TN3-isoleucine Peptide (RIIRIIRIII)

As seen in Figure 53, the TN3-isoleucine peptide structure was first placed in the water phase on the membrane in 4 pieces, with a distance of approximately 10 Å to the membrane and to each other.

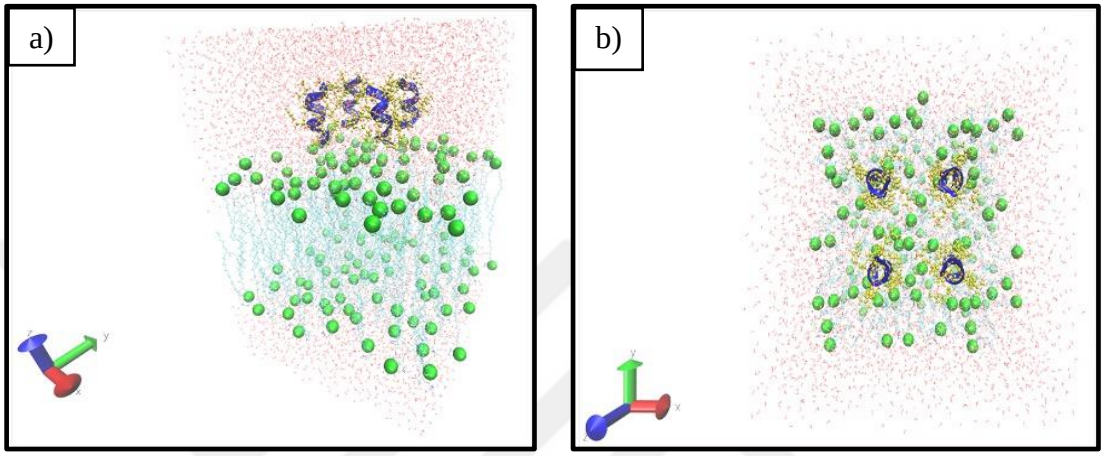

Figure 53. Positioning of the TN3-isoleucine peptide on the bacterial membrane and in water, a) lateral diagonal view, b) top view. Water molecules are shown in red-white, phosphate molecules in green balls, membrane lipids in light blue, alpha helix structure of peptides in blue and atoms in yellow.

After the simulation system shown in the figure above was prepared, it was used as the initial input and a 10 ns MD simulation was carried out. In Figure 54, this simulation result of the TN3-isoleucine peptide is visualized from the top and the side. As visualized in this way, it was observed that TN3-isoleucine molecules tended towards the membrane during this short simulation time of 10ns.

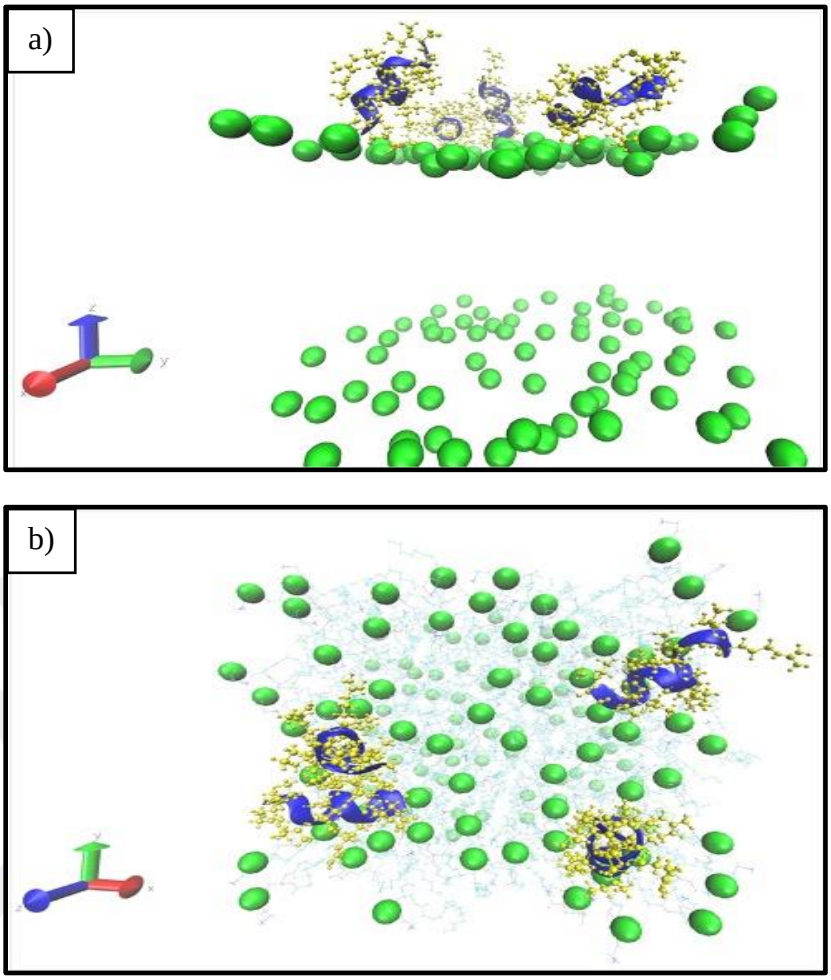

Figure 54. As a result of molecular simulation lasting 10ns after positioning the TN3-isoleucine peptide on the bacterial membrane and in water, a) side view (lipid ends and water molecules are eliminated for better observation of the approach to the membrane), b) top view. Water molecules are shown in red-white, phosphate molecules in green balls, membrane lipids in light blue, alpha helix structure of peptides in blue and atoms in yellow.

The graph of the distance (Angstrom) of the TN3-isoleucine peptide to the membrane according to the time step is given in Figure 55, and the root mean square deviation graph is given in Figure 56.

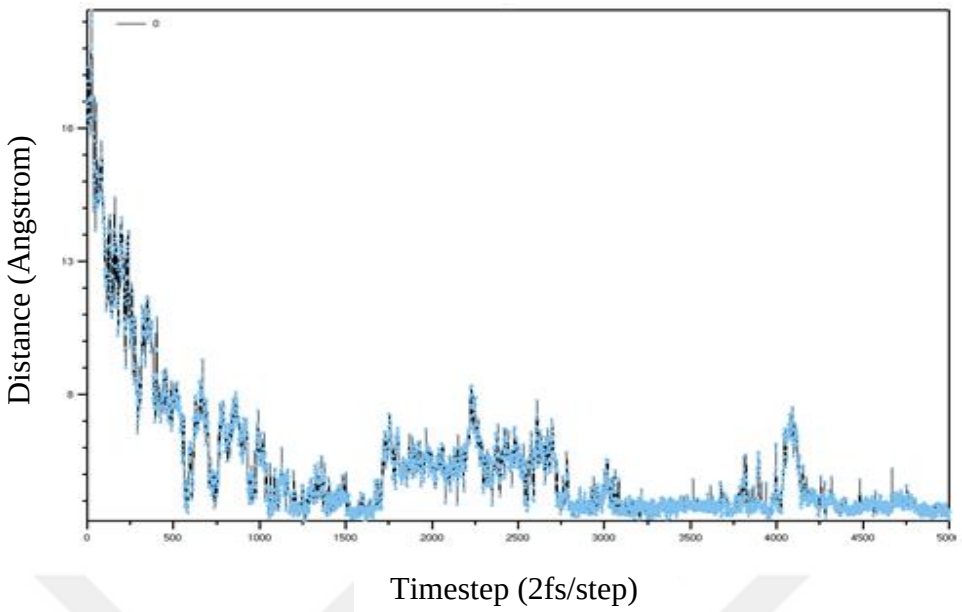

Figure 55. Graph of the distance (Angstrom) of the TN3-isoleucine peptide from the membrane over time.

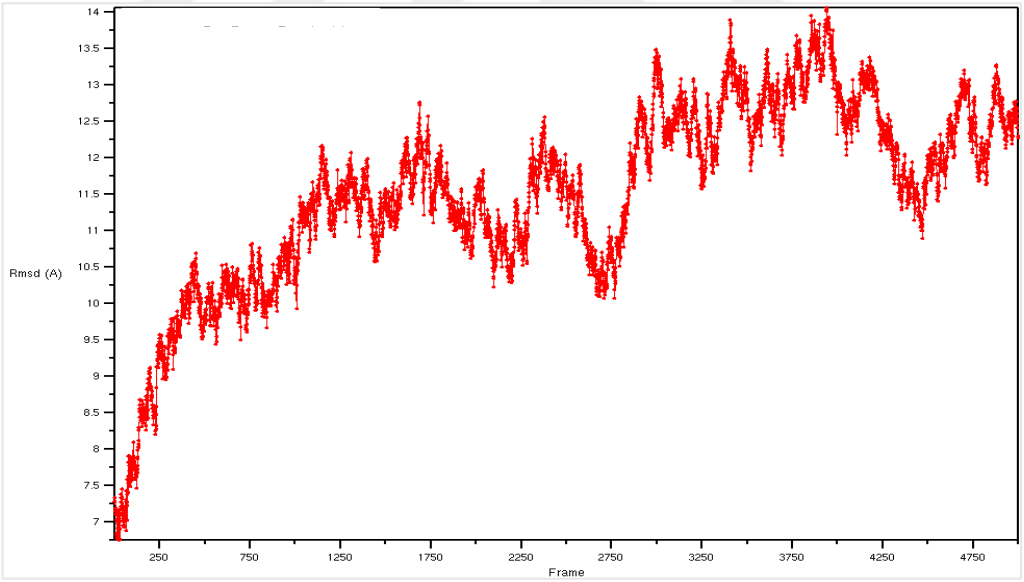

Figure 56. Graph of root mean square deviation of TN3-isoleucine peptide with respect to time step.

TN3-valine Peptide (RVVRVVRVVV)

The TN3-valine peptide structure was placed in the water phase on the membrane as shown in Figure 57, in 4 pieces, with a distance of approximately 10 Å to the membrane and to each other.

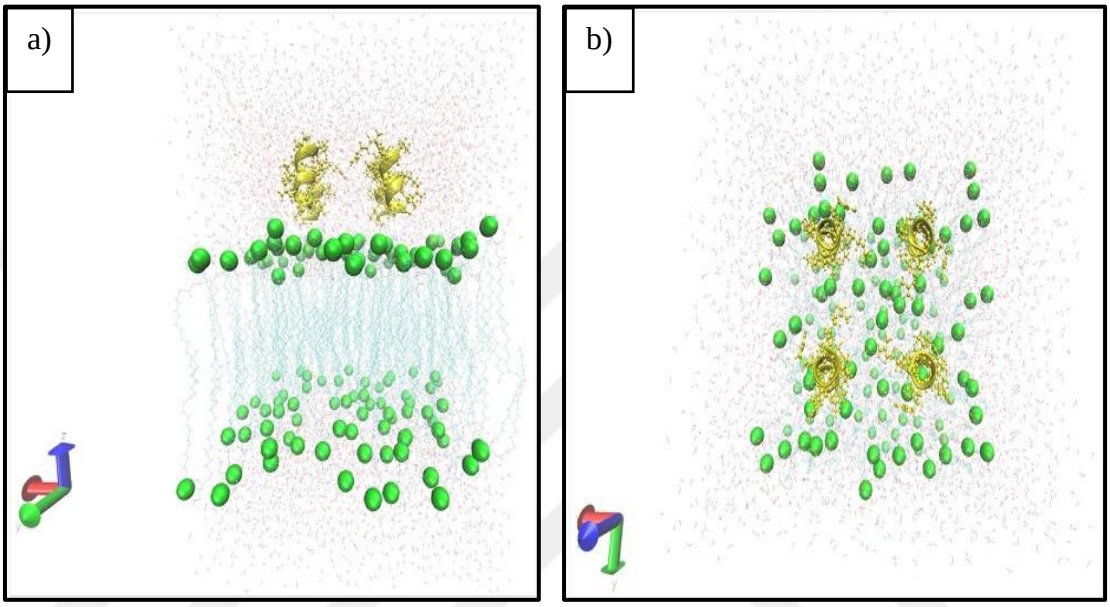

Figure 57. Positioning of the TN3-valine peptide on the bacterial membrane and in water, a) lateral diagonal view, b) top view. Water molecules are shown in red-white, phosphate molecules in green balls, membrane lipids in light blue, alpha helix structure of peptides and atoms in yellow.

After the simulation system shown in the figure above was prepared, it was used as the initial input and a 10 ns MD simulation was performed. In Figure 58, this simulation result of the TN3-valine peptide is visualized from the top and the side. It was observed that TN3-valine molecules tended towards the membrane during this short simulation time of 10 ns.

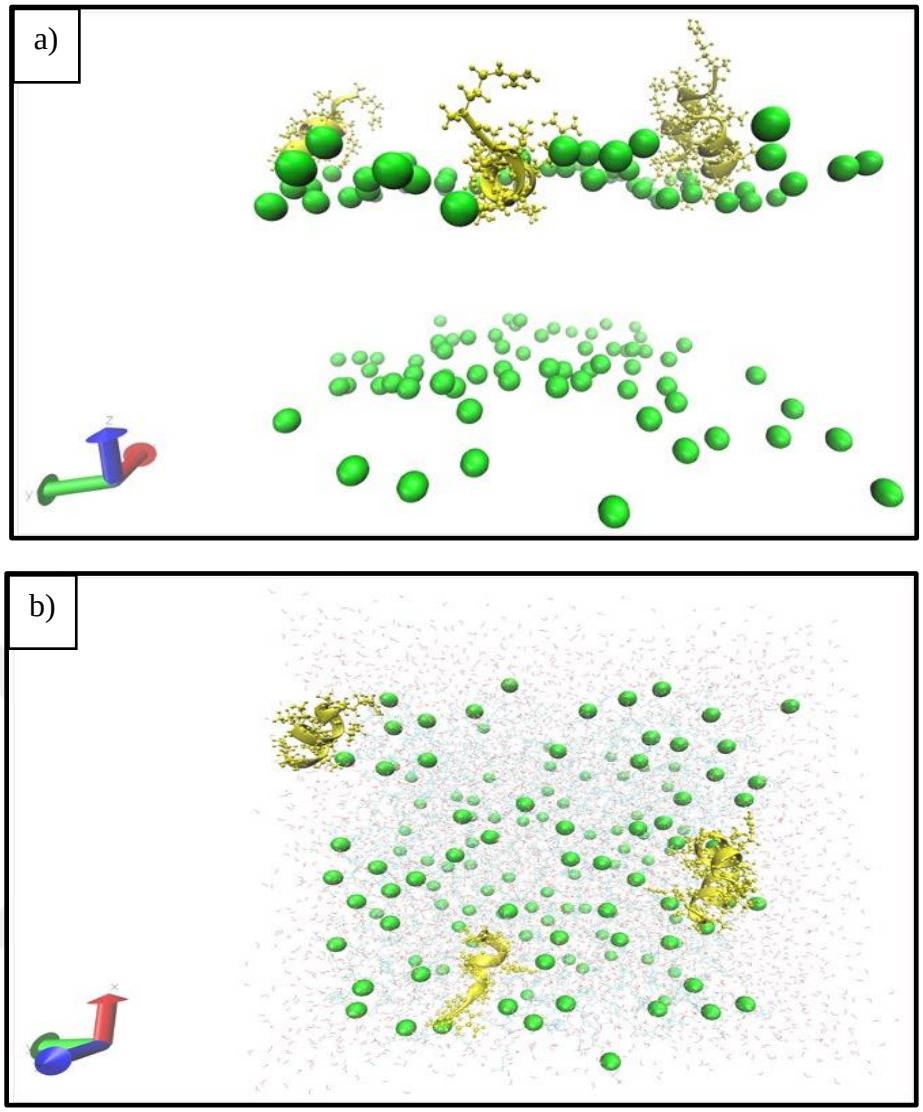

Figure 58. Representation the result of molecular simulation lasting 10ns after positioning the TN3-valine peptide on the bacterial membrane and in water, a) side view (lipid ends and water molecules are closed for better observation of the approach to the membrane), b) top view. Water molecules are shown in red-white, phosphate molecules in green balls, membrane lipids in light blue, alpha helix structure of peptides and atoms in yellow. (There are 3 peptides in the simulation box because one of the peptides goes outside the periodic boundary conditions).

The graph of the distance (Angstrom) of the TN3-valine peptide from the membrane is given in Figure 59, and the graph of root mean square deviation is given in Figure 60.

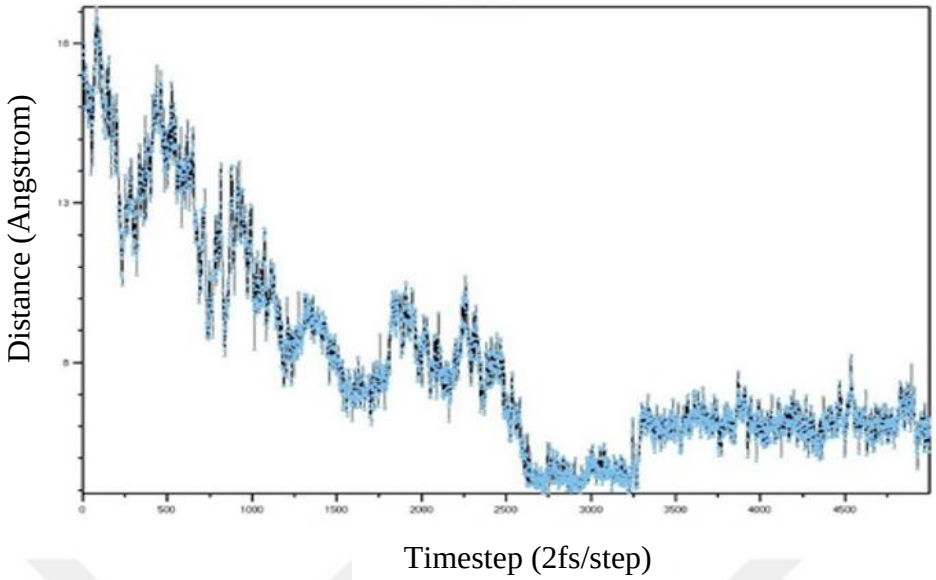

Figure 59. Graph of the distance (Angstrom) of the TN3-valine peptide from the membrane over time.

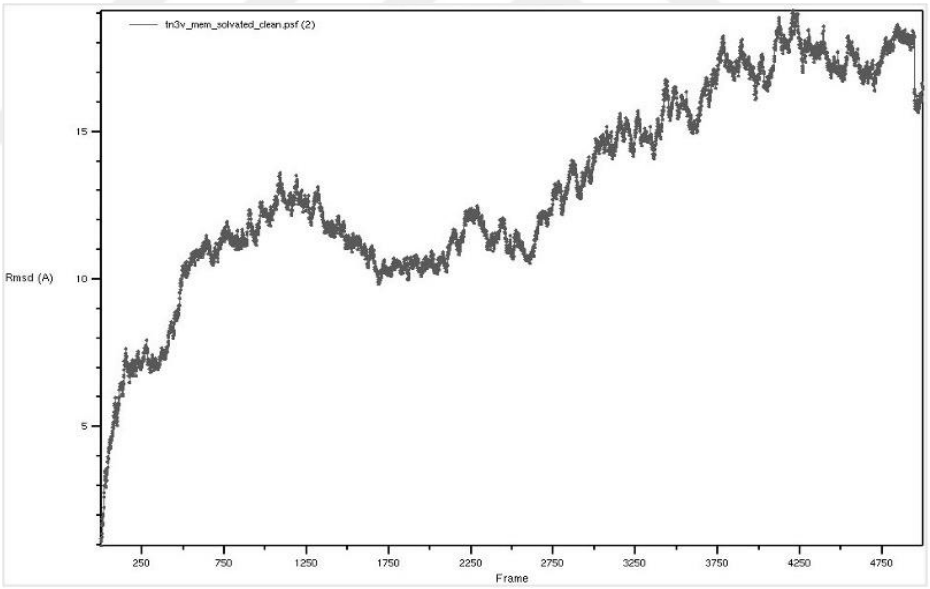

Figure 60. Time step-dependent root mean square deviation plot of TN3-valine peptide.

TN1-isoleucine Peptide (RIIRIIIIRIIR)

As seen in Figure 61, the TN1-isoleucine peptide structure was first placed in the water phase on the membrane as 4 pieces, with a distance of approximately 10 Å to the membrane and to each other.

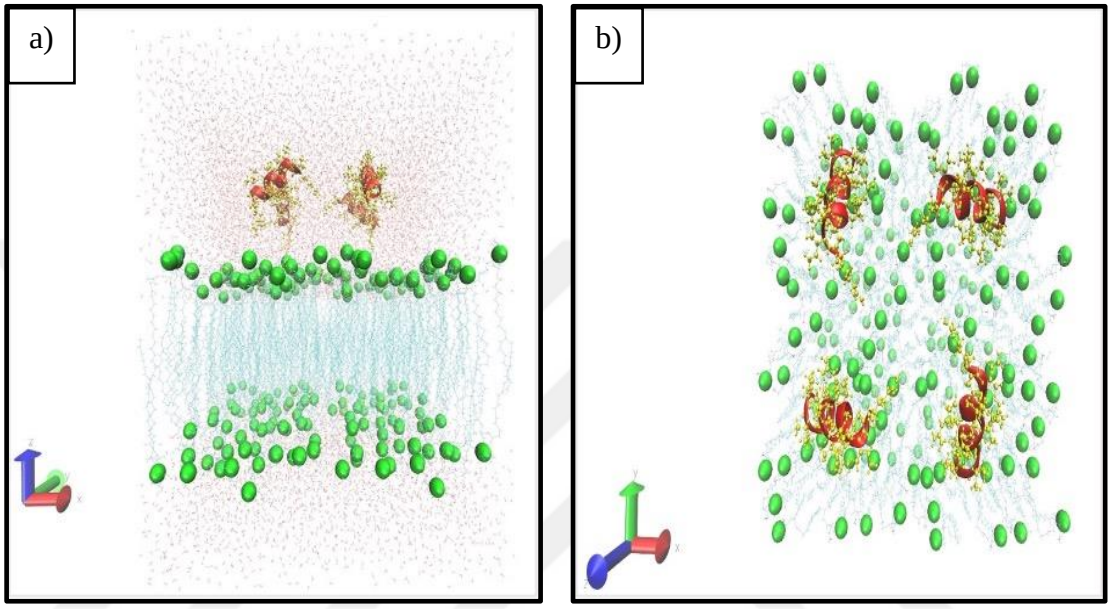

Figure 61. Positioning of the TN1-isoleucine peptide on the bacterial membrane and in water, a) lateral diagonal view, b) top view. Water molecules are shown in red-white, phosphate molecules in green balls, membrane lipids in light blue, alpha helix structure of peptides in red and atoms in yellow.

After the simulation system shown in the figure above was prepared, it was used as the initial input and a 10ns MD simulation was carried out. In Figure 62, this simulation result of the TN1-isoleucine peptide is visualized from the top and the side. It was observed that TN1-isoleucine molecules tended towards the membrane during this short simulation time of 10ns.

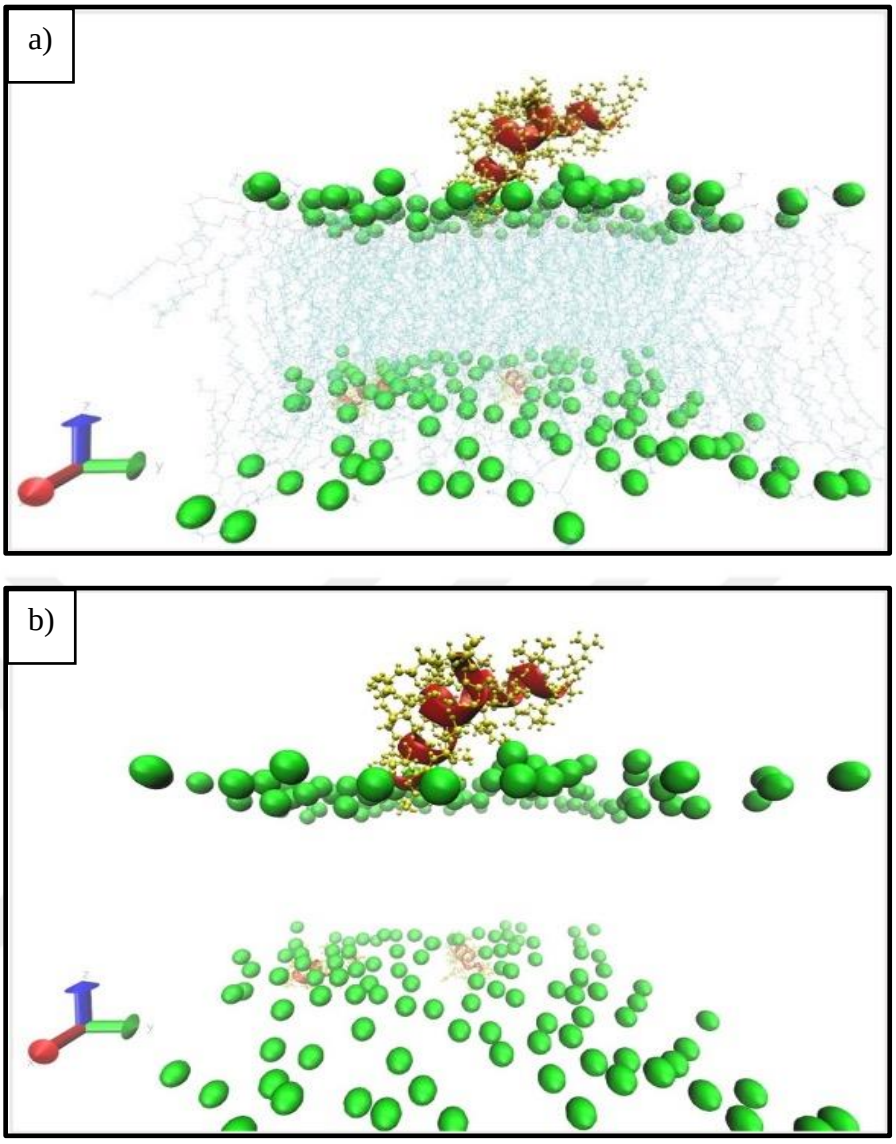

Figure 62. Representation the result of the molecular simulation lasting 10ns after the TN1-isoleucine peptide was positioned on the bacterial membrane and in water, a) side view, b) lipid ends and water molecules were closed in order to better observe the approach to the membrane. Water molecules are shown in red-white, phosphate molecules in green balls, membrane lipids in light blue, alpha helix structure of peptides in red and atoms in yellow. (As one of the peptides crosses its periodic boundary, it is located below in the simulation box).

The graph of the distance (Angstrom) of the TN1-isoleucine peptide to the membrane according to the time step is given in Figure 63, and the root mean square deviation graph is given in Figure 64.

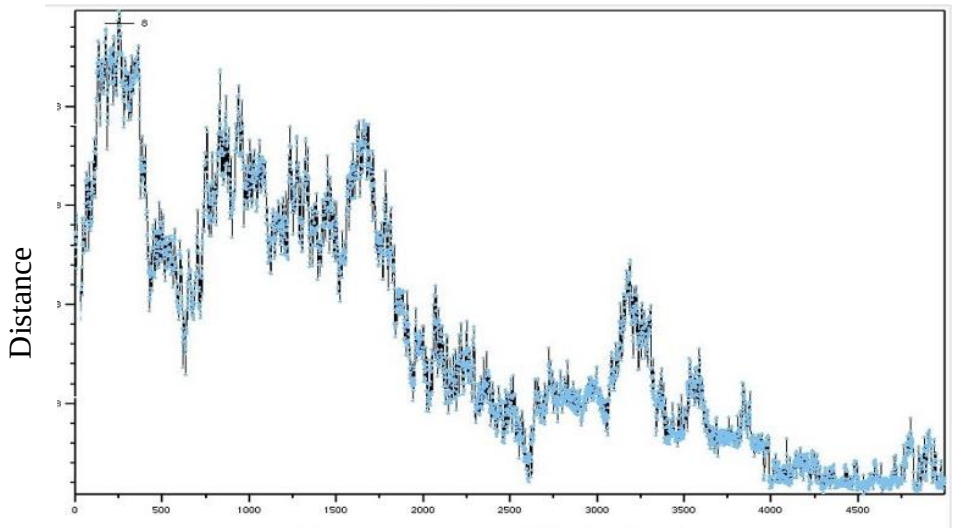

Figure 63. Graph of the distance (Angstrom) of the TN1-isoleucine molecule from the membrane over time.

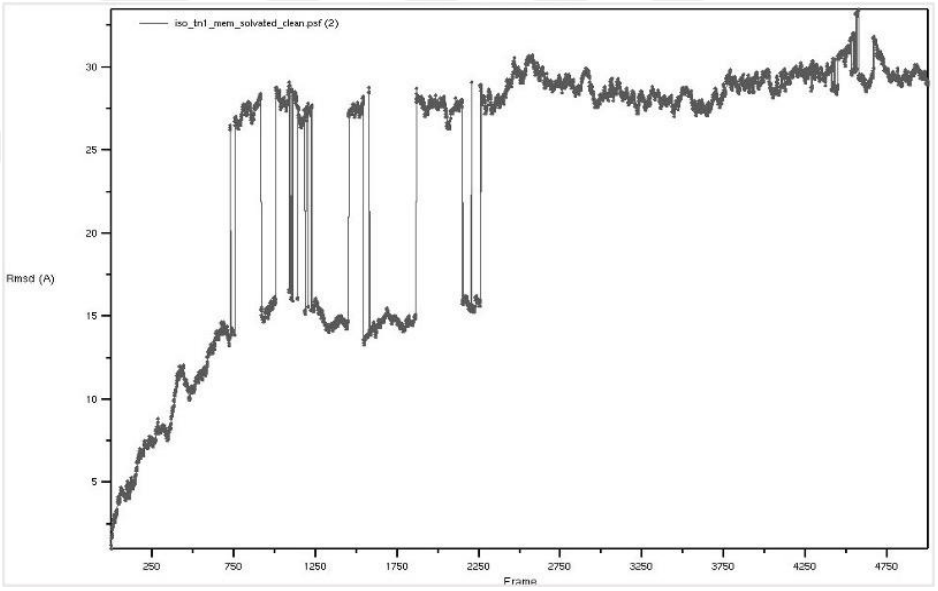

Figure 64. Graph of root mean square deviation of TN1-isoleucine peptide with respect to time step.

TN1-valine Peptide (RVVRVVVVRVVR)

The TN1-valine peptide structure was first placed in the water phase on the membrane as shown in Figure 65, in 4 pieces, with a distance of approximately 10 Å to the membrane and to each other.

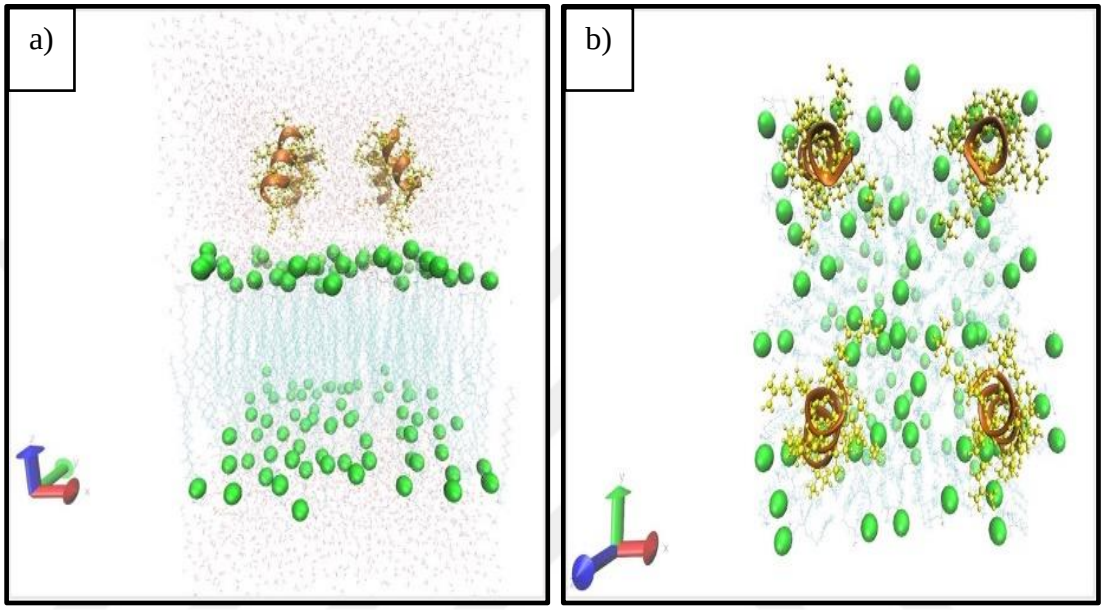

Figure 65. Positioning of the TN1-valine peptide on the bacterial membrane and in water, a) side view, b) top view. Water molecules are shown in red-white, phosphate molecules in green balls, membrane lipids in light blue, alpha helix structure of peptides in orange and atoms in yellow.

After the simulation system shown in the figure above was prepared, it was used as the initial input and a 10ns MD simulation was carried out. In Figure 66, this simulation result of the TN1-valine peptide is visualized from the top and the side. It was observed that TN1-valine molecules tended towards the membrane during this short simulation time of 10ns.

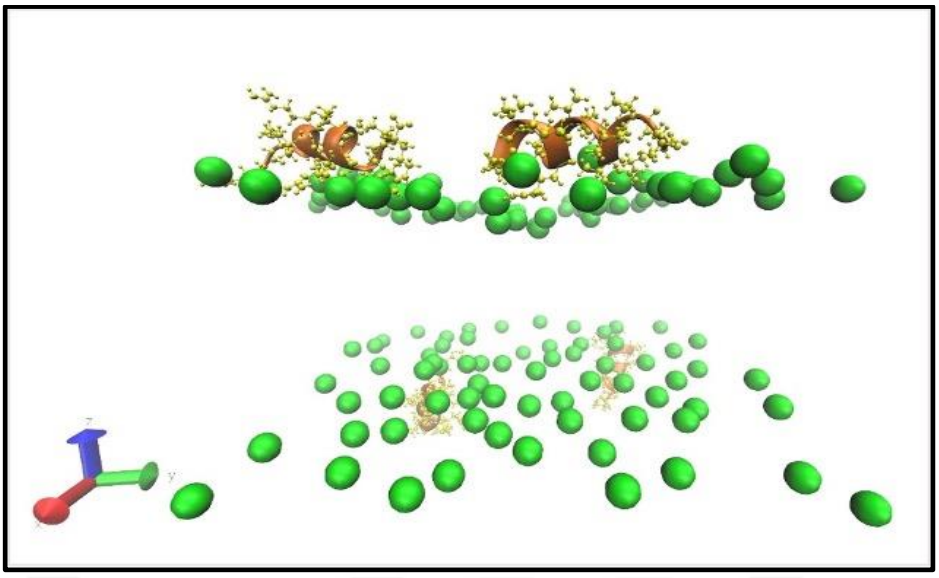

Figure 66. Side view of the TN1-valine peptide as a result of molecular simulation lasting 10ns after positioning the TN1-valine molecule on the bacterial membrane and in water (lipid ends and water molecules are closed for better observation of the approach to the membrane). Phosphate molecules are green balls, the alpha helix structure of peptides is shown in orange and atoms in yellow. (As two of the peptides go outside the periodic boundary conditions, they are listed below in the simulation box).

The graph of the distance (Angstrom) of the TN1-valine peptide from the membrane according to the time step is given in Figure 67, and the root mean square deviation graph is given in Figure 68.

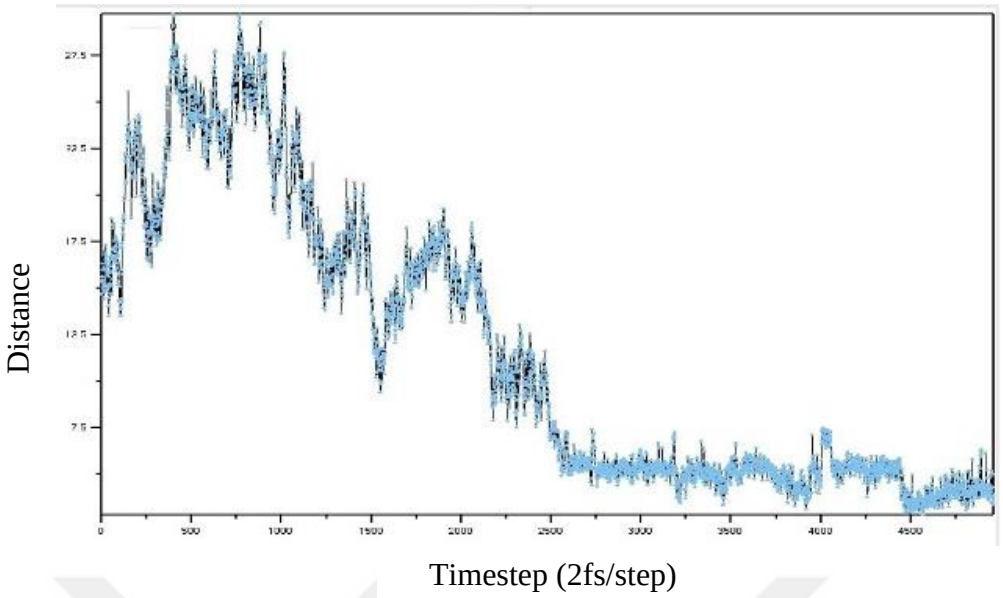

Figure 67. Graph of the distance (Angstrom) of the TN1-valine peptide from the membrane over time.

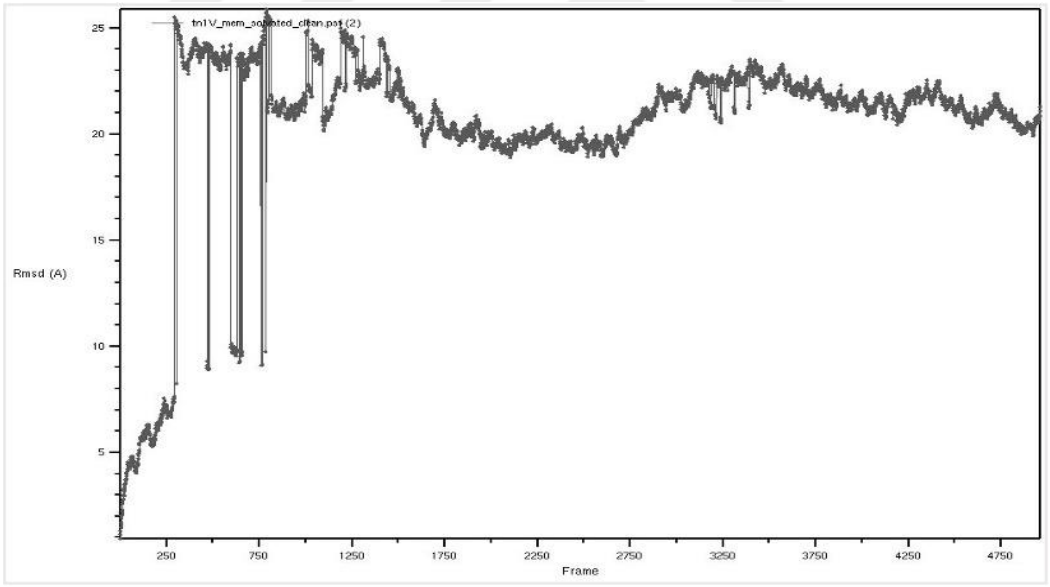

Figure 68. Time step-dependent root mean square deviation plot of TN1-valine peptide.

TN6 Peptide (RLLRLLLRLLR)

The TN6 peptide structure was first placed in the water phase on the membrane as shown in Figure 69, in 4 pieces, with a distance of approximately 10 Å to the membrane and to each other.

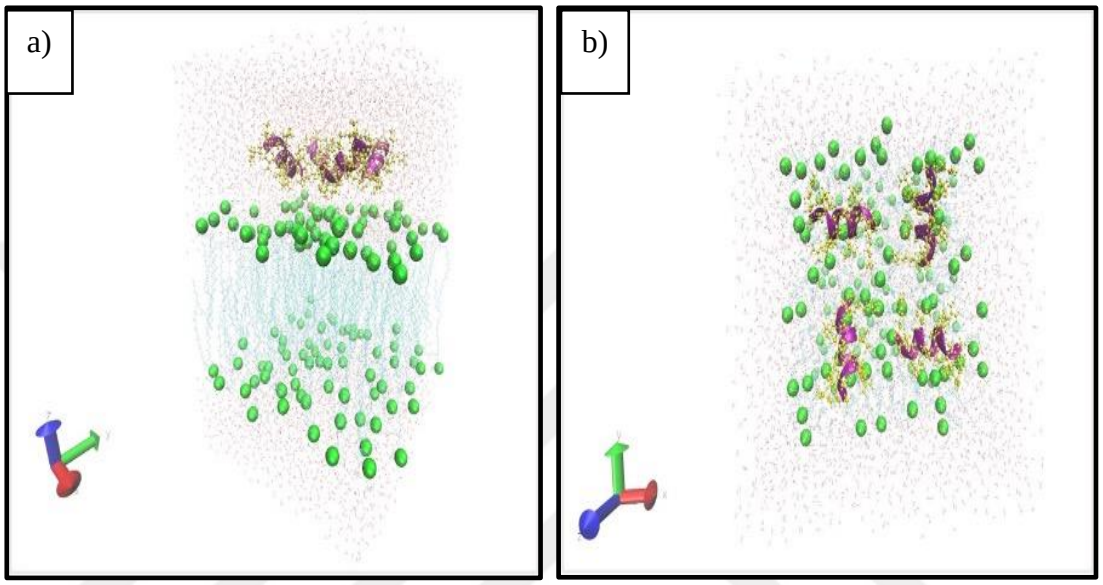

Figure 69. Positioning of the TN6 peptide on the bacterial membrane and in water, a) side view, b) top view. Water molecules are shown in red-white, phosphate molecules in green balls, membrane lipids in light blue, alpha helix structure of peptides in purple and atoms in yellow.

After the simulation system shown in the figure above was prepared, it was used as the initial input and a 100ns MD simulation was carried out. In Figure 70, this simulation result of the TN6 peptide is visualized from the top and the side. It was observed that TN6 molecules tended to move towards the membrane and penetrate the membrane during this simulation period of 100ns.

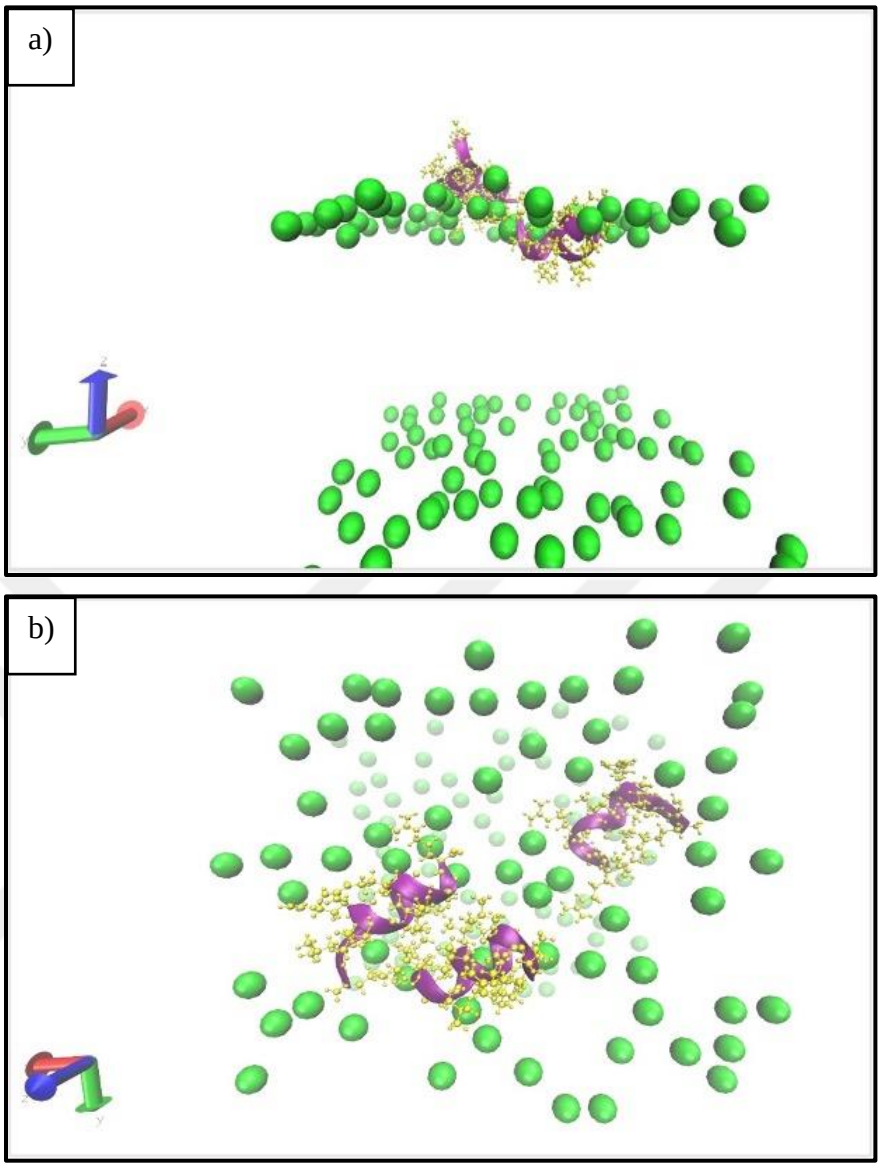

Figure 70. Molecular simulation lasting 100ns after positioning the TN6 peptide on the bacterial membrane and in water, a) side view, b) top view. Water molecules are shown in red-white, phosphate molecules in green balls, membrane lipids in light blue, alpha helix structure of peptides in purple and atoms in yellow. (Since one of the peptides goes to the other side of the membrane through the periodic boundary, 3 peptides appear in the simulation box).

The graph of the distance (Angstrom) of the TN6 peptide from the membrane according to the time step is given in Figure 71, and the root mean square deviation graph is given in Figure 72.

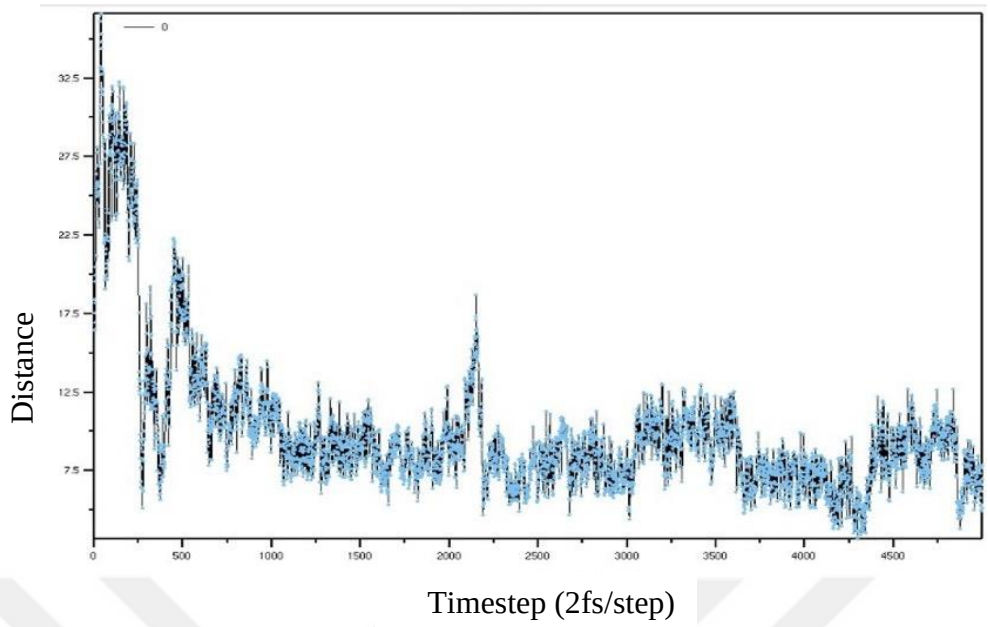

Figure 71. Graph of TN6 peptide's distance from the membrane (Angstrom) versus time step.

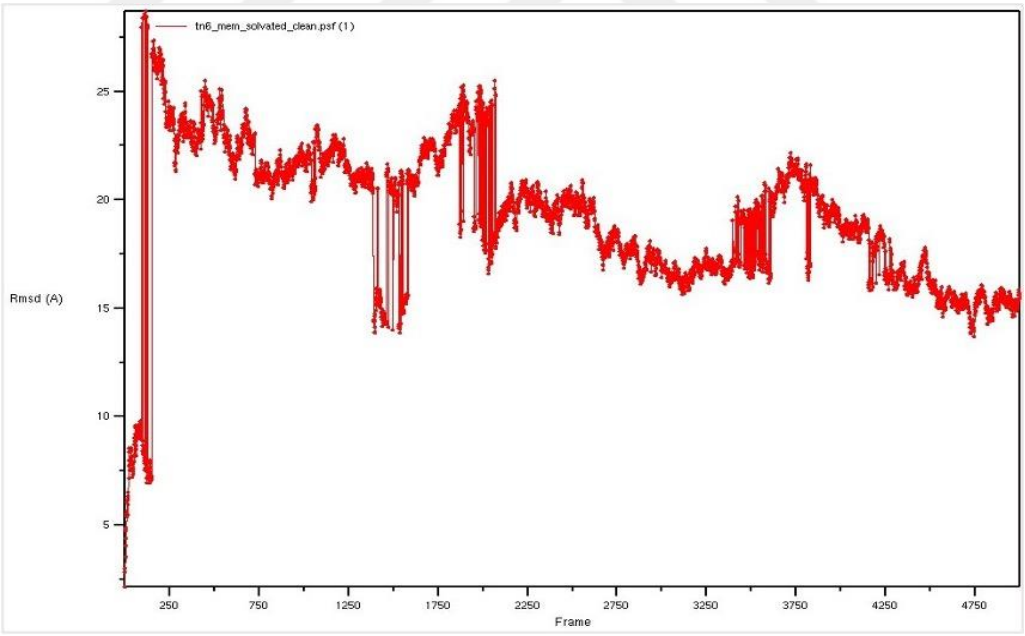

Figure 72. Graph of root mean square deviation of TN6 peptide with respect to time step.

The ratios of the interaction period of the phosphate ends of the bacterial membrane with each amino acid of the TN6 peptide (L-form) chosen as an example to

examine in which amino acids the peptide interaction with the membrane is higher is shown in Table 8.

Table 8. Comparison of the interaction period between the amino acid portions of the TN6 peptide and the phosphate ends of the bacterial membrane.

Amino acid	**First contact area with the membrane**	**Percentage of contact time versus total time analyzed**	**Total time frame in contact (5000 frame(s) analyzed)**
ARG	Phosphate ends	91.5 %	4574 frame(s)
LEU	Phosphate ends	91.8 %	4590 frame(s)
LEU	Phosphate ends	92.2 %	4611 frame(s)
ARG	Phosphate ends	95.5 %	4775 frame(s)
LEU	Phosphate ends	93.8 %	4692 frame(s)
LEU	Phosphate ends	92.0 %	4598 frame(s)
LEU	Phosphate ends	94.4 %	4721 frame(s)
ARG	Phosphate ends	95.9 %	4797 frame(s)
LEU	Phosphate ends	92.8 %	4640 frame(s)
LEU	Phosphate ends	86.8 %	4342 frame(s)
ARG	Phosphate ends	96.4 %	4821 frame(s)

D-TN6 Peptide D(RLLRLLLRLLR)

The D-TN6 peptide structure was placed in the water phase on the membrane as shown in Figure 73, in 4 pieces, with a distance of approximately 10 Å to the membrane and to each other.

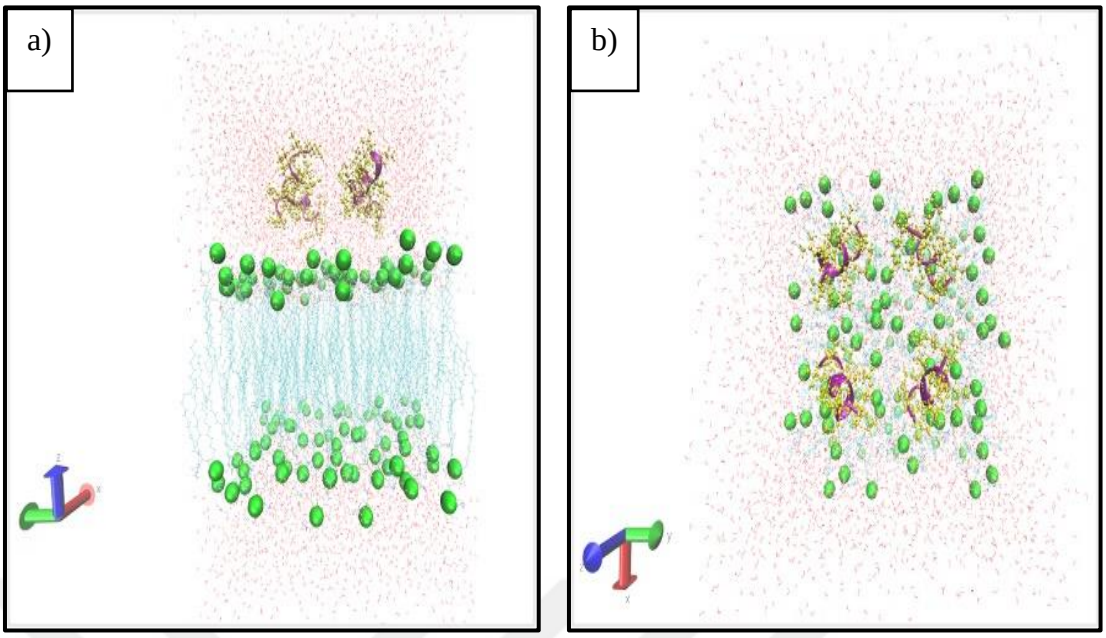

Figure 73. Positioning of the D-TN6 peptide on the bacterial membrane and in water, a) side view, b) top view. Water molecules are shown in red-white, phosphate molecules in green balls, membrane lipids in light blue, alpha helix structure of peptides in purple and atoms in yellow.

After the simulation system shown in the figure above was prepared, it was used as the initial input and a 100ns MD simulation was carried out. In Figure 74, the side section of this simulation result of the D-TN6 peptide is visualized. It was observed that D-TN6 molecules tended to move towards the membrane and penetrate the membrane during this simulation period of 100ns.

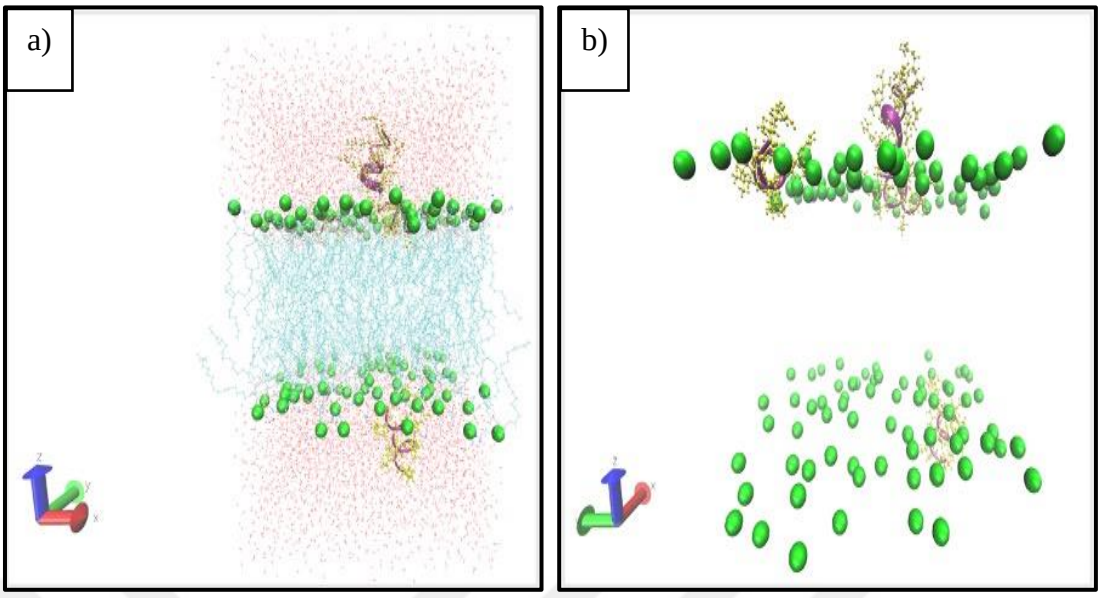

Figure 74. Representation the result of molecular simulation lasting 100 ns after the D-TN6 peptide is positioned on the bacterial membrane and in water, a) side view, b) water molecules and lipid ends are closed for better observation of penetration into the membrane. Water molecules are shown in red-white, phosphate molecules in green balls, membrane lipids in light blue, alpha helix structure of peptides in purple and atoms in yellow. (As one of the peptides crosses the periodic boundary, it is placed below in the simulation box).

The graph of D-TN6 peptide's distance to the membrane (Angstrom) in 100 ns simulation according to time step is given in Figure 75, and the root mean square deviation graph is given in Figure 76.

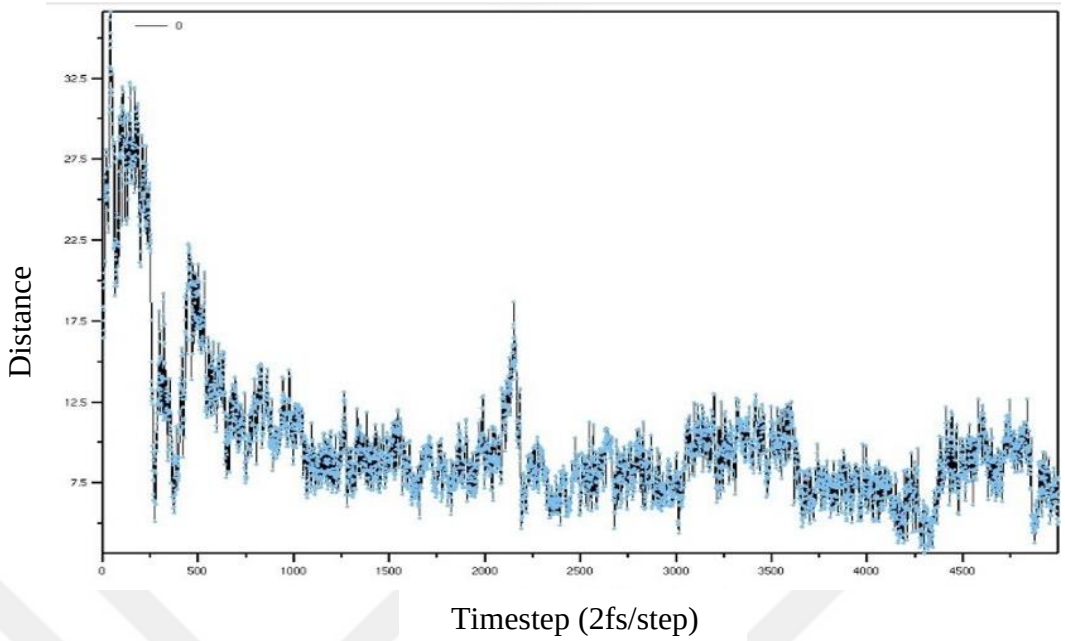

Figure 75. Graph of D-TN6 peptide distance from membrane (Angstrom) versus time step.

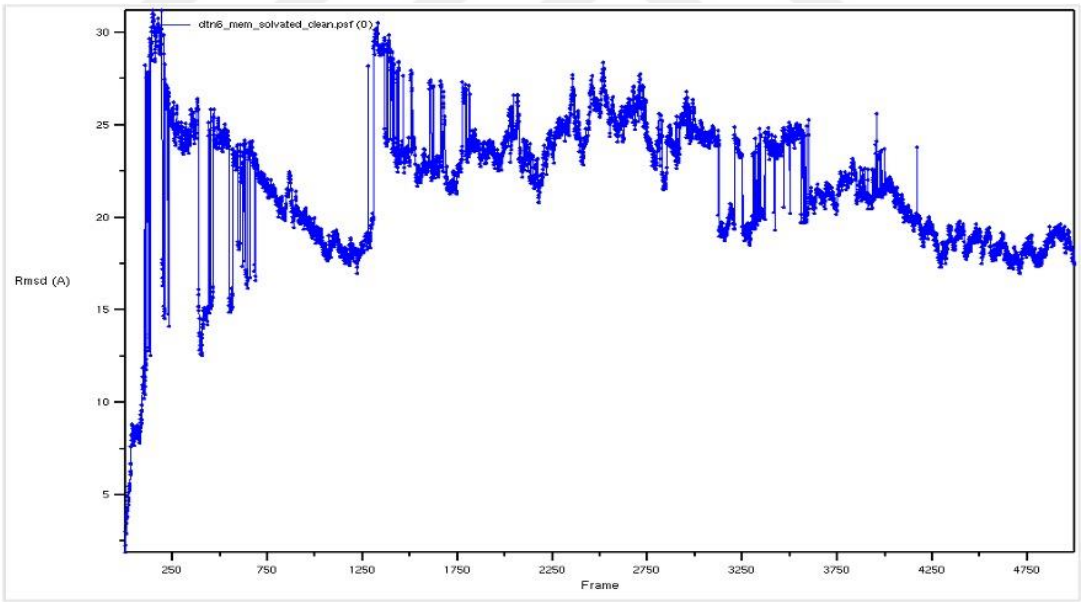

Figure 76. Time step-dependent root mean square deviation plot of D-TN6 peptide.

It is supported by laboratory results that the D form of TN6 peptide is more resistant to proteases. For this reason, the simulation time of the D form was extended

up to 300 ns, and its mechanism of action on bacteria was examined in more detail as seen in Figure 77.

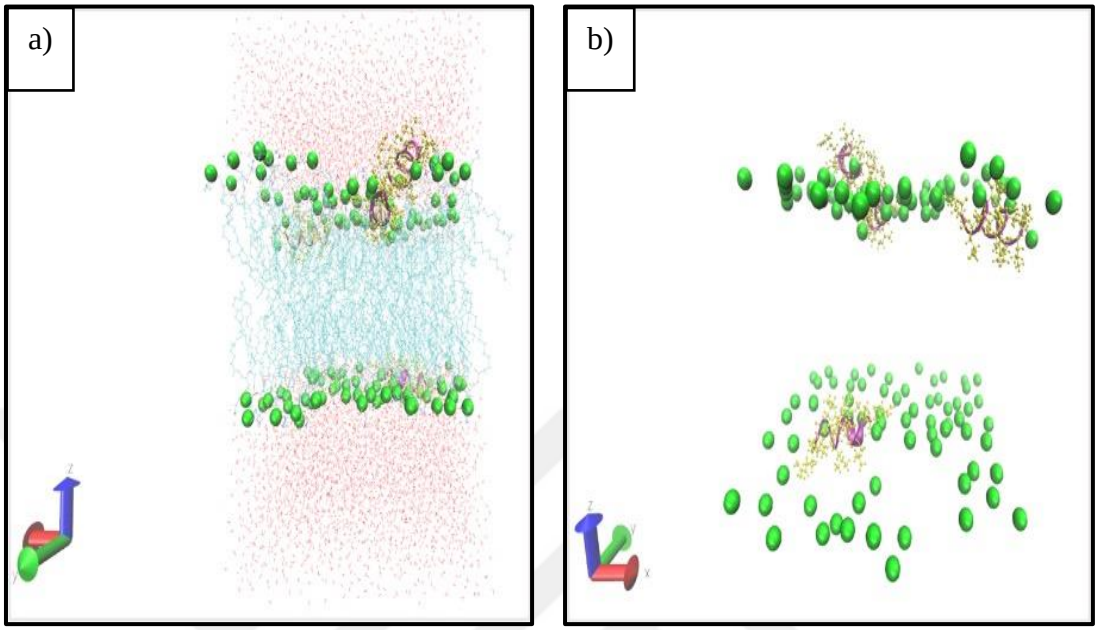

Figure 77. Representation the result of molecular simulation lasting 300 ns after the D-TN6 peptide is positioned on the bacterial membrane and in water, a) side view, b) water molecules and lipid ends are closed for better observation of penetration into the membrane. Water molecules are shown in red-white, phosphate molecules in green balls, membrane lipids in light blue, alpha helix structure of peptides in purple and atoms in yellow. (As one of the peptides goes outside the periodic boundary conditions, it is located below in the simulation box).

The graph of distance (Angstrom) of the D-TN6 to the membrane in a 300 ns extended simulation of the D-TN6 peptide is given in Figure 78, and the root mean square deviation graph is given in Figure 79.

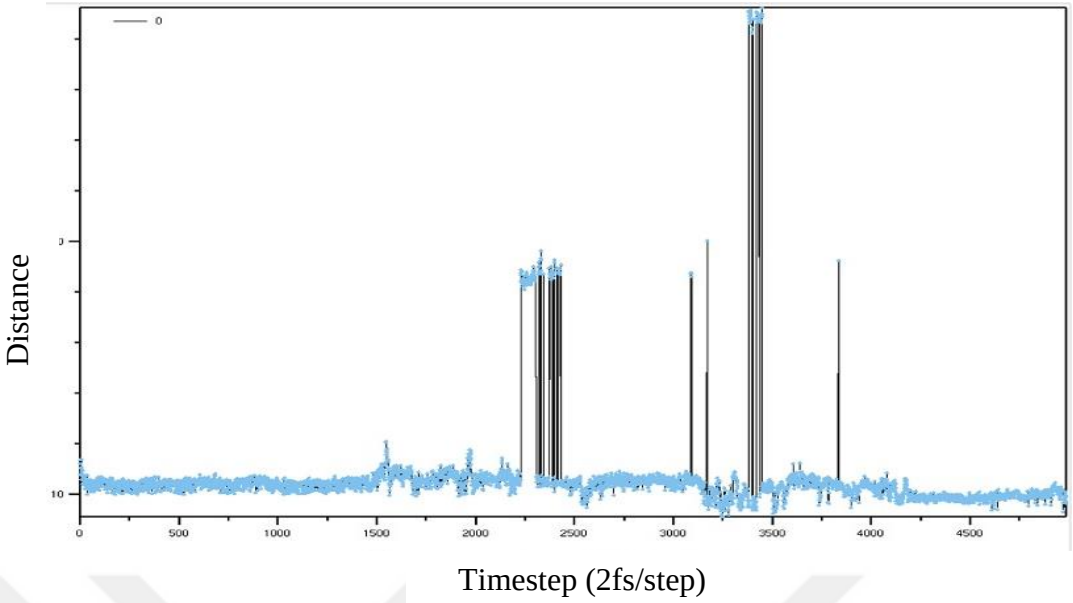

Figure 78. Graph of D-TN6 peptide distance from membrane (Angstrom) versus time step (300 ns total).

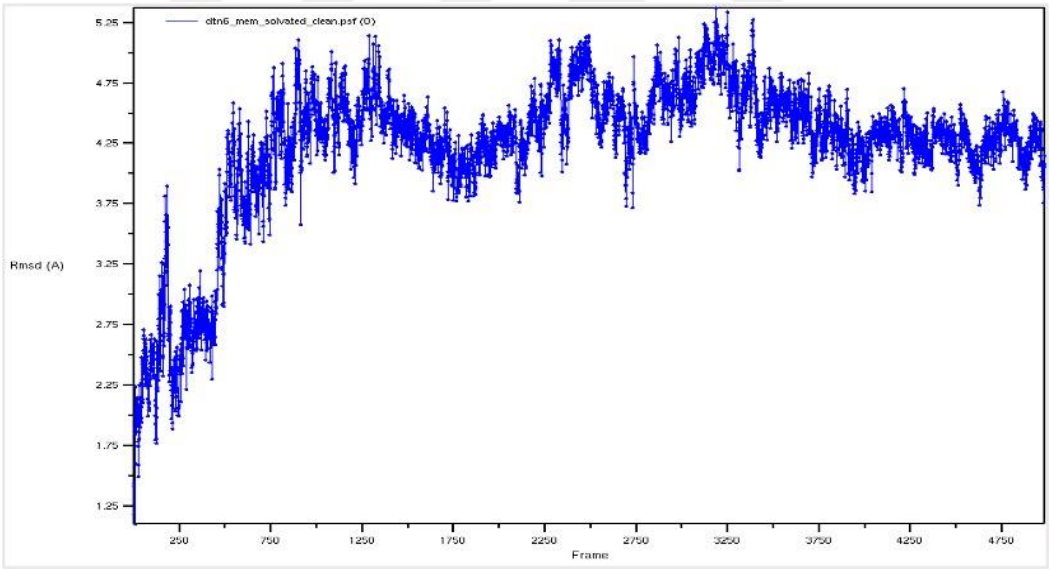

Figure 79. Graph of root mean square deviation of D-TN6 peptide based on time step (300ns total).

In order to compare the D-TN6 peptide with the L form, and to examine which amino acids have more membrane-peptide interaction, the comparison of the interaction period of time of each amino acid of the selected D-TN6 peptide with the phosphate ends of the bacterial membrane as percentage is shown in Table 9.

Table 9. Comparison of the interaction period of time between the amino acid portions of the D-TN6 peptide and the phosphate ends of the bacterial membrane.

Amino acid	First contact area with the membrane	Percentage of contact time versus total time analyzed	Total time frame in contact (5000 frame(s) analyzed)
DAR	Phosphate ends	98.3 %	4915 frame(s)
DLE	Phosphate ends	98.5 %	4925 frame(s)
DLE	Phosphate ends	99.1 %	4957 frame(s)
DAR	Phosphate ends	99.8 %	4992 frame(s)
DLE	Phosphate ends	99.4 %	4971 frame(s)
DLE	Phosphate ends	98.2 %	4909 frame(s)
DLE	Phosphate ends	99.4 %	4972 frame(s)
DAR	Phosphate ends	99.7 %	4983 frame(s)
DLE	Phosphate ends	99.4 %	4968 frame(s)
DLE	Phosphate ends	99.3 %	4965 frame(s)
DAR	Phosphate ends	99.9 %	4994 frame(s)

Section 2:

After positioning the designed sample polymer molecule (DABCO-based double cationic charged polymer) on the bacterial membrane in water, a molecular dynamicss simulation lasting 150 ns was created.

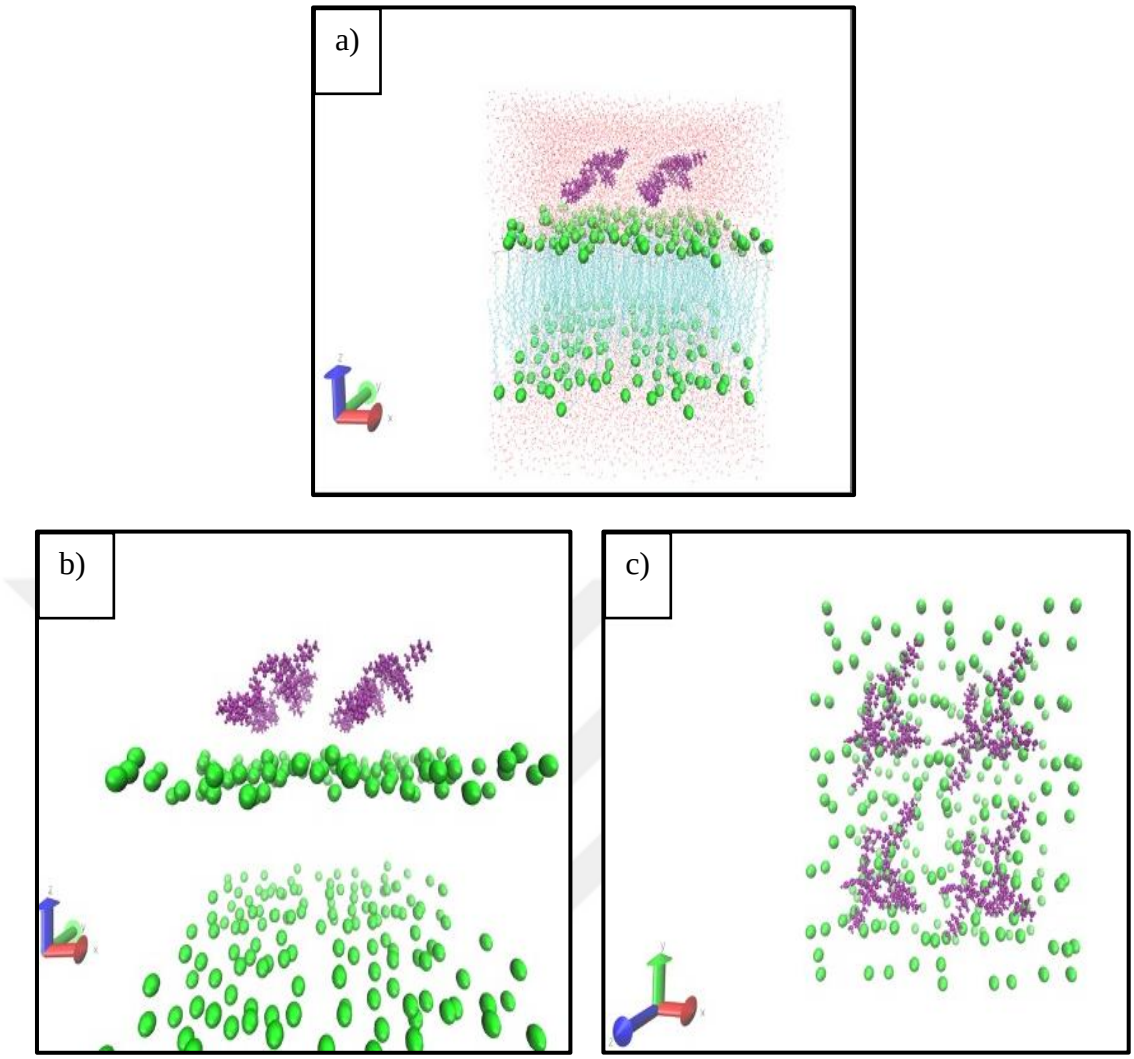

Figure 80. Positioning of the DABCO-polymer molecule on the bacterial membrane and in water. Water molecules are shown in red-white, phosphate molecules in green balls, membrane lipids in blue, polymer CPK notation and purple color. a) A cross-sectional view of the membrane and polymer was taken. b) In order to better see the positioning of the polymers on the membrane, the water molecules and lipid ends are eliminated, and the simulation box is shown more closely. c) In order to better see the positioning of the 4 polymers with each other, the membrane and the polymer were viewed from above.

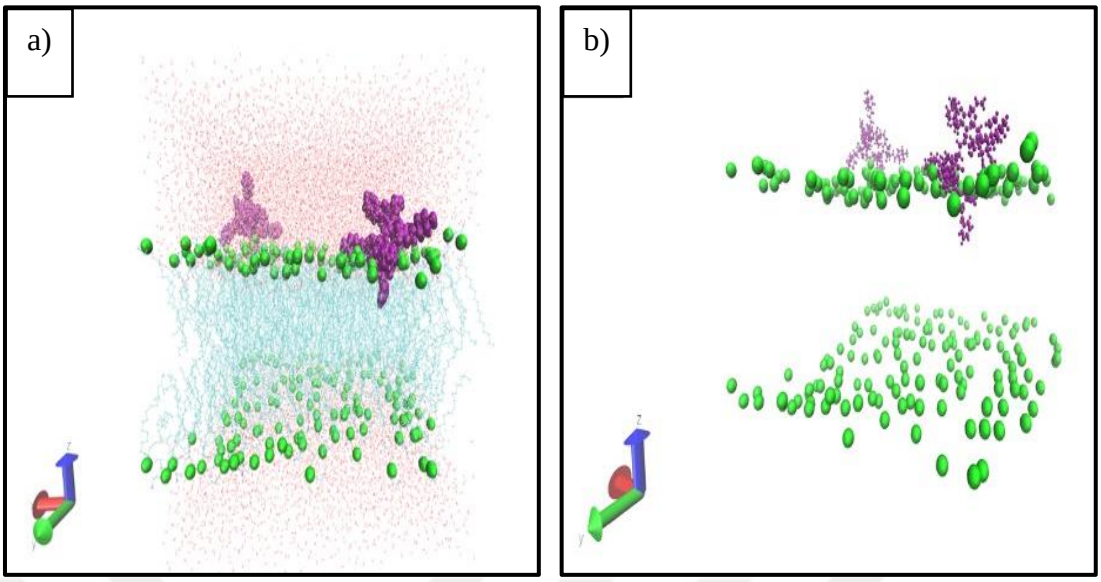

Figure 81. The result of the molecular simulation, which was carried out after the DABCO-polymer molecule was positioned in the bacterial membrane and water and lasted for 150ns. a) Water molecules are shown as red-white, phosphate molecules as green spheres, membrane lipids in blue, polymer VDW surface representation. b) In order to better see the interaction between the polymer and the membrane, the lipid ends, and water molecules are eliminated, and the polymer is shown with the CPK notation.

When the simulations were examined, it was observed that the polymer oriented towards the membrane and interacted with the membrane in the simulation. Meanwhile, it is visualized that the polymer forms a stable conformation, as can be seen from the graph demonstrated in Figure 82, that the root mean square deviation graph of the polymer molecules also converges depending on the time step.

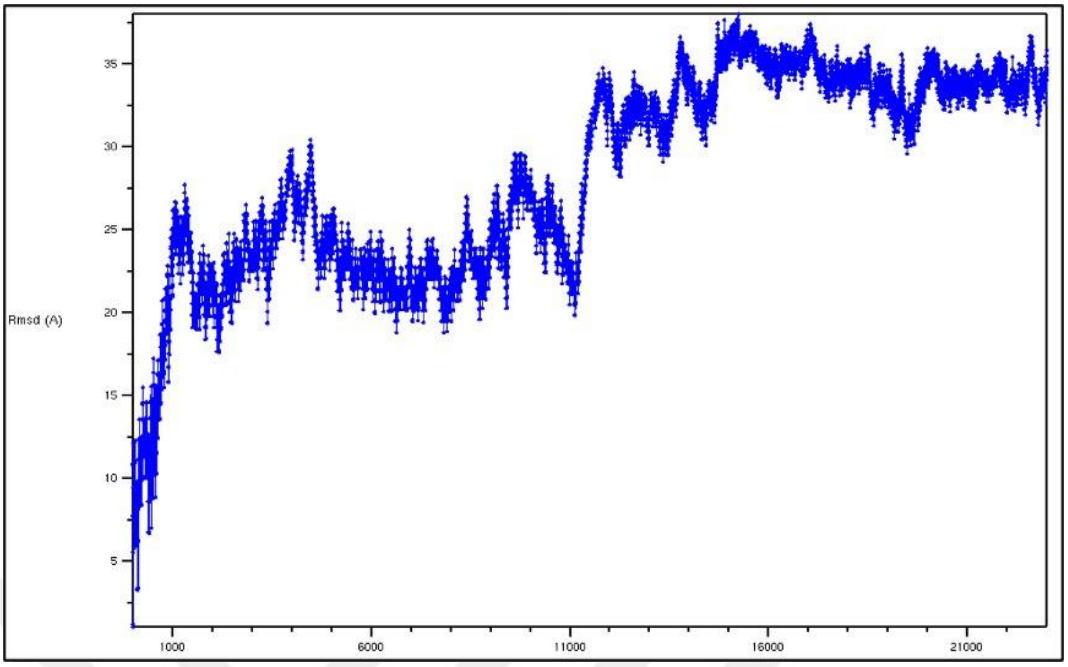

Figure 82. Root mean square deviation (RMSD) plot of the DABCO-polymer molecule with respect to time step.

The graph of the distance (Å) of the polymer to the membrane in the simulation according to the time step is given in Figure 83. When the graph is examined, it is seen that the polymer molecule, which was first located at an average distance of 17 Å from the center of gravity, converges to the membrane with back-and-forth movements, and the distance between polymer and the membrane becomes 0 in the 6000th step, each of which is 2 fs, that is, in approximately 12 ns. When the simulation was examined, it was observed that the phenyl group penetrated the membrane after adhering to the membrane.

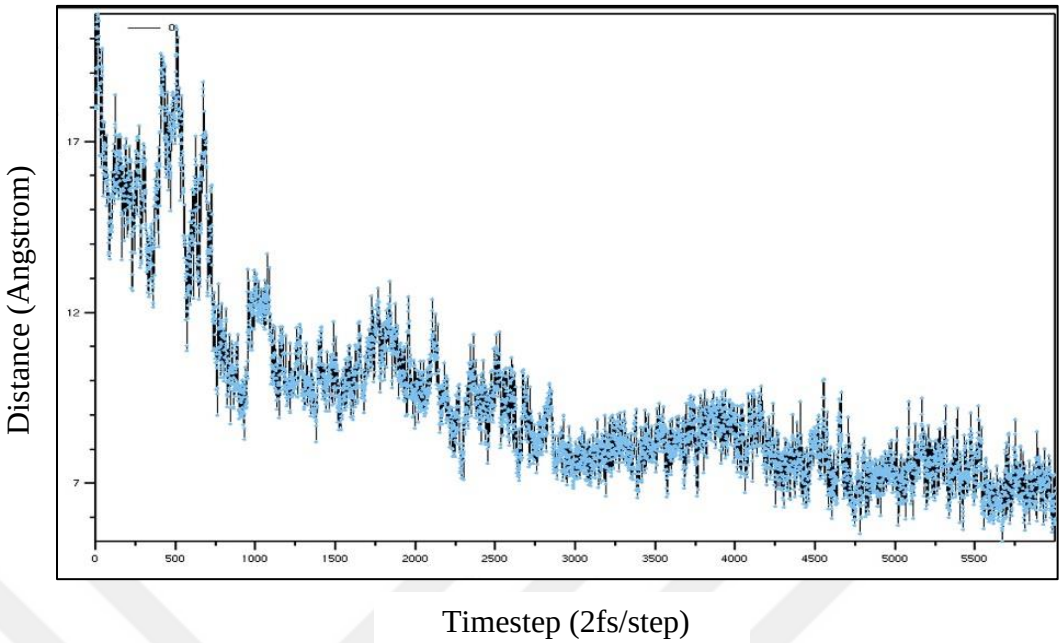

Figure 83. Graph of the DABCO-polymer molecule distance from the membrane (Angstrom) versus time step.

Section 3:

D-TN6 (RLLRLLLRLLR) peptide was first placed in 4 pieces in the water phase on the membrane, with a distance of approximately 10 Å to the membrane and to each other, and then the 300ns MD simulation was modeled for a total of 600ns by extending +300ns as visualized in Figure 84.

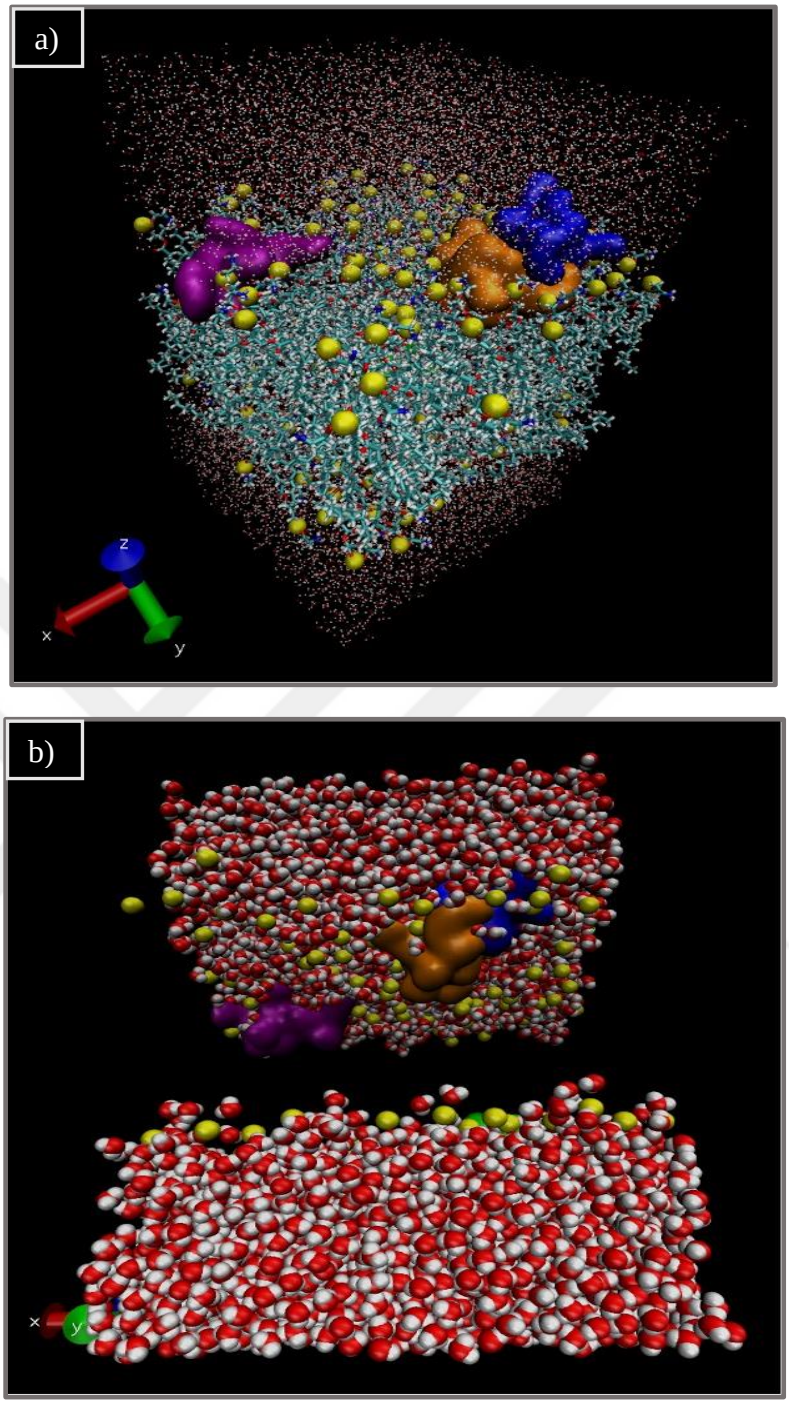

Figure 84. Positioning the D-TN6 peptide on the bacterial membrane and in water, a) Water molecules are red-white dots, phosphate molecules are yellow VDW, membrane lipids are light blue as Bond, peptides are blue, orange, and purple with the QuickSurf surface method, b) Water molecules red-white, phosphate molecules are yellow VDW, membrane lipids are not shown, peptides are visualized in blue, orange, and purple by the QuickSurf surface method.

After obtaining the simulation system shown in the figure above, these simulation results at 300 ns were used as the initial input and a total of 600ns MD simulation was carried out. As visualized in Figure 84, it was observed that during this simulation period of 600ns, D-TN6 molecules penetrated into the membrane, and two of them moved together as embedded in the membrane, while the other two remained embedded in the membrane individually.

In Figure 85, an example of some structures formed by water molecules during this simulation of the D-TN6 peptide and the transition of water from the lipid layer to the other water layer are visualized.

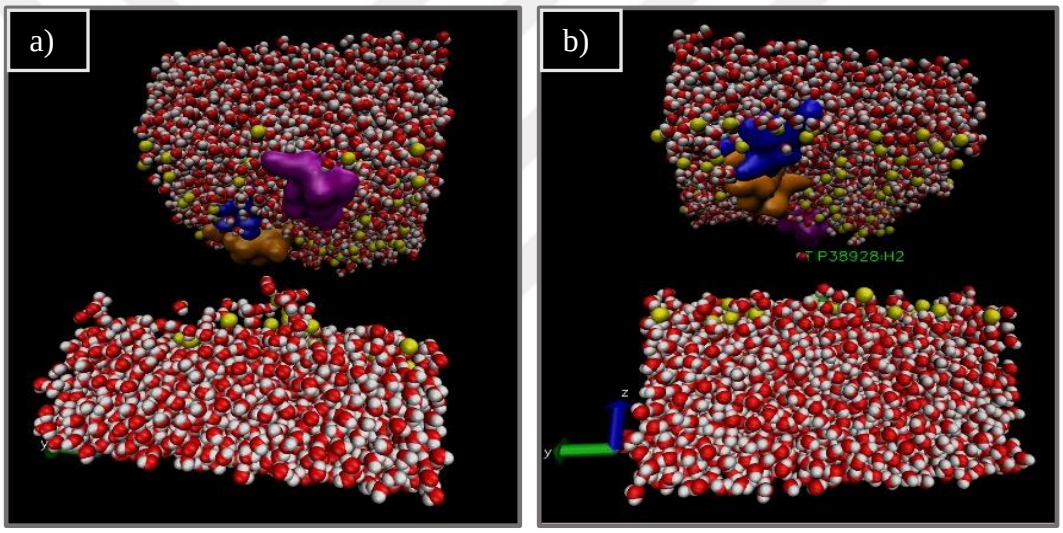

Figure 85. During the molecular simulation carried out after the D-TN6 molecule is positioned on the bacterial membrane and in water, which lasts for 600 ns in total, a) some water molecules bind to each other and form structures that extend to the lipid layer, b) TIP38928:H2 water hydrogen atom at ~396ns, c) TIP32615 A cross-section of the :H2 water hydrogen atom at ~439ns, d)TIP3220:OH2 water oxygen atom from the lipid membrane layer to the other water layer at ~471ns. For better visualization of the membrane interior, the lipid ends were visualized by capping them. Water molecules are red-white, membrane phosphate atoms are yellow VDW, peptides are shown in blue, orange, and purple with QuickSurf surface representation. (Since one of the peptides crosses the periodic boundary, it is located in the water layer under the lipids in the simulation box and is not visible in the image).

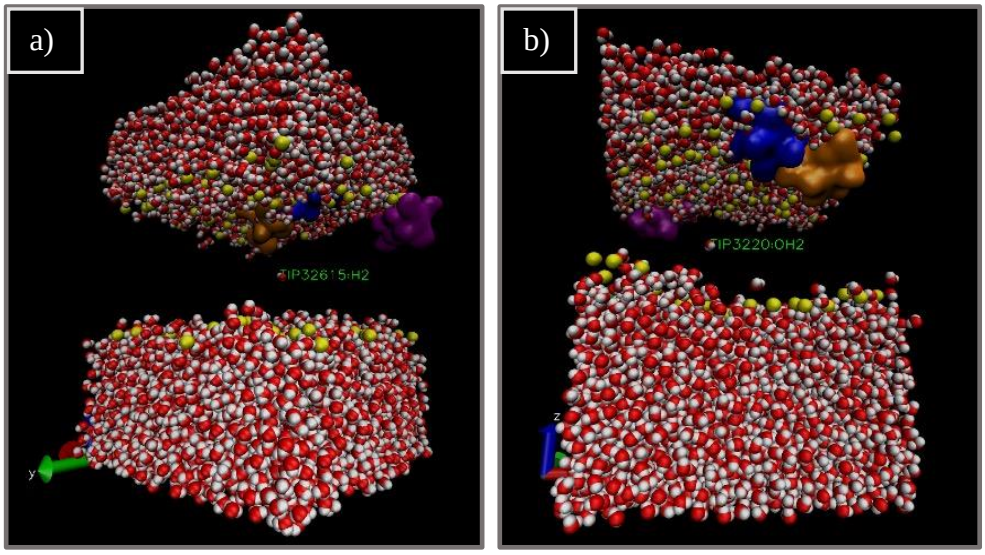

Figure 85. During the molecular simulation carried out after the D-TN6 molecule is positioned on the bacterial membrane and in water, which lasts for 600 ns in total, a) some water molecules bind to each other and form structures that extend to the lipid layer, b) TIP38928:H2 water hydrogen atom at ~396ns, c) TIP32615 A cross-section of the :H2 water hydrogen atom at ~439ns, d)TIP3220:OH2 water oxygen atom from the lipid membrane layer to the other water layer at ~471ns. For better visualization of the membrane interior, the lipid ends were visualized by capping them. Water molecules are red-white, membrane phosphate atoms are yellow VDW, peptides are shown in blue, orange, and purple with QuickSurf surface representation. (Since one of the peptides crosses the periodic boundary, it is located in the water layer under the lipids in the simulation box and is not visible in the image) (continued).

5 DISCUSSION

5.1 First Study

First study of this thesis comprises of three parts. In this study set, experiments conducted to investigate how catelicidin-like antimicrobial peptides interact with bacterial-similar membrane and with itself by using molecular modelling and computational methods. The analysis of the results was carried out simultaneously with the experimental studies and their compatibility with the experimental results was considered.

In the first section of the study, short (2 ns) simulations were run for Model1, Model2, Model3, Model4 separately. Long (~50 ns) simulations were run for Model4 P2 in L-form peptides and Model4 P4 in D-form peptides. The reason why P2 and P4 peptides selected for this section is to compare D-form and L-form containing peptides. By making short simulations (2 ns) of the designed 4 peptide models, their tendency towards the membrane from the water-phase was investigated so that it is determined that which model is worth to use for following experiments.

Since D-form peptides are identical to L-forms in all respects except for their chirality, the parameters of D-amino acids are nearly the same as their L-structured counterparts. For this reason, molecular dynamicss models were performed based on CHARMM27 force field parameters, as in other peptides. The only difference between the two molecules is the reverse chirality of the methyl side chain and the HA atom at the CA or alpha-carbon atom. For this reason, a new topology file was prepared for the D-form by changing the L-chiral center in the CA atom in the existing topology file for the L-form of the amino acids.

Screenshots introcudes below are the topology file containing atomic informations of amino acids demonstrates bonding between atoms of Alanine L-form (on the left) and D-form (on wright).

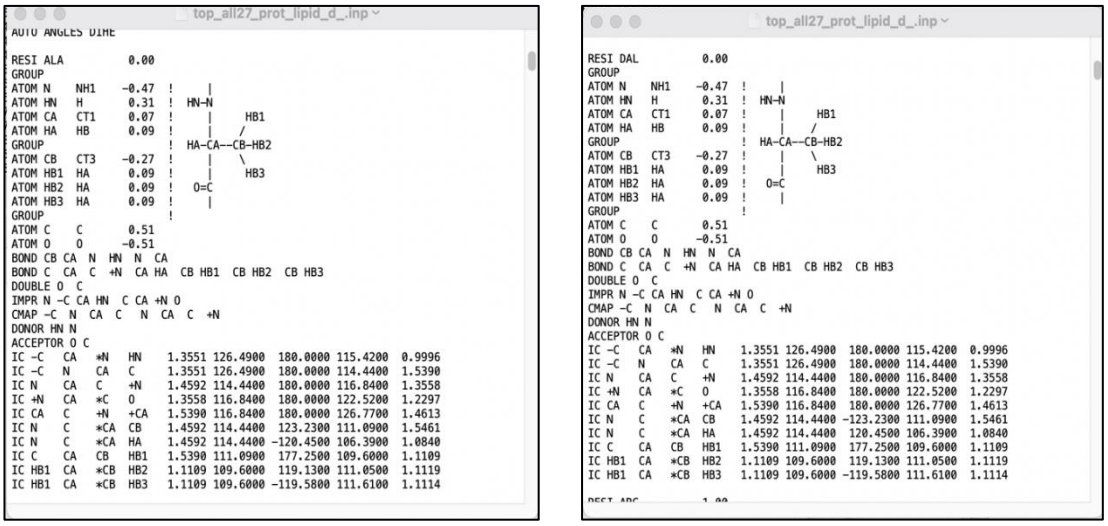

Figure 86. Topology file "top_all27_prot_lipid_d_.inp"downloaded from CHARMM-GUI web page (103).

The reason why 4 identical peptides were located in rectangular form and the distances of the peptides to each other and to the membrane is 10 Å, is to determine whether the peptides interact with each other and with the membrane without leaving the periodic boundary conditions in MD.

Since it is unable to generate 3D structures of D-form peptides via protein prediction tools such as PEP-FOLD3 at that time, a script specific to the purpose of converting L-form amino acids to D-form amino acids was developed. In this sense, a new method that can contribute to similar studies has been introduced during this study.

It has been observed that the antimicrobial properties (MIC values) of the peptides that interact with each other in the water phase and do not migrate to the membrane are not convenient, and based on this, an evaluation has been made to determine whether a eliminating can be made between the 4 peptide models. Since it was seen in the molecular dynamicss models that all of them were directed towards the membrane, it was understood that no elimination could be made depending on this criterion.

As a result of the molecular modelling studies for the first section of the first set of three studies, the interaction of the molecules with the antimicrobial effect mechanism with the membrane was examined, and it was ensured that the newly designed molecules were based on rational rather than random basis.

Some important considerations have been taken into account when designing antimicrobial peptides; Priority was given to the peptides being hydrophobic to approach the membrane and positively charged for better interaction with the negatively charged cell membrane. One of the important points to be considered in peptide design is the termination of the peptide with an amide group. It has been determined that the amide group peptide at the C-terminal end causes the peptide to approach the membrane more perpendicularly and to be taken into the cell faster, and it has an effect on increasing the membrane permeability. In addition, it also shows activity in the resistance of the peptide to proteases (117). Furthermore, amino acid sequences in the D-form affect peptide activity by making them more stable as well as more resistant to protease. That's why, both L-form and D-form amino acids were used in amino acid sequences for peptides' resistance to proteases, lower toxicity, and better antimicrobial activity.

In the second section, C-P1 and P1-C peptides were designed by adding cysteine amino acids separately to the amide and carboxyl ends of the Model 4-P1 peptide, since it has showed the best MIC results compared to the other peptides terminated with arginine amino acids. The addition of the amino acid cysteine to the peptides is required for the surface coating investigation in the experimental studies. The modified antibacterial peptides will bind to the UV/Ozone activated catheter surface using the Thiol-in reaction.

For this section, only the Model4 P1 peptide were simulated in peptide-membrane-water system in order to test the behavior of the P1 peptides generated in mixes form (D-form and L-form) by using developed new method whether the P1 peptide maintain its form in water-phase and when contacting membrane or one another. As it was in the first section, 4 identical peptides located above the POPE

membrane. Unlike previous peptide simulations, the P1 peptide is positioned at a distance of more than 10 Å from the membrane and each other, as it focuses on eliminating the problem in its parameterization. Simulation run was arranged to take ~50 ns.

After the simulation runs, it was not observed any deformation or detachment of the molecules belonging to formation of P1 peptide. Therefore, it is decided that P1 peptide can be added cystine for next simulation experimentation.

In the last section of the first study, C-P1 peptide which was observed to have good antimicrobial properties as a result of experimental studies, was modeled in a double-layered lipid membrane (POPE) system in water as in previous sections, and its mechanism of action on the membranes of microorganisms was investigated. It is aimed to compare the experimental inferences made with the C-P1 peptide with the results of MD modelling. To be more precise with the results, simulation run for C-P1 peptide were set for 100 ns.

Furthermore, addition to previously developed method for converting L-form amino acids to D-form amino acids in a peptide, a new software tool was tried to generate 3D structure of P1 peptide in mixed configuration containing both L-form and D-form. Since mixed formed peptides are more difficult to generate computationally, a practical tool to form 3D structure of a molecule makes it easier this process compared to the writing a coding script manually. Also, it can lower the possibility of making error since writing script is a detailed and challenging way to proceed. New software that we used is the Discovery Studio 2021 Software having a tool for converting L-form amino acids to D-forms.

The fact that the C-P1 peptide contains L- and D-form amino acids causes the main difficulty in creating 3D structure files of C-P1 which is named with the extension of “pdb”. PDB file format is a text-based file used to store descriptions of the 3D structures of molecules found in a data base named The Protein Data Bank. In

PDB files, amino acids' three letter abbreviations are written in fourth column originally.

However, amino acids in the D-form are denoted as 4-letter, with the letter D prefixed to their 3-letter notation as shown below. When a peptide contains mixed form of amino acids, order in PDB file in which L-form amino acids denoted as 3-letter and D-forms denoted as 4-letter, is disrupted so that dysregulation in PDB file causes error during computational processes such as MD simulation. For this reason, PDB file of a peptide must be carefully generated.

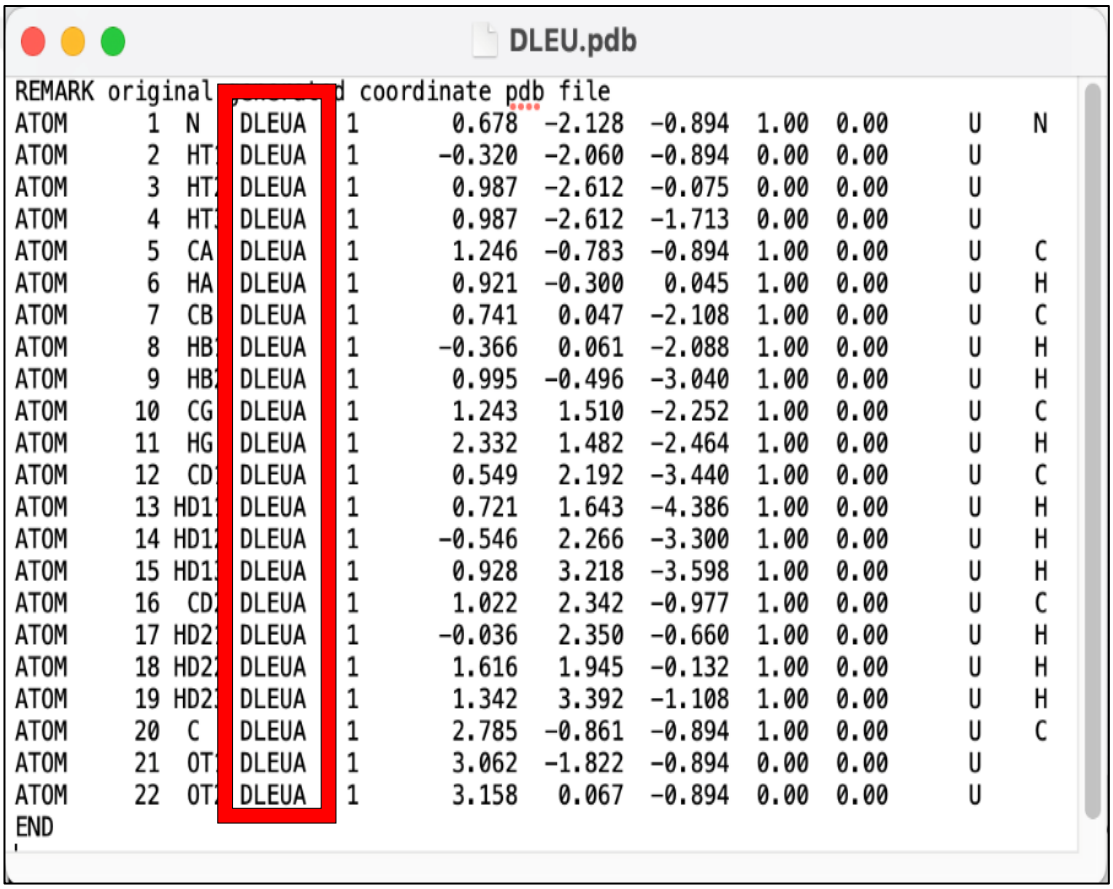

Figure 87. PDB file formats of C-P1 peptide in both L-form and D-form and of DLEU amino acid. Demonstration of the difference between D- and L-form in PDB file.

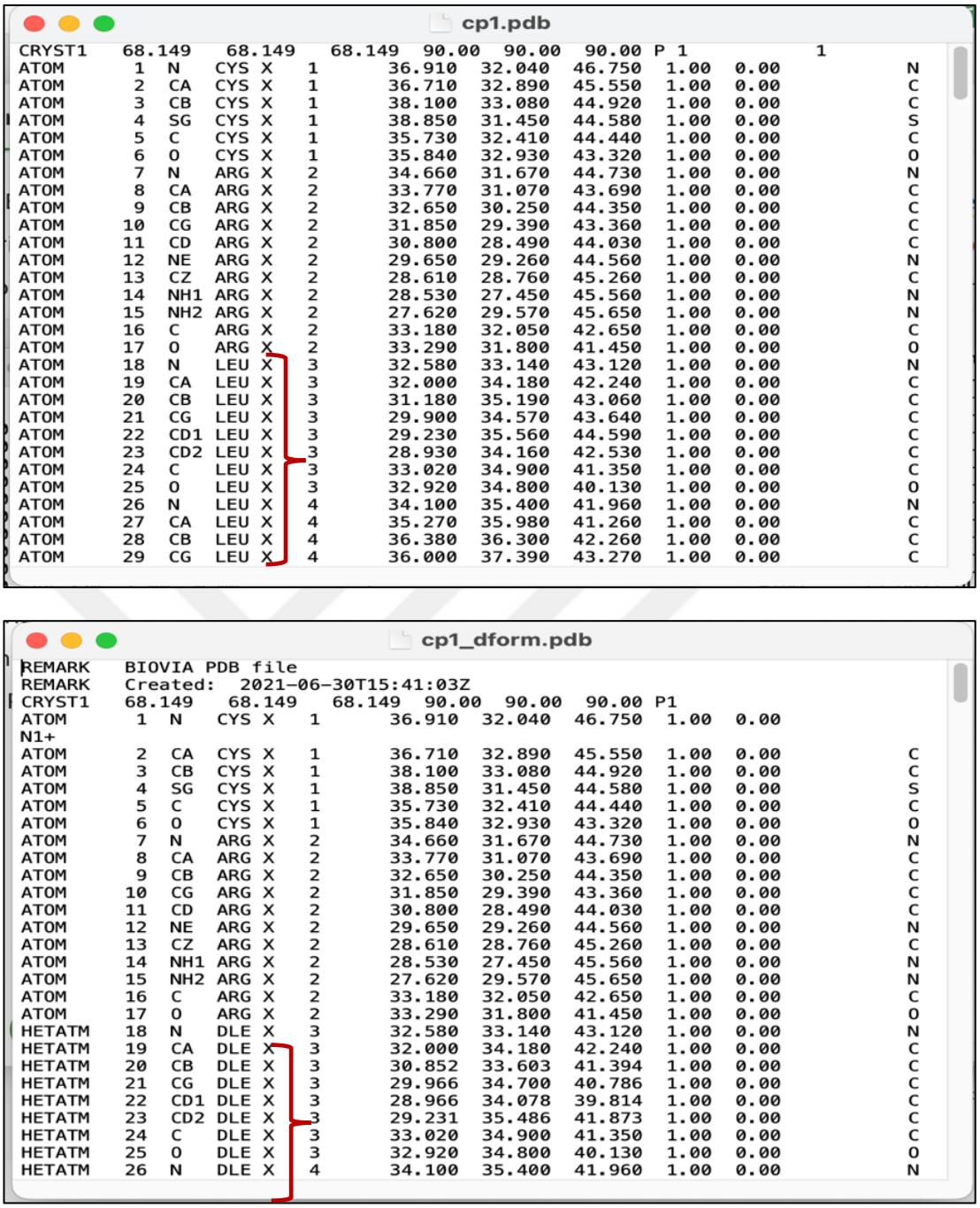

cp1.pdb

```
CRYST1   68.149   68.149   68.149  90.00  90.00  90.00 P 1           1
ATOM      1  N   CYS X   1      36.910  32.040  46.750  1.00  0.00           N
ATOM      2  CA  CYS X   1      36.710  32.890  45.550  1.00  0.00           C
ATOM      3  CB  CYS X   1      38.100  33.080  44.920  1.00  0.00           C
ATOM      4  SG  CYS X   1      38.850  31.450  44.580  1.00  0.00           S
ATOM      5  C   CYS X   1      35.730  32.410  44.440  1.00  0.00           C
ATOM      6  O   CYS X   1      35.840  32.930  43.320  1.00  0.00           O
ATOM      7  N   ARG X   2      34.660  31.670  44.730  1.00  0.00           N
ATOM      8  CA  ARG X   2      33.770  31.070  43.690  1.00  0.00           C
ATOM      9  CB  ARG X   2      32.650  30.250  44.350  1.00  0.00           C
ATOM     10  CG  ARG X   2      31.850  29.390  43.360  1.00  0.00           C
ATOM     11  CD  ARG X   2      30.800  28.490  44.030  1.00  0.00           C
ATOM     12  NE  ARG X   2      29.650  29.260  44.560  1.00  0.00           N
ATOM     13  CZ  ARG X   2      28.610  28.760  45.260  1.00  0.00           C
ATOM     14  NH1 ARG X   2      28.530  27.450  45.560  1.00  0.00           N
ATOM     15  NH2 ARG X   2      27.620  29.570  45.650  1.00  0.00           N
ATOM     16  C   ARG X   2      33.180  32.050  42.650  1.00  0.00           C
ATOM     17  O   ARG X   2      33.290  31.800  41.450  1.00  0.00           O
ATOM     18  N   LEU X   3      32.580  33.140  43.120  1.00  0.00           N
ATOM     19  CA  LEU X   3      32.000  34.180  42.240  1.00  0.00           C
ATOM     20  CB  LEU X   3      31.180  35.190  43.060  1.00  0.00           C
ATOM     21  CG  LEU X   3      29.900  34.570  43.640  1.00  0.00           C
ATOM     22  CD1 LEU X   3      29.230  35.560  44.590  1.00  0.00           C
ATOM     23  CD2 LEU X   3      28.930  34.160  42.530  1.00  0.00           C
ATOM     24  C   LEU X   3      33.020  34.900  41.350  1.00  0.00           C
ATOM     25  O   LEU X   3      32.920  34.800  40.130  1.00  0.00           O
ATOM     26  N   LEU X   4      34.100  35.400  41.960  1.00  0.00           N
ATOM     27  CA  LEU X   4      35.270  35.980  41.260  1.00  0.00           C
ATOM     28  CB  LEU X   4      36.380  36.300  42.260  1.00  0.00           C
ATOM     29  CG  LEU X   4      36.000  37.390  43.270  1.00  0.00           C
```

cp1_dform.pdb

```
REMARK    BIOVIA PDB file
REMARK    Created:  2021-06-30T15:41:03Z
CRYST1   68.149   68.149   68.149  90.00  90.00  90.00 P1
ATOM      1  N   CYS X   1      36.910  32.040  46.750  1.00  0.00
N1+
ATOM      2  CA  CYS X   1      36.710  32.890  45.550  1.00  0.00           C
ATOM      3  CB  CYS X   1      38.100  33.080  44.920  1.00  0.00           C
ATOM      4  SG  CYS X   1      38.850  31.450  44.580  1.00  0.00           S
ATOM      5  C   CYS X   1      35.730  32.410  44.440  1.00  0.00           C
ATOM      6  O   CYS X   1      35.840  32.930  43.320  1.00  0.00           O
ATOM      7  N   ARG X   2      34.660  31.670  44.730  1.00  0.00           N
ATOM      8  CA  ARG X   2      33.770  31.070  43.690  1.00  0.00           C
ATOM      9  CB  ARG X   2      32.650  30.250  44.350  1.00  0.00           C
ATOM     10  CG  ARG X   2      31.850  29.390  43.360  1.00  0.00           C
ATOM     11  CD  ARG X   2      30.800  28.490  44.030  1.00  0.00           C
ATOM     12  NE  ARG X   2      29.650  29.260  44.560  1.00  0.00           N
ATOM     13  CZ  ARG X   2      28.610  28.760  45.260  1.00  0.00           C
ATOM     14  NH1 ARG X   2      28.530  27.450  45.560  1.00  0.00           N
ATOM     15  NH2 ARG X   2      27.620  29.570  45.650  1.00  0.00           N
ATOM     16  C   ARG X   2      33.180  32.050  42.650  1.00  0.00           C
ATOM     17  O   ARG X   2      33.290  31.800  41.450  1.00  0.00           O
HETATM   18  N   DLE X   3      32.580  33.140  43.120  1.00  0.00           N
HETATM   19  CA  DLE X   3      32.000  34.180  42.240  1.00  0.00           C
HETATM   20  CB  DLE X   3      30.852  33.603  41.394  1.00  0.00           C
HETATM   21  CG  DLE X   3      29.966  34.700  40.786  1.00  0.00           C
HETATM   22  CD1 DLE X   3      28.966  34.078  39.814  1.00  0.00           C
HETATM   23  CD2 DLE X   3      29.231  35.486  41.873  1.00  0.00           C
HETATM   24  C   DLE X   3      33.020  34.900  41.350  1.00  0.00           C
HETATM   25  O   DLE X   3      32.920  34.800  40.130  1.00  0.00           O
HETATM   26  N   DLE X   4      34.100  35.400  41.960  1.00  0.00           N
```

Figure 87. PDB file formats of C-P1 peptide in both L-form and D-form and of DLEU amino acid. Demonstration of the difference between D- and L-form in PDB file (continued).

In the 100 ns simulation (see in Figure 29), the peptides started attaching to the membrane beginning from about 15 ns. It was observed that they move in a membrane-bound manner throughout the simulation. The peptides, which were first bound

vertically to the membrane from the cystine end, then moved to the horizontal position and remained attached to the membrane, remaining somewhat embedded on the membrane surface with both the cystine end and leucine amino acids.

This is an expected result, since the functional group at the cystine amino acid end of the C-P1 molecule is very active. Although the orientation of the C-P1 peptide to the membrane can be seen by performing the molecular dynamics simulation of the C-P1 peptide on the membrane, it would be more appropriate to simulate a C-P1 peptide-like structure on the membrane, which is attached to the catheter (polymer) surface from the cystine ends, in future studies.

The reason for choosing the POPE membrane in MD simulations is that PE (Phosphatidylethanolamine) lipids are generally more abundant on the cytoplasmic side of the bacterial membrane and PE lipids are frequently used to mimic the bacterial membrane in previous studies (118).

5.2 Second Study

Second study of this thesis consists of four sections. In order to examine the interactions of synthetically designed polymers (Triphenylphosphonium:mannose 5:2) with microorganism-specific antimicrobial peptides designed earlier (99) and a reference peptide (magainin) found in nature, it is intended in this study to develop model membrane structures belonging to specific species.

To this purpose, in the first section, Top6 model membrane involving the 6 main lipid species most abundant in E. coli (102) were designed. For a more thorough investigation of the membrane-polymer activation by MD simulation processes, parameter sets of the antimicrobial similar polymers were generated. Additionally, a simulation box was created using model membrane and water (in Figure 30). Antimicrobial peptides, the source of the polymer in this study (99), and magainin protein, a reference peptide found in nature, were 3D modeled and compared to provide a better insight.

Second section of the study were conducted with Triphenylphosphonium:mannose 5:2 polymer – POPE membrane system with different simulation time and different P atom charges. 3D structure of the polymer used in these experiments were obtained by different research laboratory since it was required to perform quantum simulations and our computational power was not qualified for these kinds of procedures.

In order to examine the interactions of the mannose part of the designed Triphenylphosphonium:Mannose 5:2 polymer molecule with the lectin protein, which is thought to have metabolic importance for the cell, the binding energies and binding positions of the molecules were calculated and examined using the method called molecular docking. Binding score was found as -1,14 which falls in the range considered as showing good binding affinity.

In the first simulation, the electronic charge on the P atom is set to -0.15095, and simulation was set for 100 ns (Figure 32). Then, a second simulation was made by changing the simulation duration to 60 ns and the charge on the P atom to +1 within these parameter sets, considering that it would be more compatible with the Br- anion (Figure 33). Thus, it was also investigated whether the electronic charge on the P atom affects the interaction of the polymer with the membrane.

Although it has been emphasized in the literature that production simulations with a duration of at least 100-200 ns should be observed in order to observe the interaction properties of membrane and antimicrobial polymers (119), the Triphenylphosphonium: Mannose 5:2 polymer designed as a result of the simulations we have done in this project can also be used with two different P electronic load parameters. It is seen that it starts to penetrate the membrane in less than 100 ns. Natural peptides with similar antimicrobial properties were studied in the models in the previous preliminary study (101), and it was predicted that in the case where it is assumed to enter the membrane, it causes the membrane to break down due to the passage of water molecules or a few of the peptides combine to lose their antimicrobial effect.

In this study, synthetically designed polymers are polymers inspired by these natural peptides. Thus, the existing simulations reported in Section 2 were extended to 200 ns in the Section 3 to observe whether the polymer has fully penetrated the membrane and generates an environment that is favorable to water passage, and to observe a similar antimicrobial effect and/or which functional groups play an active role in this effect.

In the simulations carried out in the second section of the study, when the distance (Å) of the Triphenylphosphonium:Mannose 5:2 polymer to the membrane is analyzed according to the time step graph, it is seen that the polymer molecule deployed at a distance of 12.5 Angstrom first converges to the membrane with back-and-forth movements, and it is seen that the distance between the membrane and the membrane is 0 in the 16000th step (each step is 2 fs), that is approximately 32 ns. When the part of the simulation up to 100 ns is examined, it has been observed that the Triphenylphosphonium group first enters the membrane after adhering to the membrane, but then comes out, while the mannose group remains there during the simulation period after it enters the membrane. In the simulation range of 100-200 ns, it was observed that both polymers remained in the same plane with the P atoms on the surface but did not achieve the expected vertical deployment between membrane lipids.

Although it has been emphasized in the literature that production simulations with a duration of at least 100-200 ns should be observed in order to observe the interaction properties of membrane and antimicrobial polymers (120), as a result of the simulations we have done in this project, the Triphenylphosphonium:Mannose 5:2 polymer designed with two different P electronic charges starts to enter the membrane in less than 100 ns, and remains in the membrane by maintaining its horizontal orientation with the membrane in the range of 100-200 ns. However, vertical (and parallel to lipids) deployment of the polymer in the membrane in the range of 100-200 ns has not yet been observed.

Natural peptides with similar antimicrobial properties were studied in the models in a preliminary study (101), and it was predicted that in the case where it is assumed to enter the membrane, it causes the membrane to break down due to the passage of water molecules or a few of the peptides combine to lose their antimicrobial effect. On the other hand, in this project, synthetically designed polymers are polymers inspired by these natural peptides. Therefore, to observe whether the polymer fully penetrates into the membrane and to observe a similar antimicrobial effect and/or which functional groups play an active role in this effect, the available simulations reported here may require to be interpreted, compared with the experimental results, and further extended and analyzed if necessary.

For the last section of the second study, Triphenylphosphonium:Mannose 5:2 polymer and 3D-formed red blood cell membrane were modeled by MD simulation with 100 ns simulation duration with 50,000,000 timesteps and 50,000 frames. P charge parameter was set as +1 (Figure 38 & 39). In the simulation created, the electronic charge on the P atom was set as +1 considering its compatibility with the Br-anion. The reason for this is to observe the system for a longer period of time and to evaluate more accurately whether the polymer reaches equilibrium, at which step it has reached equilibrium, and its interaction with the membrane. Besides, the mannose-lectin and galactose-lectin interactions were examined by docking.

According to result of the simulations and to distance and RMSD graph, polymer on the red blood cell membrane reached to the point where they showed a stable conformation. Furthermore, It is observed that the polymer molecule, which was initially placed at a distance of around 15, moves back and forth toward the membrane. After 30000 steps, the distance between the polymer and the membrane is reduced to zero in 2 fs steps, or in roughly 60 ns. The triphenylphosphonium group first entered the membrane after adhering to the membrane, but then came out. In contrast, the mannose group entered the membrane and stayed there throughout the simulation period.

Docking results shows that the binding score (affinity) of Lectin and Mannose was -6.4. Lectin-galactose docking interaction score was -6.5 It is intended to compare how mannose and galactose interact through this process. showed that mannose and galactose showed a negligible difference when interacting with the lectin protein. Therefore, it can be said that the galactose group can be another alternative for designing antimicrobial peptide inspired polymers.

5.3 Third Study

Last study of the thesis consists of three sections. In the first sections previously designed AMPS in different but related project (101). Most active peptides, TN1 and TN3, were investigated to understand whether they have antimicrobial property by locating them on doble-layered POPE membrane in water with different placements and different amounts. TN6 and D-TN6 peptides were also simulated.

TN3 peptide was placed on the membrane first as 12 identical peptides in rectangular and circular form. After that they were placed as 4 identical peptides on the membrane. The reason for high number of peptides; It has been shown in the literature that ideal pore-forming peptides in the bacterial membrane can permeate the lipid vesicle with at least 10 peptides bound per vesicle or 1 peptide per 10,000 lipids (121). For this reason, since using 4 peptides may not be enough to observe the mechanism of action, it was decided to observe at least 12 peptides on the membrane and in the water in a sample study. Furthermore, the reason for the difference in positioning is to examine the effect of the initial position of the peptides on the approach to the membrane. The reason why we chose 10 Å as the distance is to determine whether the peptides interact with each other and with the membrane without going out of the periodic boundary conditions in MD simulation.

Since it is observed that 12-pack of TN3 in both rectangular shape and circular shape, peptides were grouped together as they form a 4-pack of peptides which can be seen in Figure 46 and Figure 48. That’s why peptide number was reduced to 4 peptides to save time and to make it more manageable for computer power.

Simulations were continued with 4-pack of peptides. TN3-isoleucine, TN3-valine, TN1-isoleucine and TN1-valine were simulated for 10 ns to observe if the different amino acids affect the antimicrobial effect of the peptides on bacterial membrane. All peptides above demonstrated similar behavior where they towered to the membrane. It has been observed that TN1 and TN3 molecules attract the negatively charged phosphate groups of the lipids in the membrane with the positively charged amino acids on them and integrate them into the membrane. This interaction of opposite charges on the membrane and the peptide causes the membrane to shrink and decrease in thickness. In this way, it is thought that it creates a hydrophilic channel that allows water to pass between the charged groups.

Besides, randomly selected peptide, TN6 (L-form) and its D-form, D-TN6 were simulated separately for 100 ns. D-TN6 simulation duration was then extended to 300 ns. It is supported by laboratory results that the D form of TN6 peptide is more resistant to proteases. For this reason, the simulation time of the D form was extended, and its mechanism of action on bacteria was examined in more detail (in Figure 77).

Interaction time of amino acids belonging to each peptide with phosphate ends of the membrane were investigated during the performed simulations to obtain a more accurate information active site of the peptides (seen in Table 8 & 9). According to contact time percentages of each both TN6 and D-TN6, amino acids of D-form amino acids contact time percentages were detected to be higher that L-form amino acids. In accordance with these results, it can be said that the D-form peptides more active compared to L-form peptides.

In the second part, DABCO-based (double cationic charged) polymer locating above double-layered POPE membrane structure was simulated to last 150 ns. DABCO (triethylenediamine/TEDA) is an amine base which is a strongly nucleophilic organic compound. As it can be seen in Table 7, DABCO-based polymer was designed highly similar to the antimicrobial peptide TN1 which was designed to be similar to the naturally found antimicrobial peptide “magainin”.

When the simulation was examined, it was observed that the phenyl group penetrated the membrane after adhering to the membrane. Although it has been emphasized in the literature that production simulations with a duration of at least 100-200 ns should be observed to observe the interaction properties of membrane and antimicrobial polymers (120), it is seen that the designed polymer starts to penetrate the membrane in less than 100 ns as a result of the simulations that have done in this project. However, a complete penetration into the membrane was not observed during this simulation process.

Natural peptides with similar antimicrobial properties were studied in the models in the preliminary study, and it was predicted that in the case where it is assumed to enter the membrane, it causes the membrane to break down due to the passage of water molecules or a few of the peptides combine to lose their antimicrobial effect (101). Having said that, in the context of this study, synthetically designed polymers using here were specifically designed inspired by peptides mentioned in the preliminary study. 3D structural and property comparison of polymers with antimicrobial peptides were demonstrated in Table 7. Therefore, the existing simulations reported here may require increasing in simulation duration to observe whether the polymer has fully penetrated into the membrane and to observe a similar antimicrobial effect and/or which functional groups play an active role in this effect.

Last section experiment was conducted according to result of the simulations held in first section. Since the D-TN6 was found to be promising AMP as it is known that D-TN6 is more resistant to proteases, simulation of D-TN6 was extended to 600 ns from 300 ns.

When the previous molecular modelling results were examined, it was observed that both L and D forms of the TN6 peptide penetrated into the membrane during the simulation period. However, since the D form is known to be resistant to proteases, the simulation time was extended to a total of 600ns.

According to simulation results represented in Figure 85, two of the four peptides moved together and other two moved individually while all four were embedded in the membrane. Although the placement of peptide structures in the membrane layer and the transitions of water molecules were observed as a result of this long simulation presented in this study, comparisons can be made by creating and running similar simulation systems with different membrane structures in other studies. Aside from that, since merging of peptides can cause AMPs to lose their antimicrobial effects, D-TN6 peptides' antimicrobial effect might require further investigation whether their activity would get affected when they merged or whether they would remain merged if they are observed in simulation system having membrane of different organism.

6 CONCLUSION

Taken together all molecular modelling studies carried out in parallel and iteratively with the experimental studies within the scope of the thesis, it was ensured that the newly designed molecules, peptides and polymers which were expected to show antimicrobial effect, were based on rational rather than random basis by determining the regions where the molecules interact and the mechanisms of their antimicrobial effect.

Furthermore, 3D design of D-form amino acids is a relatively new method that has begun to develop within the scope of computational studies. In this regard, studies are important in terms of applying two different methods (generating a new script and Discovery Studio Client 2021 software' tool) that can contribute to the field of computational biology & chemistry and to related future studies.

This comprehensive thesis study demonstrates that molecular modelling studies offer significant advantages in biology and chemistry in terms of both time and resources due to the quickness of the data obtained using molecular dynamics methods and the adequate consistency with laboratory investigations. Since it is a relatively new technology, it still has aspects that are open to development.

7 REFERENCES

1. Greco I, Molchanova N, Holmedal E, Jenssen H, Hummel BD, Watts Jeffrey L and Håkansson J, et al. Correlation between hemolytic activity, cytotoxicity and systemic in vivo toxicity of synthetic antimicrobial peptides. Sci Rep. 2020;10(1):13206.
2. Kuroda K, Caputo GA. Antimicrobial polymers as synthetic mimics of host-defense peptides. Vol. 5, Wiley Interdisciplinary Reviews: Nanomedicine and Nanobiotechnology. 2013. p. 49–66.
3. Santos MRE, Fonseca AC, Mendonça P v., Branco R, Serra AC, Morais P v., et al. Recent developments in antimicrobial polymers: A review. Vol. 9, Materials. MDPI AG; 2016.
4. Carmona-Ribeiro AM, Araújo PM. Antimicrobial polymer−based assemblies: A review. Vol. 22, International Journal of Molecular Sciences. MDPI; 2021.
5. Clementi E. Ab initio computational chemistry. J Phys Chem. 1985;89(21):4426–36.
6. Young D. Computational chemistry: A practical guide for applying techniques to real world problems | Wiley. 2001.
7. Hall GG. The growth of computational quantum chemistry from 1950 to 1971. Chem Soc Rev. 1973;2(1):21.
8. Sayhan S. Investigation of Hydrogen Storage Capabilities and Related Properties of Various Nano-Materials by Using Computational Chemistry Methods, E.U. Applied and Natural Sciences. Izmr. 2007;
9. Stuper E, Brugger W, Jurs P. Computer-Aided Analysis of the Relation Between Chemical Structure and Biological Activity. Computer-Aided Analysis of the Relation Between Chemical Structure and Biological Activity. 1982;
10. Heller SR, Potenzone R. Computer Applications in Chemistry. In: Proceedings of the 6th International Conference on Computers in Chemical Research and Education. Amsterdam, The Netherlands: Elsevier; 1983.
11. Brandt J, Ugi IK. ChemInform abstract: Computer applications in chemical research and education. ChemInform. 1989;20(34).
12. Solomons TWG, Fryhle CB, Snyder SA . Organic Chemistry. Organic Chemistry. 2013;
13. Halliday D, Resnick R. Fundamentals of physics: V.1 & 2. 5th ed. Nashville, TN: John Wiley & Sons; 1998.
14. Straatsma TP, McCammon JA. Computational alchemy. Annu Rev Phys Chem. 1992;43(1):407–35.
15. Feynman RP. Feynman Lectures on Computation. Boulder, CO: Perseus Books; 1996.
16. Naray-Szabo G, Ferenczy GG. Molecular electrostatics. Chem Rev. 1995;95(4):829–47.
17. Whalen JW. Molecular Thermodynamicss: A Statistical Approach. NY: John Wiley & Sons;
18. Hill TL. Thermodynamicss of small systems. Mineola, NY: Dover Publications; 2002.
19. Levine IN. Physical Chemistry. 6th ed. Maidenhead, England: McGraw Hill Higher Education; 2008.

20. House JE. Fundamentals of Quantum Mechanics. San Diego: Academic Press; 1998.
21. Atkins PW, Friedman RS. Molecular Quantum Mechanics Oxford. Oxford; 1997.
22. Christo¨ersen RE. Basic Principles and Techniques of Molecular Quantum Mechanics. New York: Springer-Verlag; 1989.
23. Neese F, Atanasov M, Bistoni G, Maganas D, Ye S. Chemistry and quantum mechanics in 2019: Give us insight and numbers. J Am Chem Soc. 2019;141(7):2814–24.
24. Greiner W. Quantum Mechanics: An Introduction. 2nd ed. Berlin, Germany: Springer; 2012.
25. Murphy RB, Philipp DM, Friesner RA. A mixed quantum mechanics/molecular mechanics (QM/MM) method for large-scale modelling of chemistry in protein environments. J Comput Chem. 2000;21(16):1442–57.
26. Goodisman J. Statistical Mechanics for Chemists. New York: John Wiley & Sons; 1997.
27. Pfau D, Spencer JS, Matthews AGDG, Foulkes WMC. Foulkes Phys. Phys Rev Research. 2020;2.
28. Oppenheim I. Statistical mechanics and thermodynamicss: Claude Garrod, Oxford University Press, Oxford, 1995. J Stat Phys. 1996;82(1–2):455–6.
29. Hoover WG. Computational statistical mechanics. London, England: Elsevier Science; 1991.
30. Ramachandran KI, Deepa G, Namboori K. Computational chemistry and molecular modelling: Principles and applications. Berlin, Germany: Springer; 2010.
31. Peressi M, Baldereschi A, Baroni S. Ab initio studies of structural and electronic properties. In: Characterization of Semiconductor Heterostructures and Nanostructures. Elsevier; 2008. p. 17–54.
32. Zhang DW, Xiang Y, Zhang JZH. New advance in computational chemistry: Full quantum mechanical ab initio computation of streptavidin-biotin interaction energy. J Phys Chem B. 2003;107(44):12039–41.
33. Thiel W. Semiempirical quantum-chemical methods in computational chemistry. In: Dykstra CE, Frenking G, Kim KS, Scuseria GE, editors. Theory and Applications of Computational Chemistry. Elsevier; 2005. p. 559–80.
34. Wu X, Koslowski A, Thiel W. Semiempirical Quantum Chemistry. In: Electronic Structure Calculations on Graphics Processing Units. Chichester, UK: John Wiley & Sons, Ltd; 2016. p. 239–58.
35. Rivail JL. Molecular modelling. Semi-empirical and empirical methods of theoretical chemistry. In: Computational Advances in Organic Chemistry: Molecular Structure and Reactivity. Dordrecht: Springer Netherlands; 1991. p. 229–59.
36. Louwen JN, Vogt ETC. Semi-empirical atomic charges for use in computational chemistry of molecular sieves. J Mol Catal A Chem. 1998;134(1–3):63–77.
37. West AR. Solid state chemistry and its applications, student edition: Student Edition. 1st ed. John Wiley & Sons; 2014.
38. Dronskowski R. Computational chemistry of solid state materials: A guide for materials scientists, chemists, physicists and others. 1st ed. Weinheim, Germany: Wiley-VCH Verlag; 2008.

39. Tersoff J. Modelling solid-state chemistry: Interatomic potentials for multicomponent systems. Phys Rev B Condens Matter. 1989;39(8):5566–8.
40. Rappe AK, Casewit CJ. Molecular mechanics across chemistry. Sausalito, CA: University Science Books; 1997.
41. Vanommeslaeghe K, Guvench O, MacKerell Jr AD. Molecular mechanics. Curr Pharm Des. 2014;20(20):3281–92.
42. Hehre WJ. A guide to molecular mechanics and quantum chemical calculations. Unipd.it.
43. Kollman PA, Massova I, Reyes C, Kuhn B, Huo S and Chong L, Lee M, et al. Calculating structures and free energies of complex molecules: combining molecular mechanics and continuum models. Acc Chem Res. 2000;33(12):889–97.
44. Sadus RJ. Molecular simulation of fluids. London, England: Elsevier Science; 2002.
45. Belkin A, Rudyak V, Krasnolutskii S. Molecular dynamicss simulation of carbon nanotubes diffusion in water. Mol Simul. 2022;48(9):752–9.
46. van Gunsteren WF, Dolenc J, Mark AE. Molecular simulation as an aid to experimentalists. Curr Opin Struct Biol. 2008;18(2):149–53.
47. Frenkel D, Smit B. Understanding molecular simulation: From algorithms to applications. 2nd ed. San Diego, CA: Academic Press; 2002.
48. Davidson N. Statistical Mechanics. New York, NY: McGraw-Hill; 1962.
49. Deem MW. Recent contributions of statistical mechanics in chemical engineering. AIChE J. 1998;44(12):2569–96.
50. Randi? M. On computation of optimal parameters for multivariate analysis of structure-property relationship. J Comput Chem. 1991;12(8):970–80.
51. Newnham RE. Structure - Property Relations. Berlin, Germany: Springer; 2012.
52. Le T, Epa VC, Burden FR, Winkler DA. Quantitative structure-property relationship modelling of diverse materials properties. Chem Rev. 2012;112(5):2889–919.
53. Thanikaivelan P, Subramanian V, Raghava Rao J, Unni Nair B. Application of quantum chemical descriptor in quantitative structure activity and structure property relationship. Chem Phys Lett. 2000;323(1–2):59–70.
54. Grover I I, Singh I I, Bakshi I I. Quantitative structure-property relationships in pharmaceutical research - Part 1. Pharm Sci Technolo Today. 2000;3(1):28–35.
55. He L, Bai L, Dionysiou DD, Wei Zongsu and Spinney R, Chu C, Lin Z, et al. Applications of computational chemistry, artificial intelligence, and machine learning in aquatic chemistry research. Chem Eng J. 2021;426(131810):131810.
56. Zhavoronkov A. Artificial intelligence for drug discovery, biomarker development, and generation of novel chemistry. Mol Pharm. 2018;15(10):4311–3.
57. Leach AR. Molecular modelling: Principles and applications. London, England: Prentice-Hall; 1996.

58. Nie F, Cheuk ·, Chow L, Lau D. A Review on Multiscale Modelling of Asphalt: Development and Applications. Multiscale Science and Engineering 2022 4:1 [Internet]. 2022 May 6 [cited 2022 Dec 26];4(1):10–27. Available from: https://link.springer.com/article/10.1007/s42493-022-00076-x
59. Schlick T. Molecular Modelling and Simulation. New York, NY: Springer; 2014.
60. Jensen F. Introduction to Computational Chemistry.
61. Ramachandran KI, Deepa G, Namboori K. Computational chemistry and molecular modelling: Principles and applications. Computational Chemistry and Molecular Modelling: Principles and Applications. Springer Berlin Heidelberg; 2008. 1–397 p.
62. Hinchliffe A. Molecular modelling for beginners. 2nd ed. Hoboken, NJ: Wiley-Blackwell; 2011.
63. Hocquet A, Langgård M. An evaluation of the MM+ force field. J Mol Model [Internet]. 1998 [cited 2022 Dec 28];4(3):94–112. Available from: https://link.springer.com/article/10.1007/s008940050128
64. Saxena A, Wong D, Diraviyam K, Sept D. The Basic Concepts of Molecular Modelling.
65. Hollingsworth SA, Dror RO. Molecular Dynamicss Simulation for All. Neuron. 2018 Sep 19;99(6):1129–43.
66. Allen MP. John von Neumann Institute for Computing. Lecture Notes, Norbert Attig [Internet]. 2004 [cited 2022 Dec 28];23:1–28. Available from: http://www.fz-juelich.de/nic-series/volume23
67. Ginibre J. Statistical Ensembles of Complex, Quaternion, and Real Matrices. J Math Phys [Internet]. 2004 Dec 22 [cited 2022 Dec 28];6(3):440. Available from: https://aip.scitation.org/doi/abs/10.1063/1.1704292
68. Çagin T, Ray JR. Fundamental treatment of molecular-dynamicss ensembles. Phys Rev A (Coll Park) [Internet]. 1988 Jan 1 [cited 2022 Dec 28];37(1):247. Available from: https://journals.aps.org/pra/abstract/10.1103/PhysRevA.37.247
69. Ilievski E, Quinn E, Caux JS. From interacting particles to equilibrium statistical ensembles. Phys Rev B [Internet]. 2017 Mar 14 [cited 2022 Dec 28];95(11):115128. Available from: https://journals.aps.org/prb/abstract/10.1103/PhysRevB.95.115128
70. White JA, Román FL, González A, Velasco S. Periodic boundary conditions and the correct molecular-dynamicss ensemble. Physica A: Statistical Mechanics and its Applications. 2008 Dec 1;387(27):6705–11.
71. Makov G, Payne MC. Periodic boundary conditions in *ab initio* calculations. Phys Rev B [Internet]. 1995 Feb 15 [cited 2022 Dec 28];51(7):4014. Available from: https://journals.aps.org/prb/abstract/10.1103/PhysRevB.51.4014
72. Morris GM, Lim-Wilby M. Molecular docking. Methods in Molecular Biology [Internet]. 2008 [cited 2022 Dec 28];443:365–82. Available from: https://link.springer.com/protocol/10.1007/978-1-59745-177-2_19
73. Meng XY, Zhang HX, Mezei M, Cui M. Molecular Docking: A powerful approach for structure-based drug discovery.

74. Molecular Docking: Approaches, Types, Applications and Basic Challenges [Internet]. [cited 2022 Dec 28]. Available from: https://www.omicsonline.org/open-access/molecular-docking-approaches-types-applications-and-basic-challenges-2155-9872-1000356.pdf
75. Pagadala NS, Syed K, Tuszynski J. Software for molecular docking: a review . Biophys Rev.
76. Textbook of Drug Design and Discovery. Textbook of Drug Design and Discovery [Internet]. 2009 Oct 7 [cited 2022 Dec 29]; Available from: https://www.taylorfrancis.com/books/mono/10.1201/9781439882405/textbook-drug-design-discovery-kristian-stromgaard-povl-krogsgaard-larsen-ulf-madsen
77. Hung CL, Chen CC. Computational Approaches for Drug Discovery. Drug Dev Res [Internet]. 2014 Sep 1 [cited 2022 Dec 29];75(6):412–8. Available from: https://onlinelibrary.wiley.com/doi/full/10.1002/ddr.21222
78. Mandal S, Moudgil M, Mandal SK. Rational drug design. Eur J Pharmacol. 2009 Dec 25;625(1–3):90–100.
79. Mavromoustakos T, Durdagi S, Koukoulitsa C, Simcic M, G. Papadopoulos M, Hodoscek M, et al. Strategies in the Rational Drug Design. Curr Med Chem. 2011 Jun 6;18(17):2517–30.
80. Ramírez D. Computational Methods Applied to Rational Drug Design. Open Med Chem J [Internet]. 2016 Apr 26 [cited 2022 Dec 29];10(1):7. Available from: /pmc/articles/PMC5039900/
81. Macalino SJY, Gosu V, Hong S, Choi S. Role of computer-aided drug design in modern drug discovery. Archives of Pharmacal Research 2015 38:9 [Internet]. 2015 Jul 25 [cited 2022 Dec 29];38(9):1686–701. Available from: https://link.springer.com/article/10.1007/s12272-015-0640-5
82. Chen CH, Lu TK. Development and challenges of antimicrobial peptides for therapeutic applications. Antibiotics (Basel). 2020;9(1):24.
83. Raheem N, Straus SK. Mechanisms of action for antimicrobial peptides with antibacterial and antibiofilm functions. Front Microbiol. 2019;10:2866.
84. Hall CW, Mah TF. Molecular mechanisms of biofilm-based antibiotic resistance and tolerance in pathogenic bacteria. FEMS Microbiol Rev [Internet]. 2017 May 1 [cited 2022 Nov 19];41(3):276–301. Available from: https://academic.oup.com/femsre/article/41/3/276/3089981
85. Bocchinfuso G, Palleschi A, Orioni B, Grande G, Formaggio F, Toniolo C, et al. Different mechanisms of action of antimicrobial peptides: insights from fluorescence spectroscopy experiments and molecular dynamicss simulations. Journal of Peptide Science [Internet]. 2009 Sep 1 [cited 2022 Nov 19];15(9):550–8. Available from: https://onlinelibrary.wiley.com/doi/full/10.1002/psc.1144
86. Reygaert WC. An overview of the antimicrobial resistance mechanisms of bacteria. AIMS Microbiol. 2018;4(3):482–501.
87. Moretta A, Scieuzo C, Petrone AM, Salvia R, Manniello MD, Franco A, et al. Antimicrobial Peptides: A New Hope in Biomedical and Pharmaceutical Fields. Front Cell Infect Microbiol. 2021 Jun 14;11:453.

88. Cardoso MH, Orozco RQ, Rezende SB, Rodrigues G, Oshiro KGN, Cândido ES, et al. Computer-Aided Design of Antimicrobial Peptides: Are We Generating Effective Drug Candidates? Front Microbiol. 2020 Jan 22;10:3097.
89. Palmer N, Maasch JRMA, Torres MDT, de La Fuente-Nunez C. Molecular Dynamicss for Antimicrobial Peptide Discovery. Infect Immun [Internet]. 2021 Apr 1 [cited 2022 Nov 19];89(4). Available from: /pmc/articles/PMC8090940/
90. Torres MDT, de la Fuente-Nunez C. Toward computer-made artificial antibiotics. Curr Opin Microbiol. 2019;51:30–8.
91. Torres MDT, de la Fuente-Nunez C. Toward computer-made artificial antibiotics. Curr Opin Microbiol. 2019 Oct 1;51:30–8.
92. Lodge TP, Hiemenz PC. Polymer Chemistry: International Student Edition. 3rd ed. Boca Raton, FL: CRC Press; 2021.
93. Chanda M. Introduction to P olymer Science and Chemistry A Problem-Solving Approach.
94. Turner J, Cho Y, Dinh NN, Waring AJ, Lehrer RI. Activities of LL-37, a cathelin-associated antimicrobial peptide of human neutrophils. Antimicrob Agents Chemother [Internet]. 1998 [cited 2022 Dec 2];42(9):2206–14. Available from: https://journals.asm.org/journal/aac
95. de Breij A, Riool M, Cordfunke RA, Malanovic N, de Boer L, Koning RI, et al. The antimicrobial peptide SAAP-148 combats drug-resistant bacteria and biofilms. Sci Transl Med [Internet]. 2018 Jan 10 [cited 2022 Dec 2];10(423). Available from: https://www.science.org/doi/10.1126/scitranslmed.aan4044
96. Thévenet P, Shen Y, Maupetit J, Guyon F, Derreumaux P, Tufféry P. PEP-FOLD: an updated de novo structure prediction server for both linear and disulfide bonded cyclic peptides. Nucleic Acids Res [Internet]. 2012 Jul [cited 2022 Dec 2];40(Web Server issue). Available from: https://pubmed.ncbi.nlm.nih.gov/22581768/
97. Lamiable A, Thevenet P, Rey J, Vavrusa M, Derreumaux P, Tuffery P. PEP-FOLD3: faster de novo structure prediction for linear peptides in solution and in complex. Nucleic Acids Res [Internet]. 2016 Jul 8 [cited 2022 Dec 2];44(W1):W449–54. Available from: https://pubmed.ncbi.nlm.nih.gov/27131374/
98. Dassault Systèmes. BIOVIA Discovery Studio. San Diego; 2021.
99. Phillips JC, Braun R, Wang W, Gumbart J, Tajkhorshid E, Villa E, et al. Scalable molecular dynamicss with NAMD. J Comput Chem [Internet]. 2005 Dec 1 [cited 2022 Dec 3];26(16):1781–802. Available from: https://onlinelibrary.wiley.com/doi/full/10.1002/jcc.20289
100. Humphrey W, Dalke A, Schulten K. VMD: Visual molecular dynamicss. J Mol Graph. 1996 Feb 1;14(1):33–8.
101. Unubol N, Cinaroglu SS, Elmas MA, Akçelik S, Tugba A, Ildeniz O, et al. Peptide Antibiotics Developed by Mimicking Natural Antimicrobial Peptides.
102. Pandit KR, Klauda JB. Membrane models of E. coli containing cyclic moieties in the aliphatic lipid chain. Biochimica et Biophysica Acta (BBA) - Biomembranes. 2012 May 1;1818(5):1205–10.

103. Jo S, Kim T, Iyer VG, Im W. CHARMM-GUI: A web-based graphical user interface for CHARMM. J Comput Chem [Internet]. 2008 Aug 1 [cited 2022 Dec 7];29(11):1859–65. Available from: https://onlinelibrary.wiley.com/doi/full/10.1002/jcc.20945
104. Mayne CG, Saam J, Schulten K, Tajkhorshid E, Gumbart JC. Rapid parameterization of small molecules using the force field toolkit. J Comput Chem [Internet]. 2013 Dec 15 [cited 2022 Dec 7];34(32):2757–70. Available from: https://onlinelibrary.wiley.com/doi/full/10.1002/jcc.23422
105. NCI/CADD Group Chemoinformatics Tools and User Services [Internet]. [cited 2022 Dec 8]. Available from: https://cactus.nci.nih.gov/
106. Dennington RKTA; MJMSInc, SMK. Gauss View. 2016.
107. Savaş B, Karaca E. Türk Ulusal Bilim e-Altyapısı TRUBA'da Moleküler Dinamik Paketi GROMACS Versiyonlarının Performans Optimizasyonu GROMACS Performance Optimization at Turkish National Grid Resources TRUBA. Int J Adv Eng Pure Sci [Internet]. [cited 2022 Dec 12];2021(4). Available from: https://github.com/CSB-KaracaLab/gmx_performance_on_HPC.
108. Firaha DS, Gibalova A v, Hollóczki OH. Basic Phosphonium Ionic Liquids as Wittig Reagents. 2017 [cited 2022 Dec 8]; Available from: http://pubs.acs.org/journal/acsodf
109. Jo S, Lim JB, Klauda JB, Im W. CHARMM-GUI Membrane Builder for Mixed Bilayers and Its Application to Yeast Membranes. [cited 2022 Dec 10]; Available from: http://www.charmm-gui.org/input/membrane
110. Jo S, Kim T, Im W. Automated Builder and Database of Protein/Membrane Complexes for Molecular Dynamicss Simulations. [cited 2022 Dec 10]; Available from: www.plosone.org
111. Lee J, Patel DS, Ståhle J, Park SJ, Kern NR, Kim S, et al. CHARMM-GUI Membrane Builder for Complex Biological Membrane Simulations with Glycolipids and Lipoglycans. J Chem Theory Comput [Internet]. 2019 Jan 8 [cited 2022 Dec 10];15(1):775–86. Available from: https://pubs.acs.org/doi/pdf/10.1021/acs.jctc.8b01066
112. Shahinyan AA, Hakobyan PK, Poghosyan AH. Molecular dynamicss study of human red blood cell membrane.
113. Morris GM, Ruth H, Lindstrom W, Sanner MF, Belew RK, Goodsell DS, et al. AutoDock4 and AutoDockTools4: Automated Docking with Selective Receptor Flexibility. J Comput Chem [Internet]. 2009 Dec [cited 2022 Dec 8];30(16):2785. Available from: /pmc/articles/PMC2760638/
114. Sauer MM, Jakob RP, Eras J, Baday S, Eriş D, Navarra G, et al. Catch-bond mechanism of the bacterial adhesin FimH. Nat Commun [Internet]. 2016 Mar 7 [cited 2022 Dec 10];7. Available from: /pmc/articles/PMC4786642/
115. Berman HM, Westbrook J, Feng Z, Gilliland G, Bhat TN, Weissig H, et al. The Protein Data Bank. Nucleic Acids Res [Internet]. 2000 Jan 1 [cited 2022 Dec 10];28(1):235–42. Available from: https://academic.oup.com/nar/article/28/1/235/2384399
116. Eberhardt J, Santos-Martins D, Tillack AF, Forli S. AutoDock Vina 1.2.0: New Docking Methods, Expanded Force Field, and Python Bindings. J Chem Inf Model [Internet]. 2021 Aug 23 [cited 2022 Dec 8];61(8):3891–8. Available from: https://pubs.acs.org/doi/pdf/10.1021/acs.jcim.1c00203

117. Kim JY, Park SC, Yoon MY, Hahm KS, Park Y. C-terminal amidation of PMAP-23: Translocation to the inner membrane of Gram-negative bacteria. Amino Acids [Internet]. 2011 Jan 30 [cited 2022 Dec 5];40(1):183–95. Available from: https://link.springer.com/article/10.1007/s00726-010-0632-1
118. van Meer G, Voelker DR, Feigenson GW. Membrane lipids: where they are and how they behave. Nature Reviews Molecular Cell Biology 2008 9:2 [Internet]. 2008 Feb [cited 2022 Dec 5];9(2):112–24. Available from: https://www.nature.com/articles/nrm2330
119. Horn JN, Romo TD, Grossfield A. Simulating the mechanism of antimicrobial lipopeptides with all-atom molecular dynamicss. Biochemistry [Internet]. 2013 Aug 8 [cited 2022 Dec 8];52(33):5604. Available from: /pmc/articles/PMC4030210/
120. Horn JN, Romo TD, Grossfield A. Simulating the mechanism of antimicrobial lipopeptides with all-atom molecular dynamicss. Biochemistry [Internet]. 2013 Aug 8 [cited 2022 Dec 10];52(33):5604. Available from: /pmc/articles/PMC4030210/
121. Parente RA, Nir S, Szoka FC. Mechanism of leakage of phospholipid vesicle contents induced by the peptide GALA. Biochemistry [Internet]. 1990 Sep 1 [cited 2022 Dec 12];29(37):8720–8. Available from: https://pubmed.ncbi.nlm.nih.gov/2271552/

8 CURRICULUM VITAE